Brookhaven National Laboratory

Small x and Saturation

2026 CFNS Summer School, Stony Brook University

Björn Schenke, Brookhaven National Laboratory
6/8/2026

U.S. DEPARTMENT OF ENERGY | Office of Science

Science goals of the Electron Ion Collider

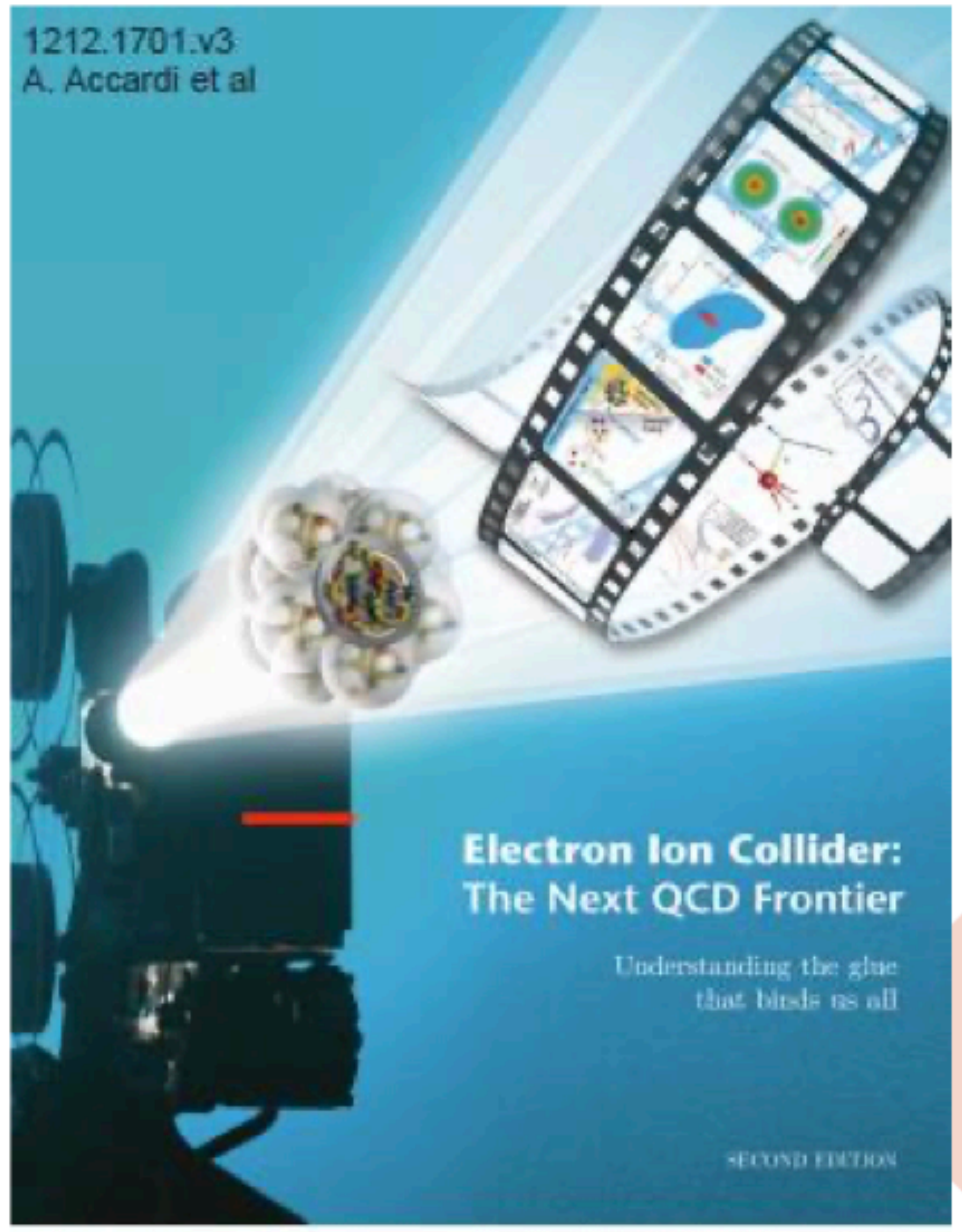

White paper
arXiv:1212.1701

Origin of nucleon mass

Origin of nucleon spin

Gluon saturation

Nucleon tomography

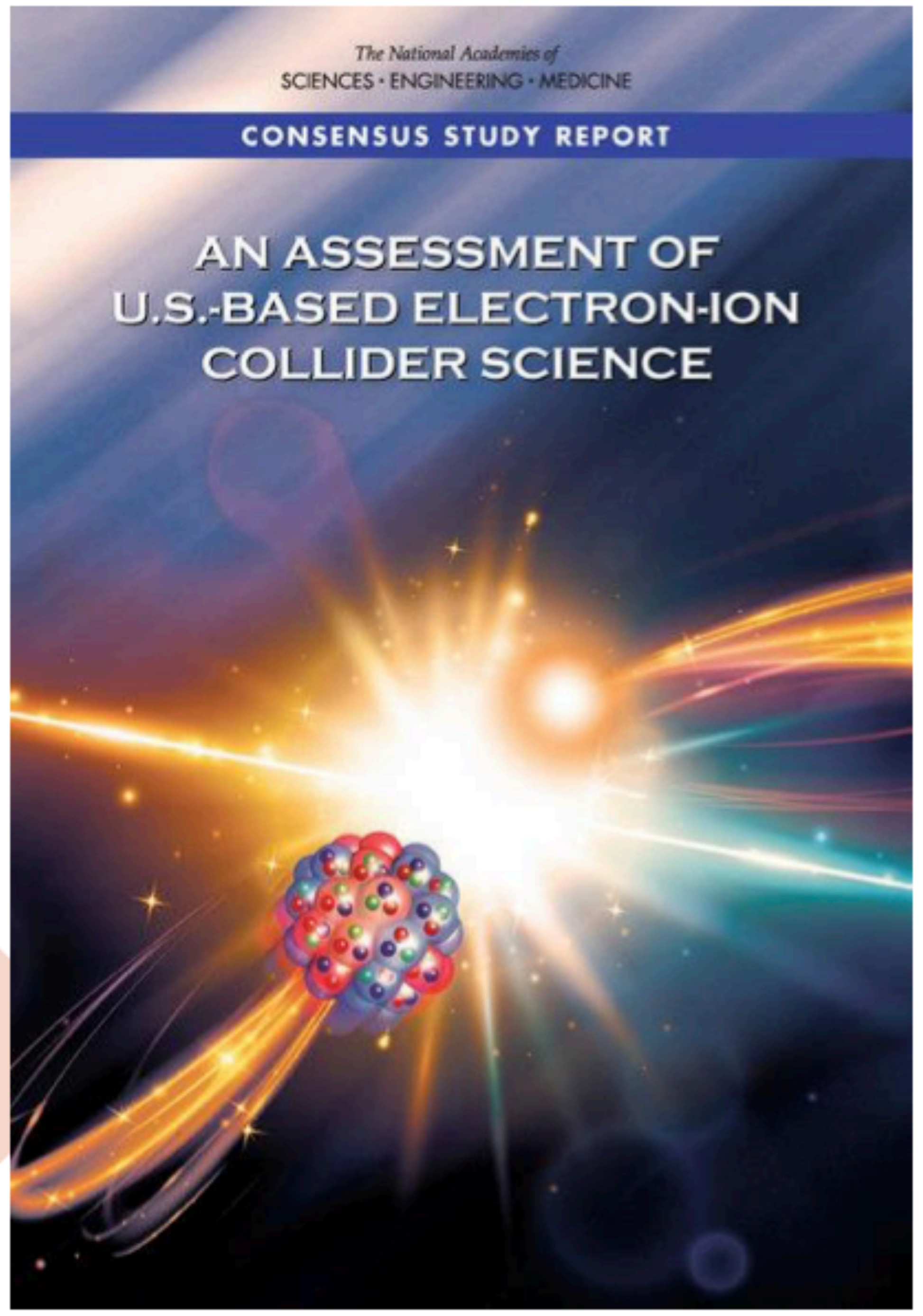

NAS report
July 2018

Science goals of the Electron Ion Collider

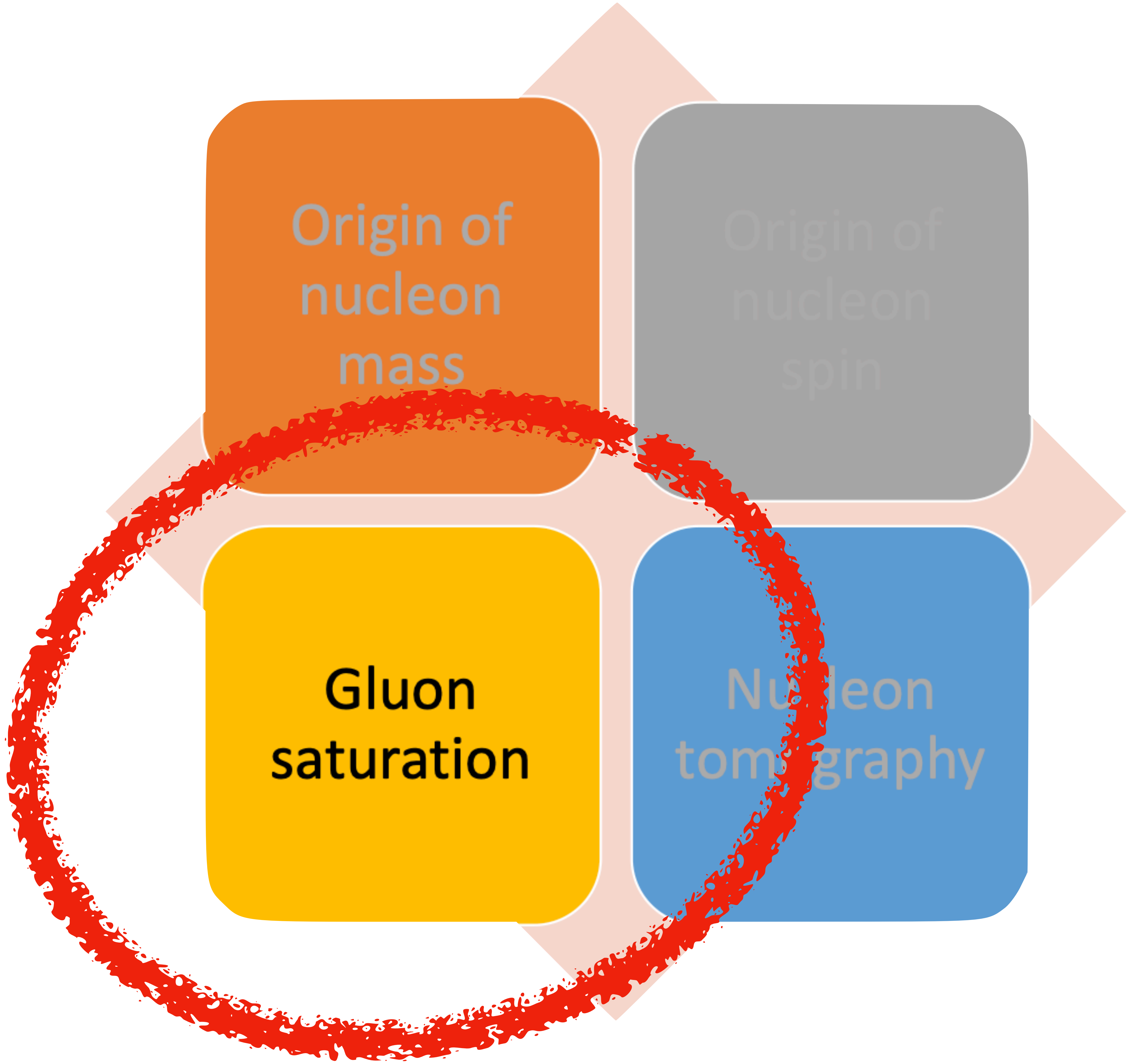

Gluon Saturation

Explosive growth of gluon density would violate unitarity

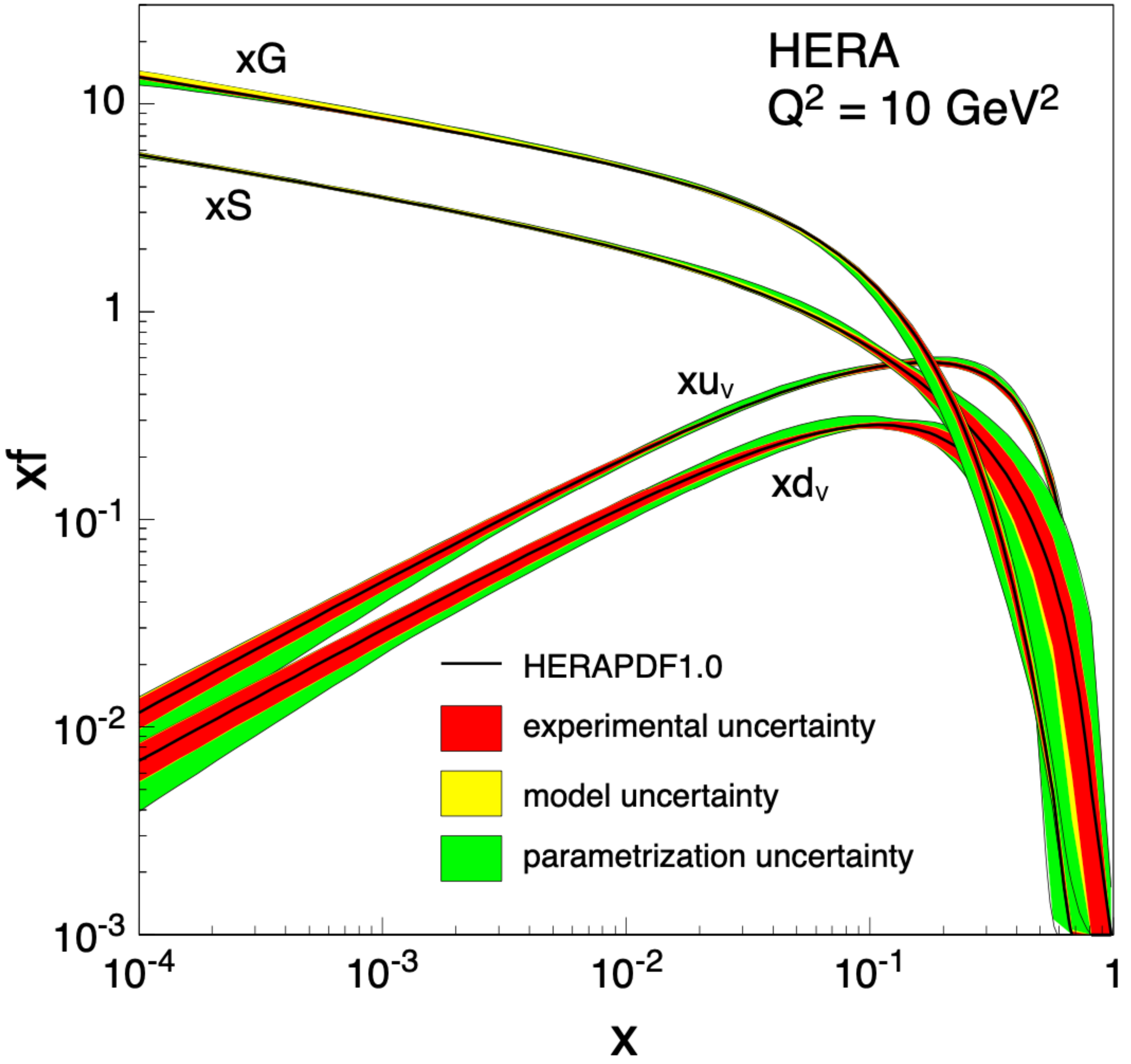

BUT: Recombination will balance gluon splittings

Need non-linear evolution equations at low *x* and low to moderate Q^2

Going to high energy

Two high energy limits: $s \to \infty$ (center of mass energy goes to infinity, $s \propto Q^2/x$)

- Bjorken limit: fixed x, $Q^2 \to \infty$
- Regge-Gribov limit: fixed Q^2, $x \to 0$

- In the Regge-Gribov limit gluons overlap, leading to a maximal occupation number of $1/\alpha_s$
- This bound is saturated for gluons with transverse momenta $k_\perp \leq Q_s$
- $Q_s(x)$ is the "saturation scale"

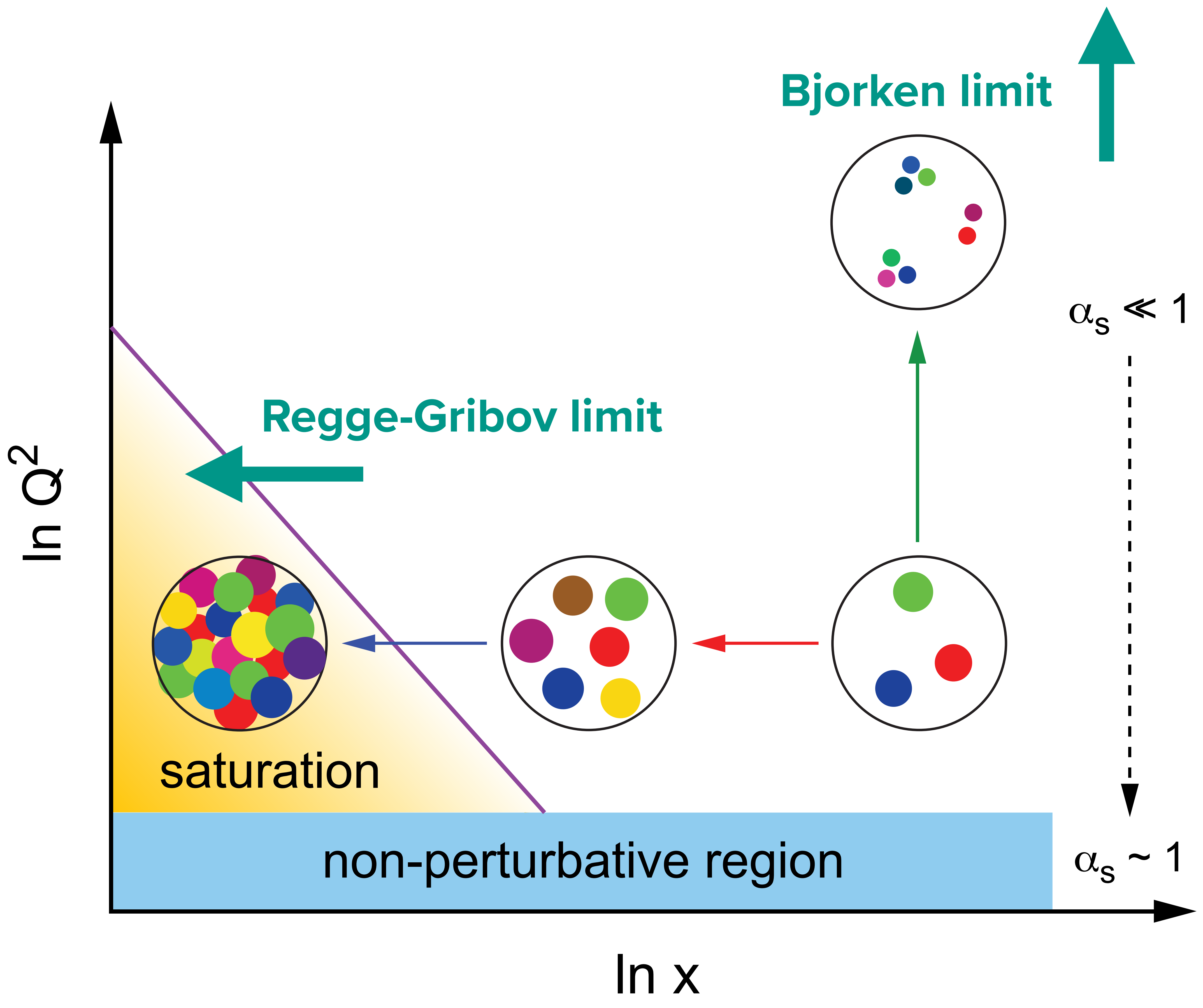

The boosted proton

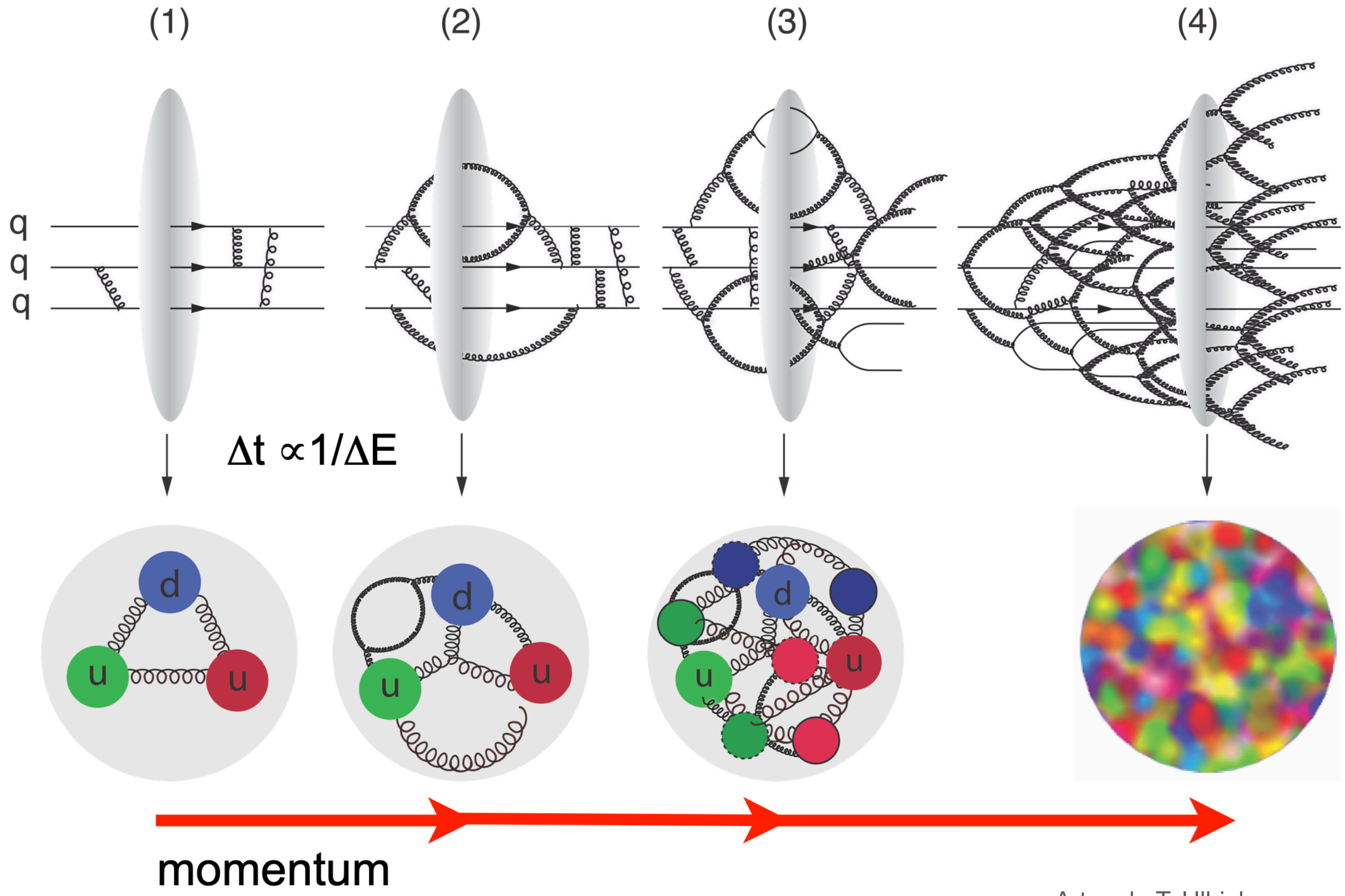

Artwork: T. Ullrich

The boosted proton

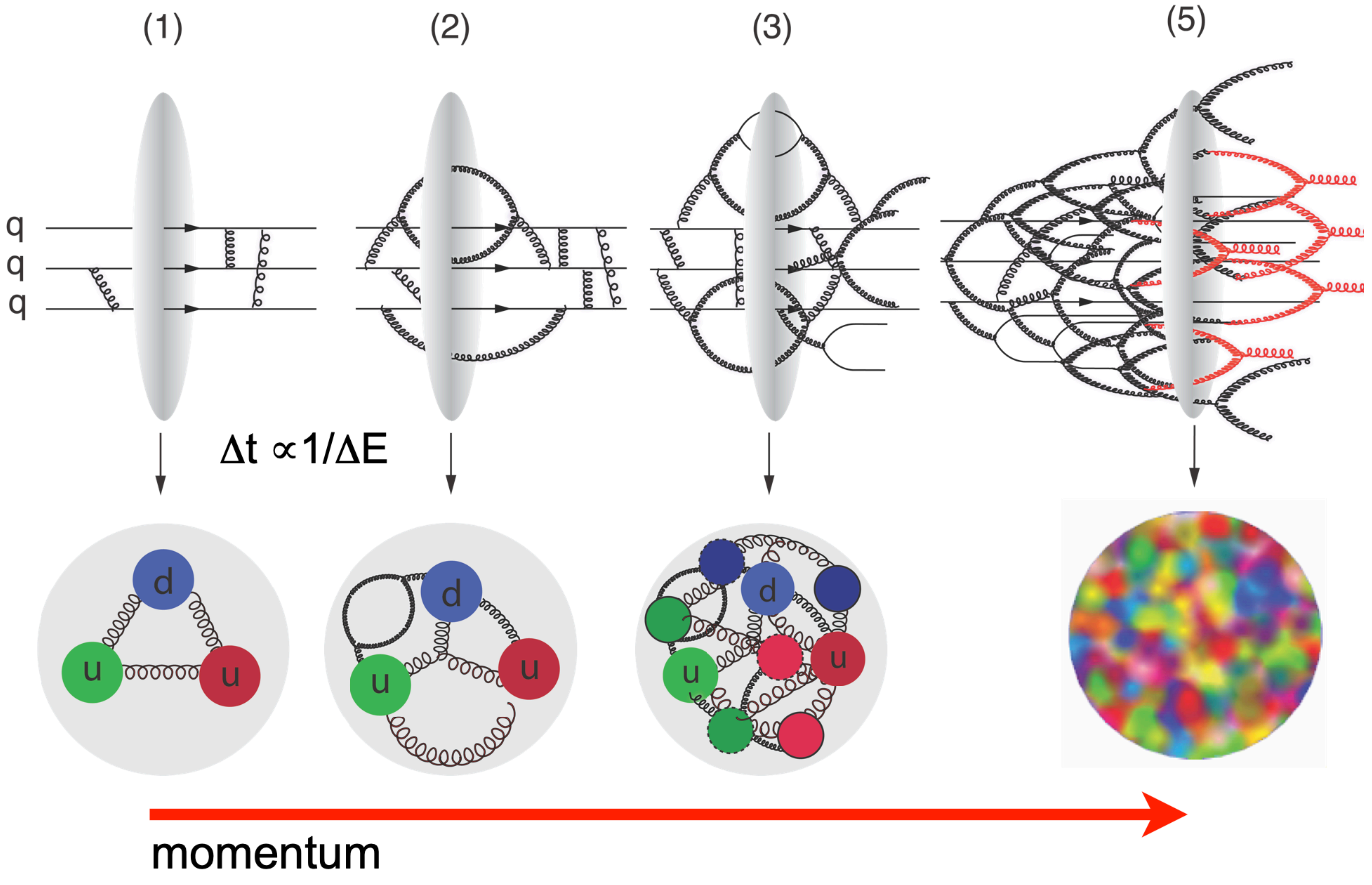

Light cone

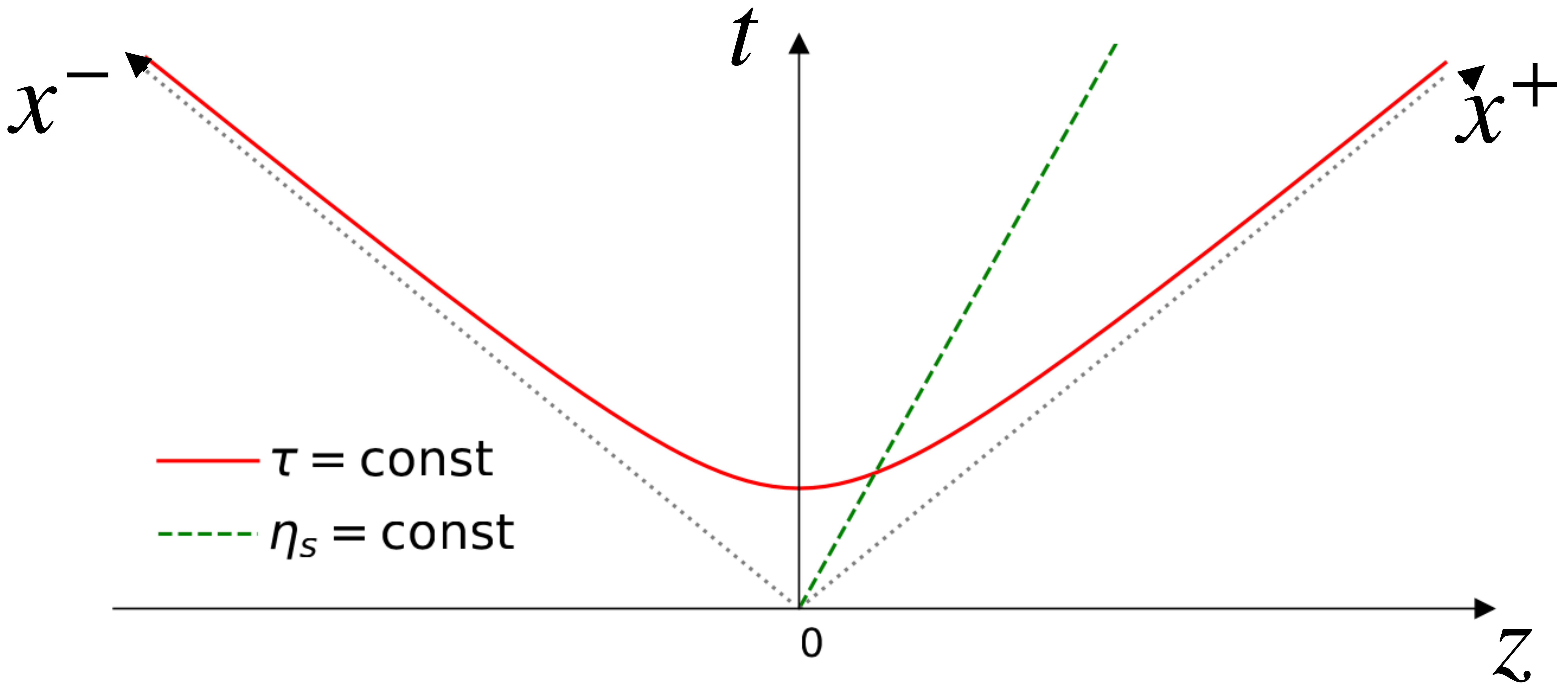

Light cone coordinates $v^{\pm} = (v^0 \pm v^3)/\sqrt{2}$

In the future light cone define $x^+ = \dfrac{\tau}{\sqrt{2}} e^{+\eta}$, and $x^- = \dfrac{\tau}{\sqrt{2}} e^{-\eta}$

or inverted $\tau = \sqrt{2x^+x^-}$, and $\eta = \dfrac{1}{2} \ln\left(\dfrac{x^+}{x^-}\right)$

Light cone

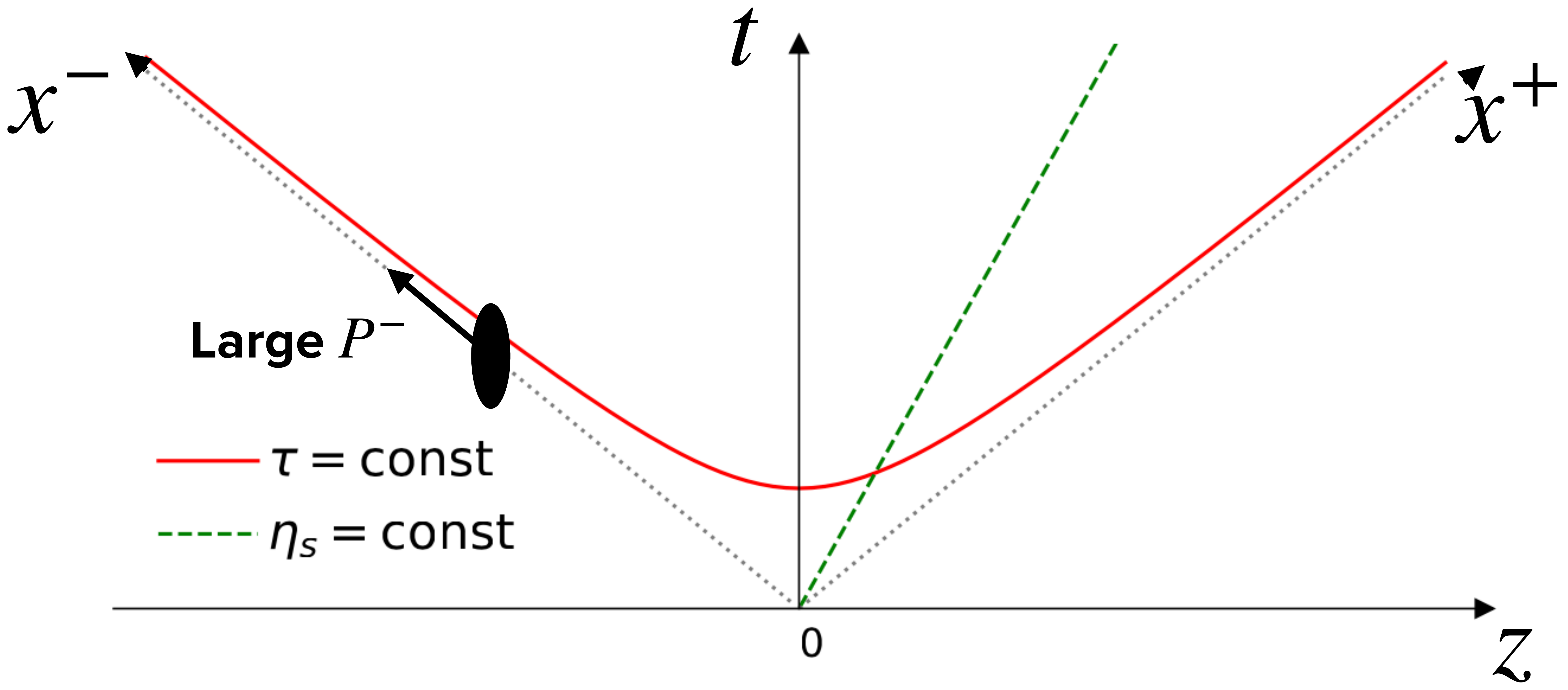

Probe hadron (or nucleus) moving with large P^- at scale $x_0 P^-$ with $x_0 \ll 1$

Separate partonic content based on longitudinal momentum $k^- = xP^-$

Large $x > x_0$: Static and localized color sources ρ

Color sources

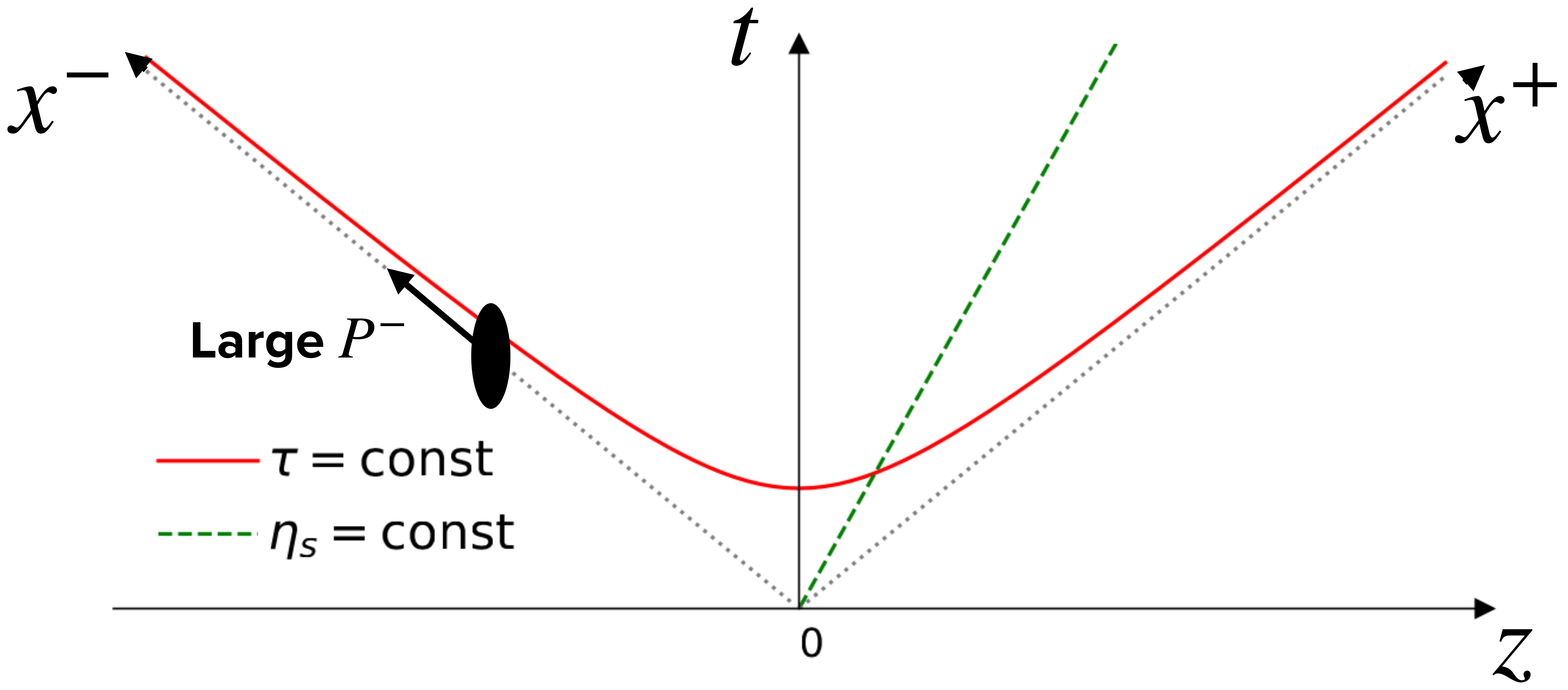

How localized are these sources? $\Delta x^+ \sim \dfrac{1}{k^-} = \dfrac{1}{xP^-}$

What is the resolution scale of the probe? $\dfrac{1}{x_0 P^-} > \dfrac{1}{xP^-}$ **for** $x > x_0$

$\rightarrow$ **Look fully localized in** x^+ **to the probe**

Color sources

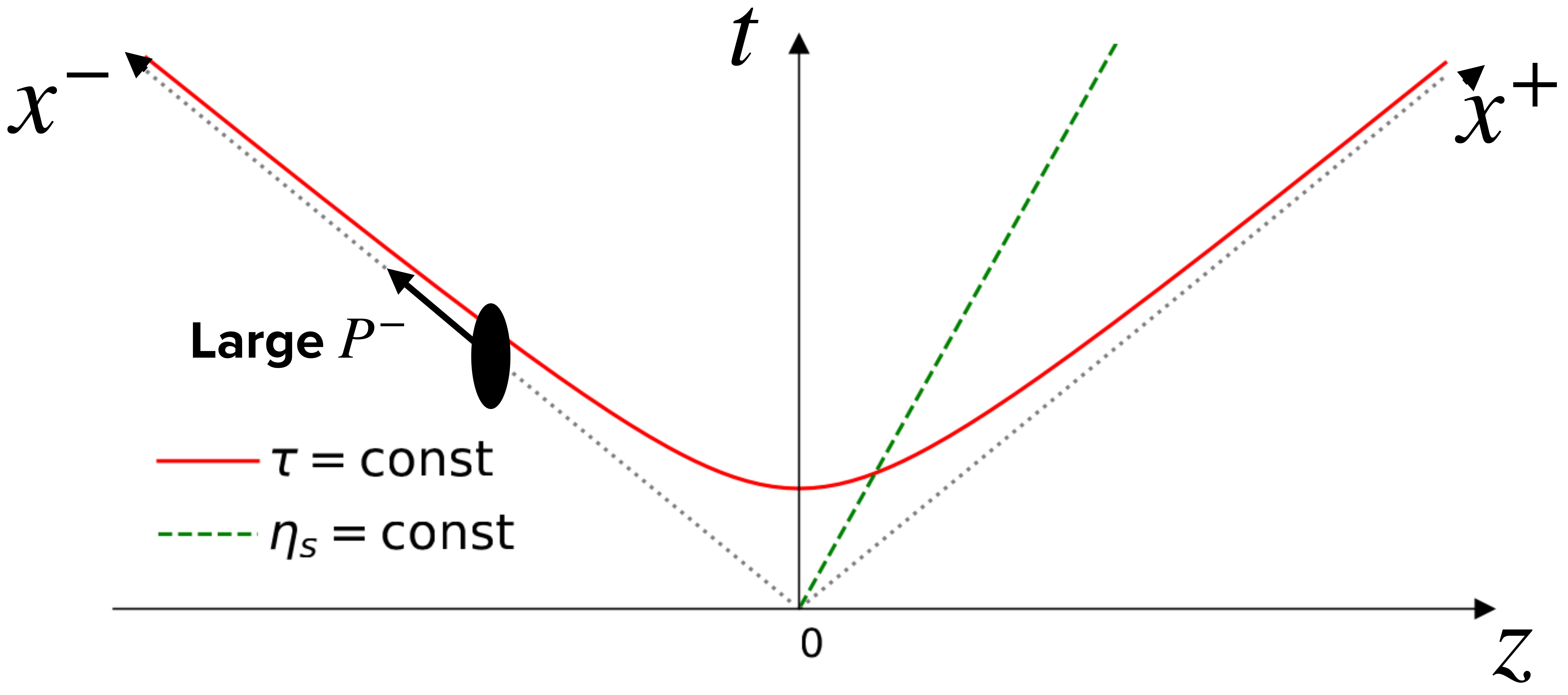

How fast do they evolve? $\Delta x^- \sim \frac{1}{k^+} = \frac{2k^-}{k_T^2} = \frac{2xP^-}{k_T^2}$ **(because** $a_\mu b^\mu = a^+b^- + a^-b^+ - \vec{a}_T \cdot \vec{b}_T$ **)**

What is the time scale of the probe? $\tau \approx \frac{2x_0P^-}{k_T^2} < \frac{2xP^-}{k_T^2}$

$\rightarrow$ **Sources look static to the probe in light cone time** x^-

Dynamic color fields

The moving color sources generate a current, independent of light cone time z^-:

$$J^{\mu,a}(z) = \delta^{\mu-}\rho^a(z^+, z_T)$$

a is the color index of the gluon
the name "color" comes from this

This current generates dynamical fields $A^{\mu,a}(z)$ described by the Yang-Mills equations

$$[D_\mu, F^{\mu\nu}] = J^\nu$$

with $D_\mu = \partial_\mu + igA_\mu$ and $F_{\mu\nu} = \frac{1}{ig}[D_\mu, D_\nu] = \partial_\mu A_\nu - \partial_\nu A_\mu + ig[A_\mu, A_\nu]$ the field strength tensor

These fields are the small $x < x_0$ degrees of freedom

They can be treated classically, because their occupation number is large $\langle AA \rangle \sim 1/\alpha_s$

the name "condensate" comes from this scaling

Color Glass Condensate: Sources and fields

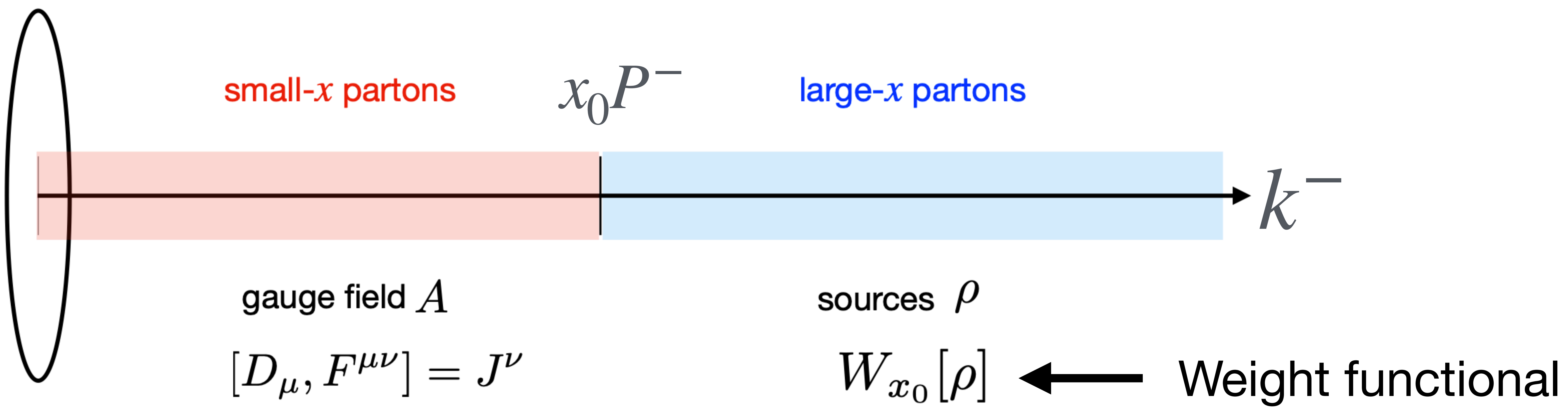

Two steps to compute expectation value of an observable $\mathcal{O}$:

1) Compute quantum expectation value $\mathcal{O}[\rho] = \langle \mathcal{O} \rangle_\rho$ for sources drawn from a given $W_{x_o}[\rho]$

2) Average over all possible configurations given the appropriate gauge invariant weight functional $W_{x_o}[\rho]$ this situation is similar to spin glasses - the name “glass” comes from this

When $x \lesssim x_0$ the path integral $\langle \mathcal{O} \rangle_\rho$ is dominated by classical solution and we are done

For smaller x we need to do quantum evolution

Weight functional

https://arxiv.org/pdf/hep-ph/0406169.pdf

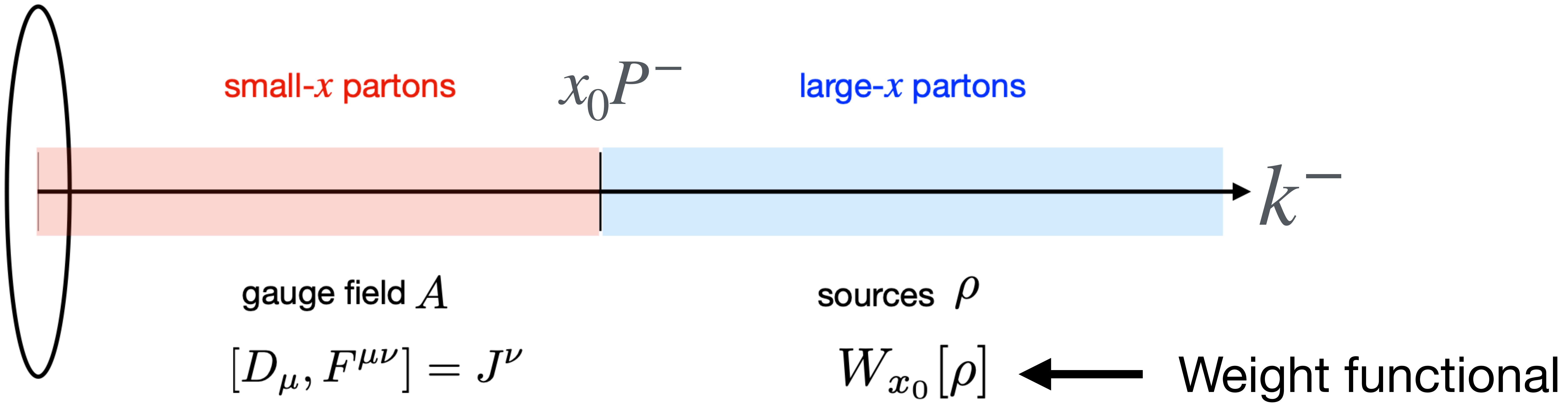

What is the weight functional?

Usually we need to model. E.g. the McLerran-Venugopalan model:

Assume a large nucleus, invoke central limit theorem. All correlations of ρ^a are Gaussian

$$W_{x_0}[\rho] = \mathcal{N} \exp\left(-\frac{1}{2} \int dx^+ d^2x_T \frac{\rho^a(x^+, x_T)\rho^a(x^+, x_T)}{\lambda_{x_0}(x^+)} \right)$$

where $\lambda_{x_0}(x^+)$ is related to the transverse color charge density distribution of the nucleus

Weight functional

https://arxiv.org/pdf/hep-ph/0406169.pdf

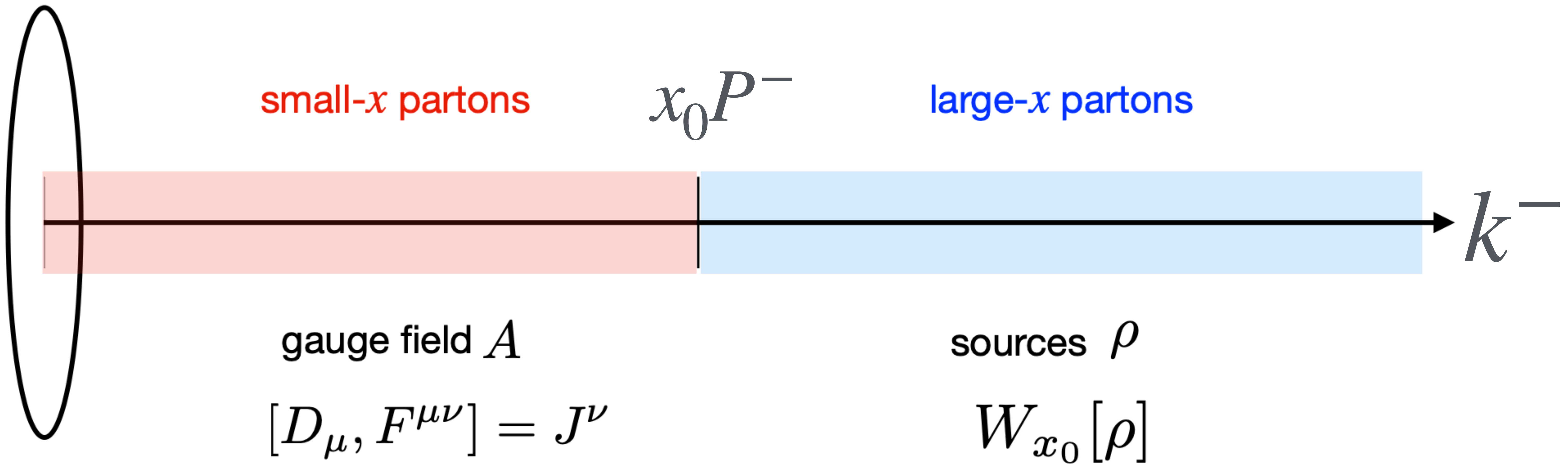

…where $\lambda_{x_0}(x^+)$ is related to the transverse color charge density distribution of the nucleus

$$\mu^2 = \int dx^+ \lambda_{x_0}(x^+) = \frac{(g^2 C_F)(A N_c)}{\pi R_A^2} \frac{1}{N_c^2 - 1} = \frac{g^2 A}{2\pi R_A^2} \sim A^{1/3}$$

normalized per color degree of freedom

We used that color charge squared of a quark is $g^2 t^a t^a = g^2 C_F$

That color charge density is related to Q_s, the saturation scale.

Wilson lines

Interaction of high energy color-charged particle with large k^+ momentum (and small $k^- = \dfrac{k_T^2}{2k^+}$)

with classical field of a nucleus can be described in the **eikonal approximation:**

The scattering rotates the color, but keeps k^+, transverse position $\vec{x}_T$, and any other quantum numbers the same.

The color rotation is encoded in a light-like Wilson line, which for a quark reads

$$V_{ij}(\vec{x}_T) = \mathscr{P} \exp\left(-ig \int_{-\infty}^{\infty} A_c^-(z^+, \vec{x}_T)\, t_{ij}^c\, dz^+ \right)$$

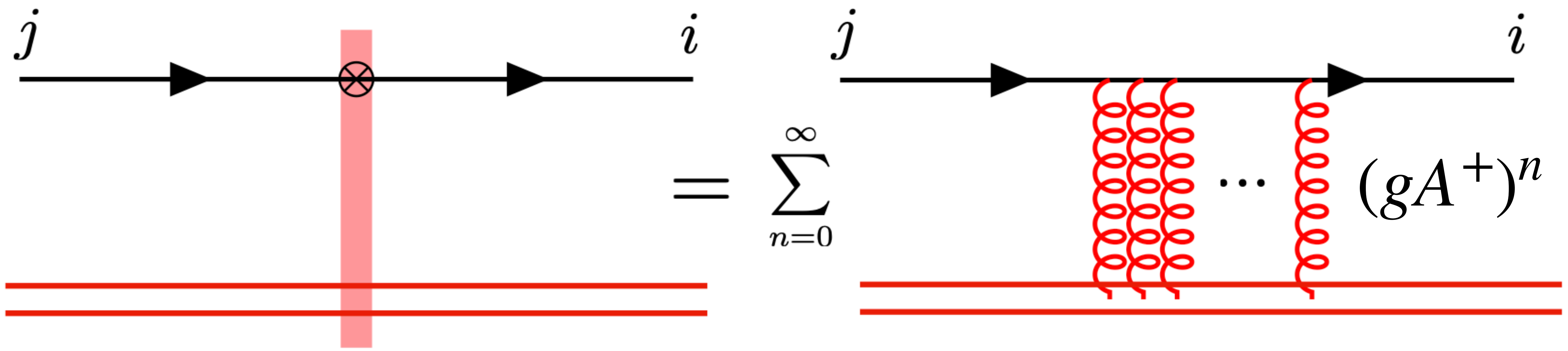

MULTIPLE INTERACTIONS NEEDED TO BE RESUMMED, BECAUSE
$A^- \sim 1/g$

Wilson lines

Interaction of high energy color-charged particle with large k^+ momentum (and small $k^- = \dfrac{k_T^2}{2k^+}$)

with classical field of a nucleus can be described in the **eikonal approximation:**

The scattering rotates the color, but keeps k^+, transverse position $\vec{x}_T$, and any other quantum numbers the same.

The color rotation is encoded in a light-like Wilson line, which for a quark reads

$$V_{ij}(\vec{x}_T) = \mathscr{P} \exp\left(-ig \int_{-\infty}^{\infty} A_c^-(z^+, \vec{x}_T)\, t_{ij}^c\, dz^+ \right)$$

path ordering

SU(3) generator (fundamental rep.)

Wilson lines and correlators

$$U_{ab}(\vec{x}_T) = \mathscr{P} \exp\left(-ig \int_{-\infty}^{\infty} A_c^-(z^+, \vec{x}_T)\, T^c_{ab}\, dz^+ \right)$$ gluon scattering

$$V_{ij}(\vec{x}_T) = \mathscr{P} \exp\left(-ig \int_{-\infty}^{\infty} A_c^-(z^+, \vec{x}_T)\, t^c_{ij}\, dz^+ \right)$$ quark scattering

These Wilson lines are the building blocks of the CGC. At the EIC for example, cross sections will be calculated as convolutions of Wilson line correlators with perturbatively calculable and process dependent impact factors

In heavy ion collisions, one can compute particle production by determining Wilson lines after the collision from the Wilson lines of the colliding nuclei.

COMPUTING PHYSICAL PROCESSES

Interactions depend on operators consisting of the Wilson lines

For example: e + A → e + A + vector meson (**exclusive** vector meson production)

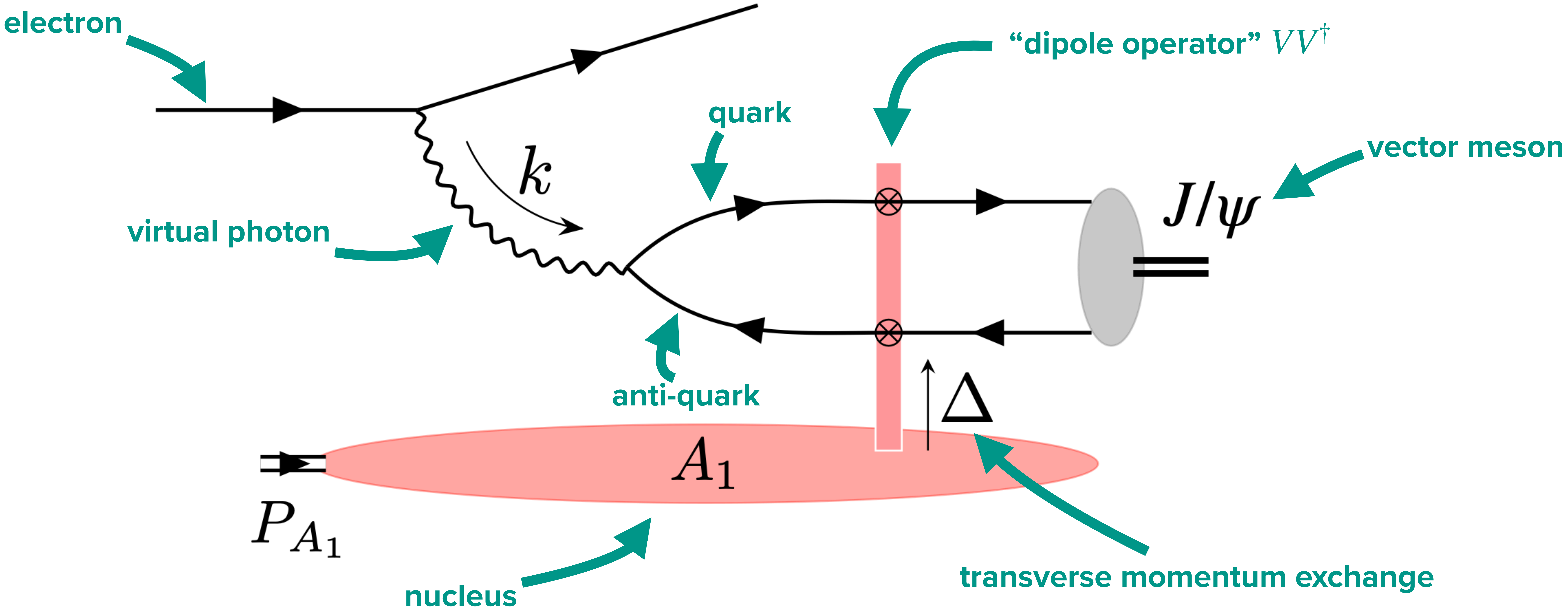

COMPUTING PHYSICAL PROCESSES

Can compute many other processes, for example:

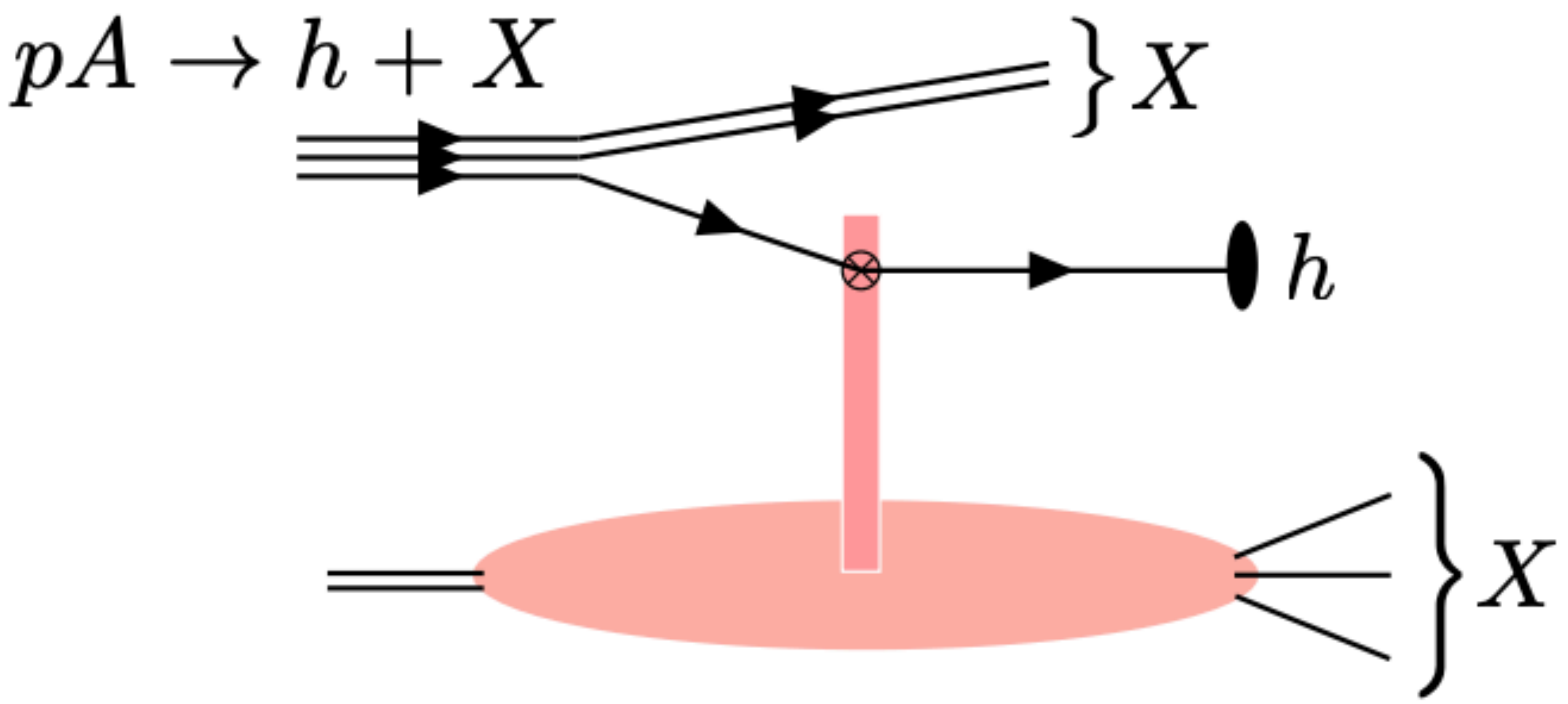

Hadron production in proton + nucleus collisions

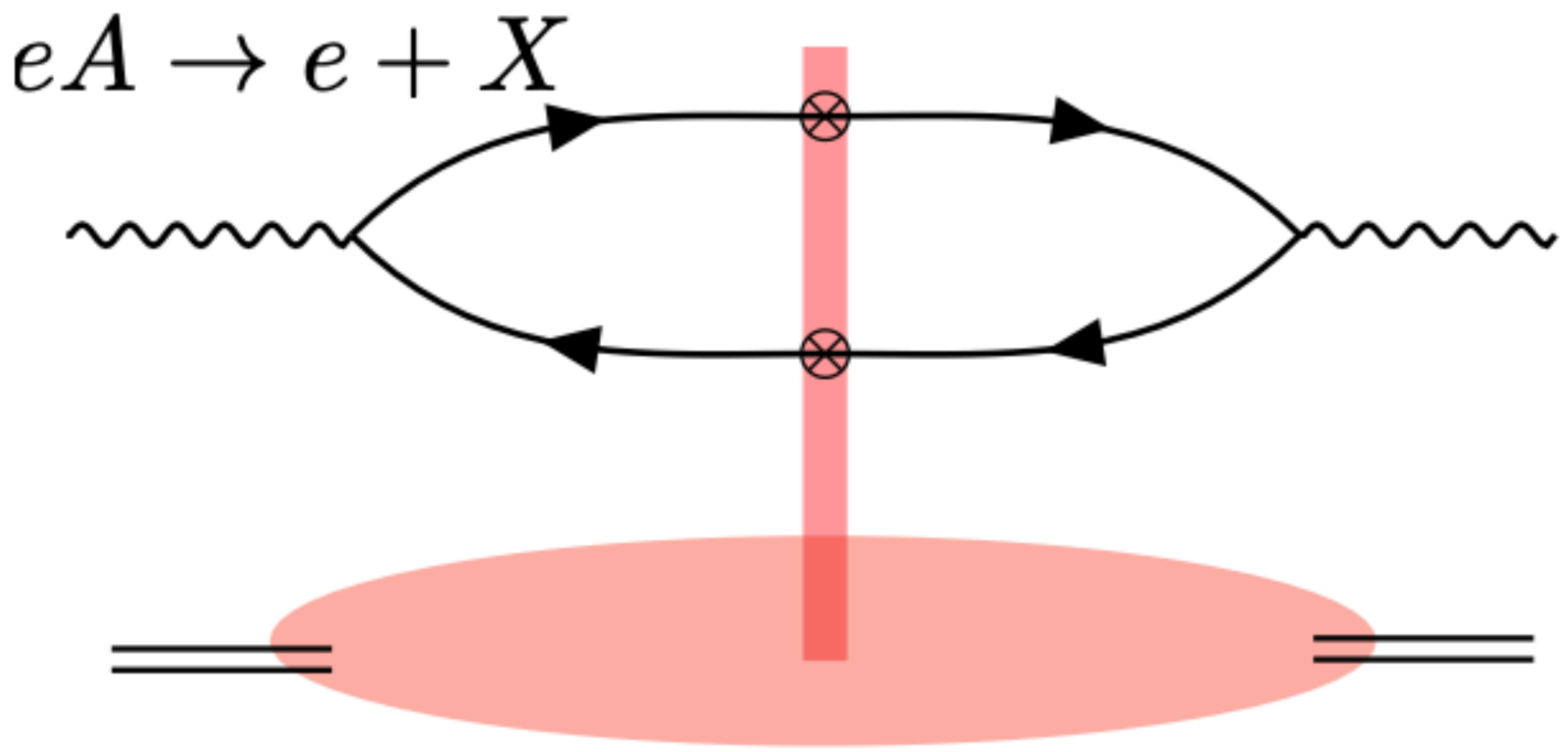

Inclusive e+A scattering

Can even use the gluon fields of nuclei computed in the CGC
as initial state for heavy-ion collisions

DIPOLE AMPLITUDE

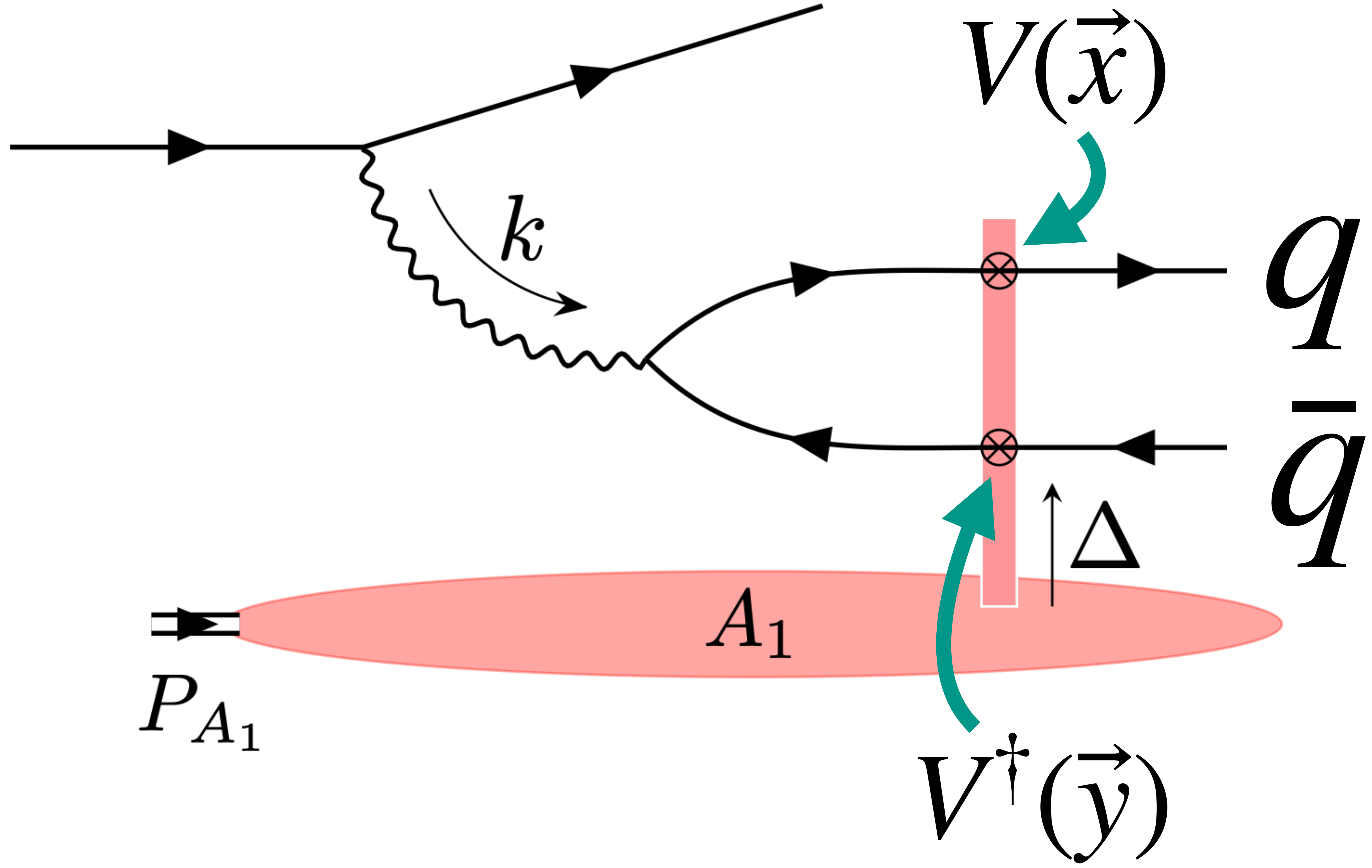

$\Rightarrow$

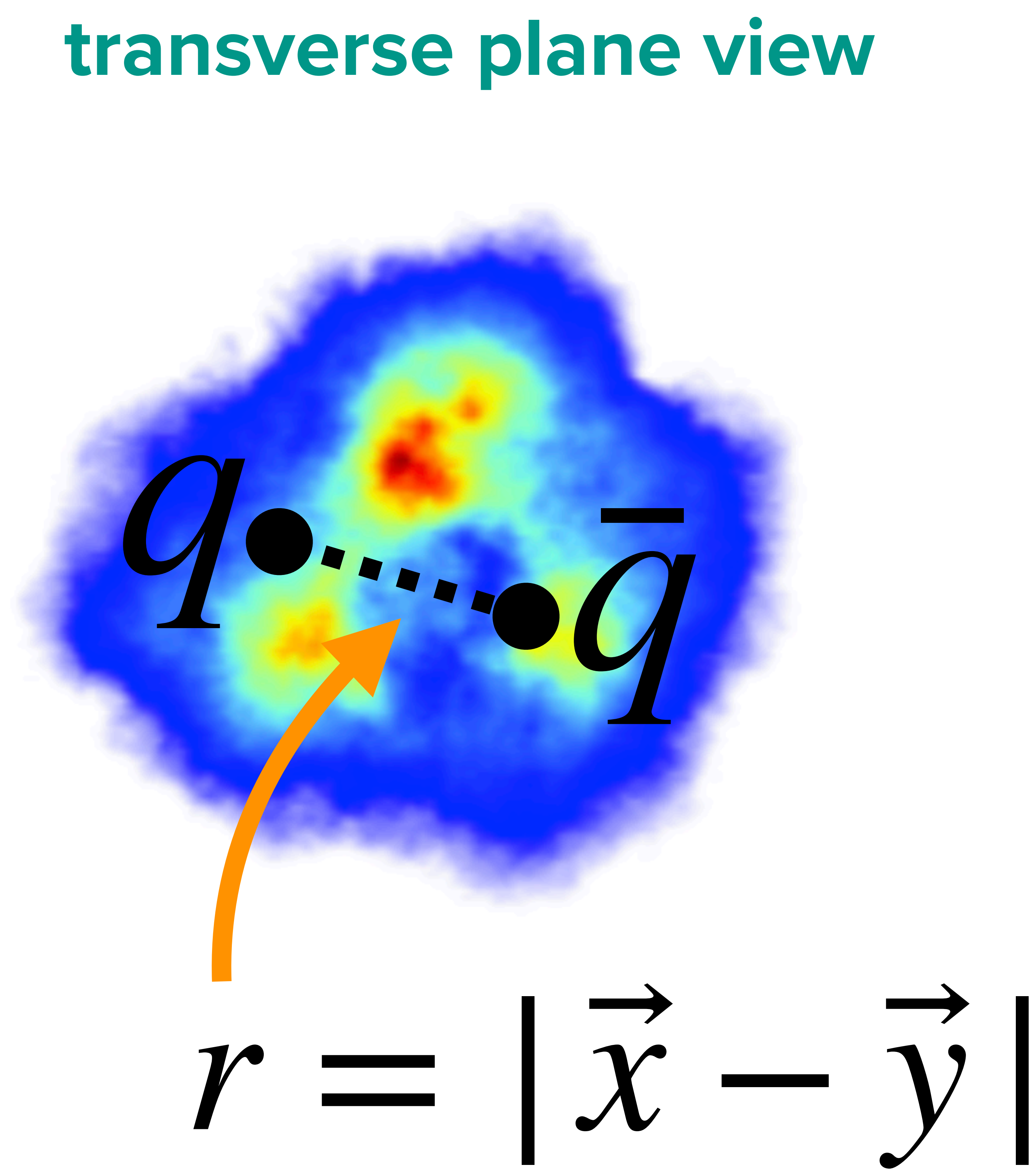

Is this one event we measure? No! We measure in momentum space.
Cross section in momentum space involves an average over all such configurations in coordinate space

DIPOLE AMPLITUDE

trace is over color (Wilson lines are color matrices)

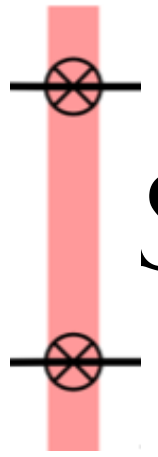

Dipole correlator $S = \langle \mathrm{Tr}[V(\vec{x})V^{\dagger}(\vec{y})] \rangle / N_c$ appears in many scattering processes

$1/3 \; tr\left(V(0)V^{\dagger}(r_{\perp})\right)$

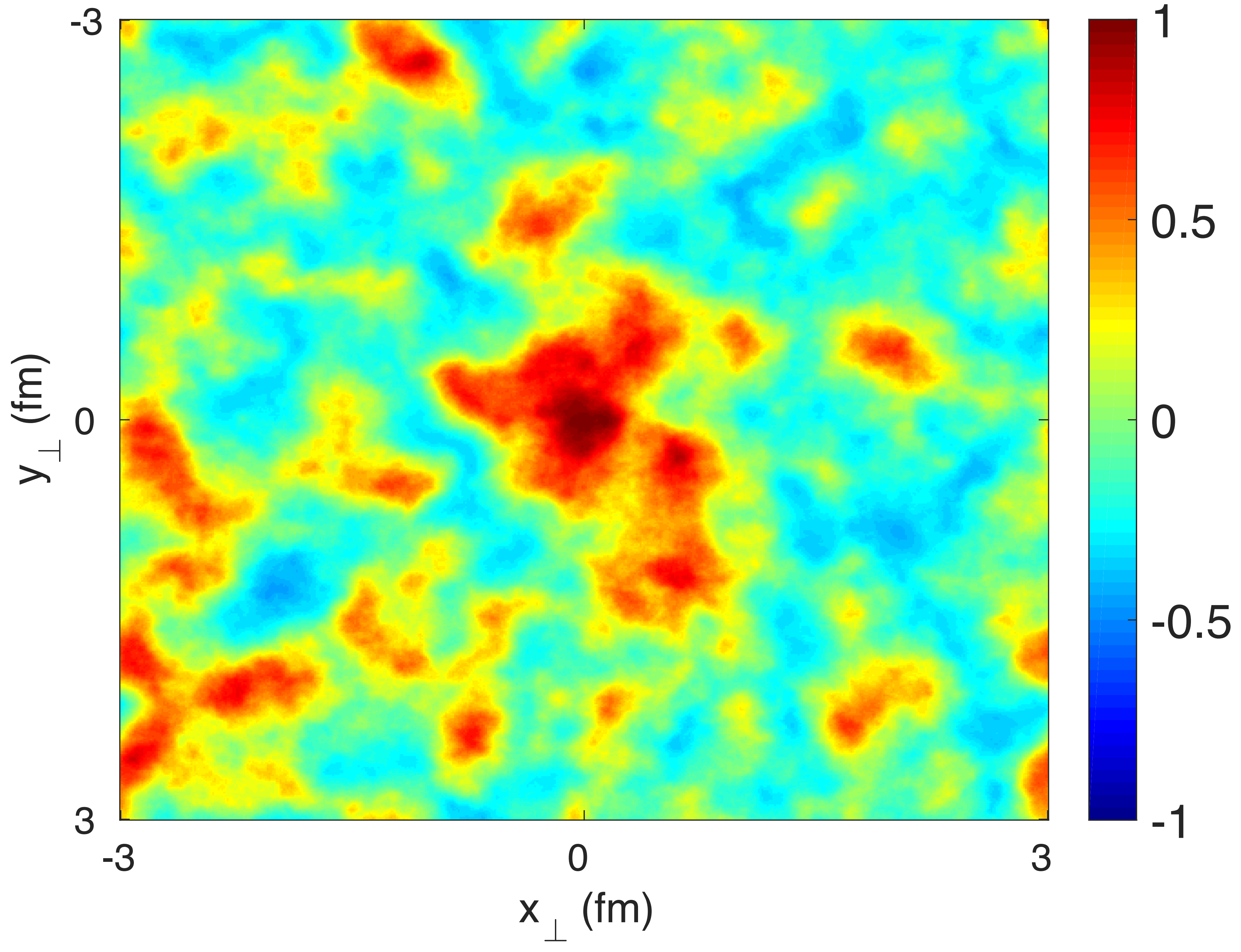

One color charge configuration

$1/3 \left\langle tr\left(V(0)V^{\dagger}(r_{\perp})\right) \right\rangle$

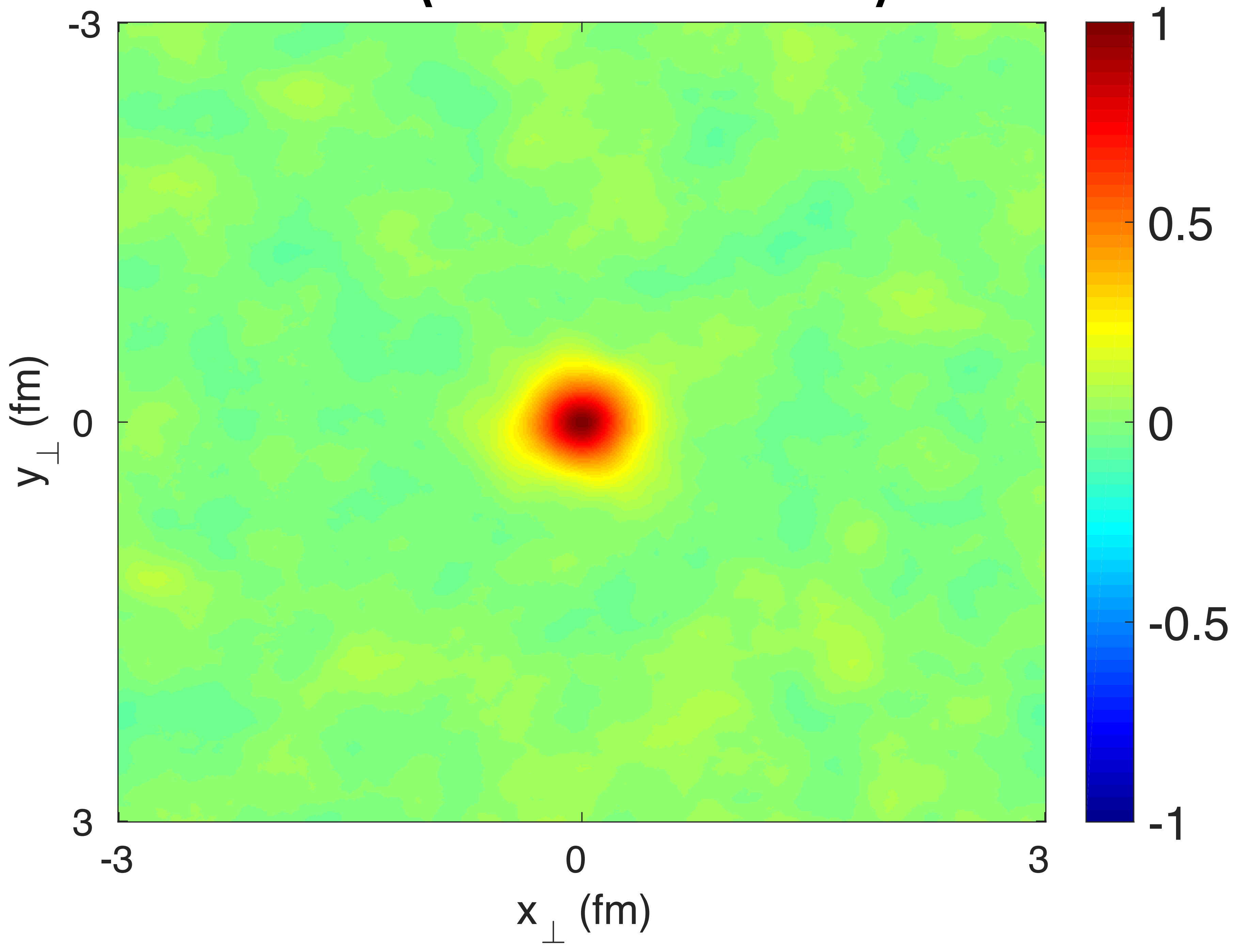

Averaged over 70 color charge configurations

DIPOLE AMPLITUDE

$$1/3 \left\langle tr\left(V(0)V^{\dagger}(r_{\perp})\right)\right\rangle$$

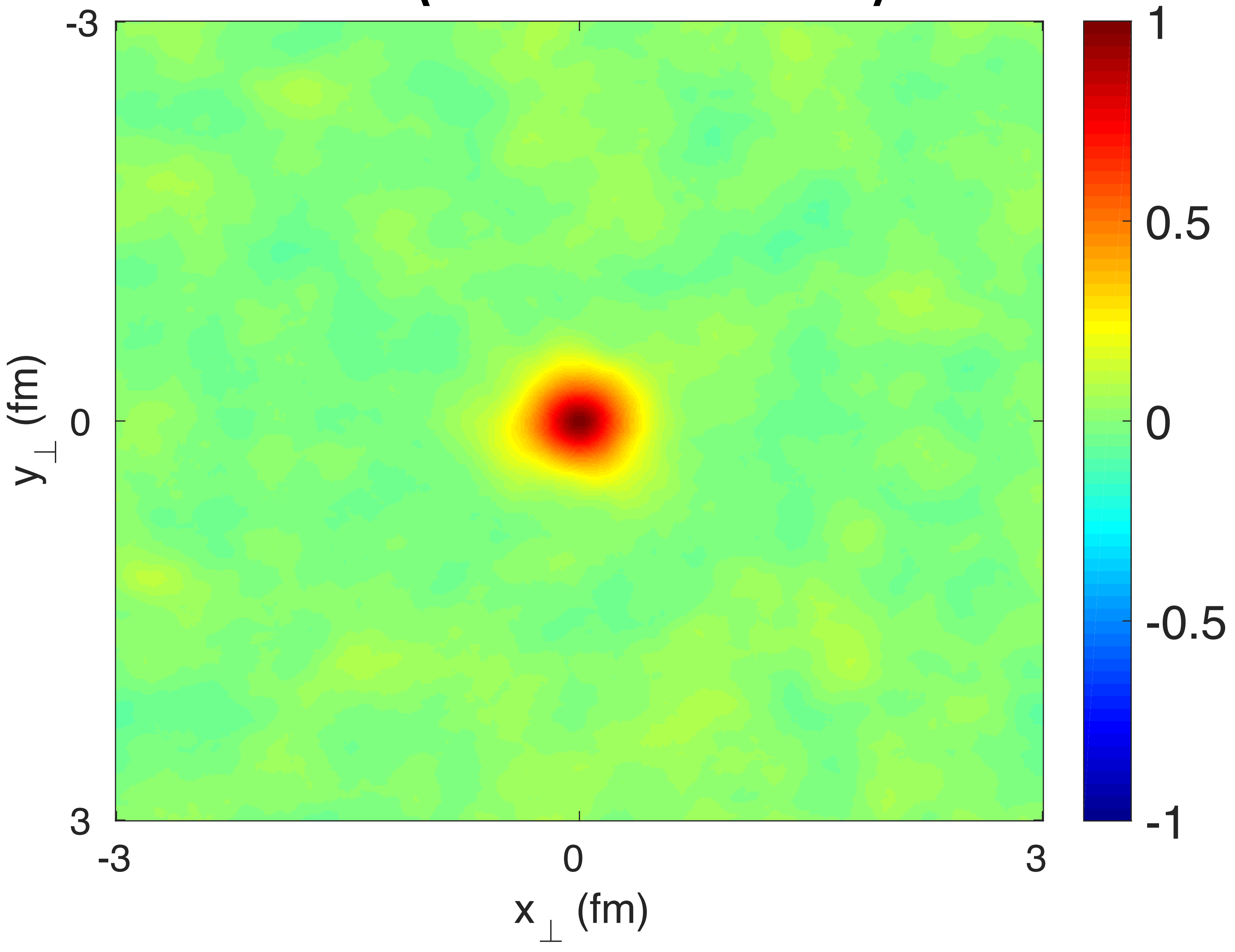

$$\equiv S$$

like a probability amplitude for no scattering

$\Rightarrow$ $N = 1 - S$

defines Q_s (two examples)

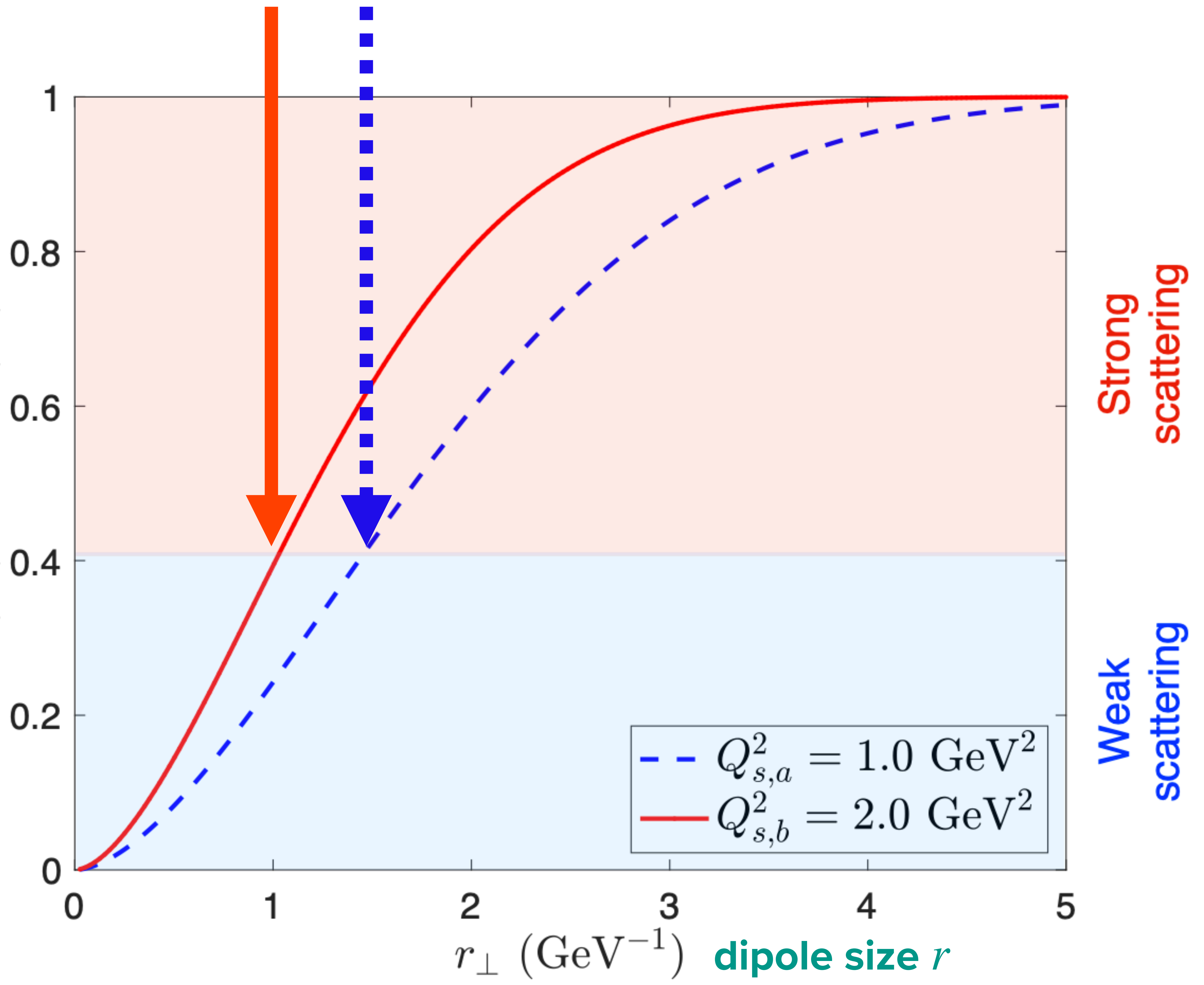

THE SATURATION SCALE

$N = 1 - S$

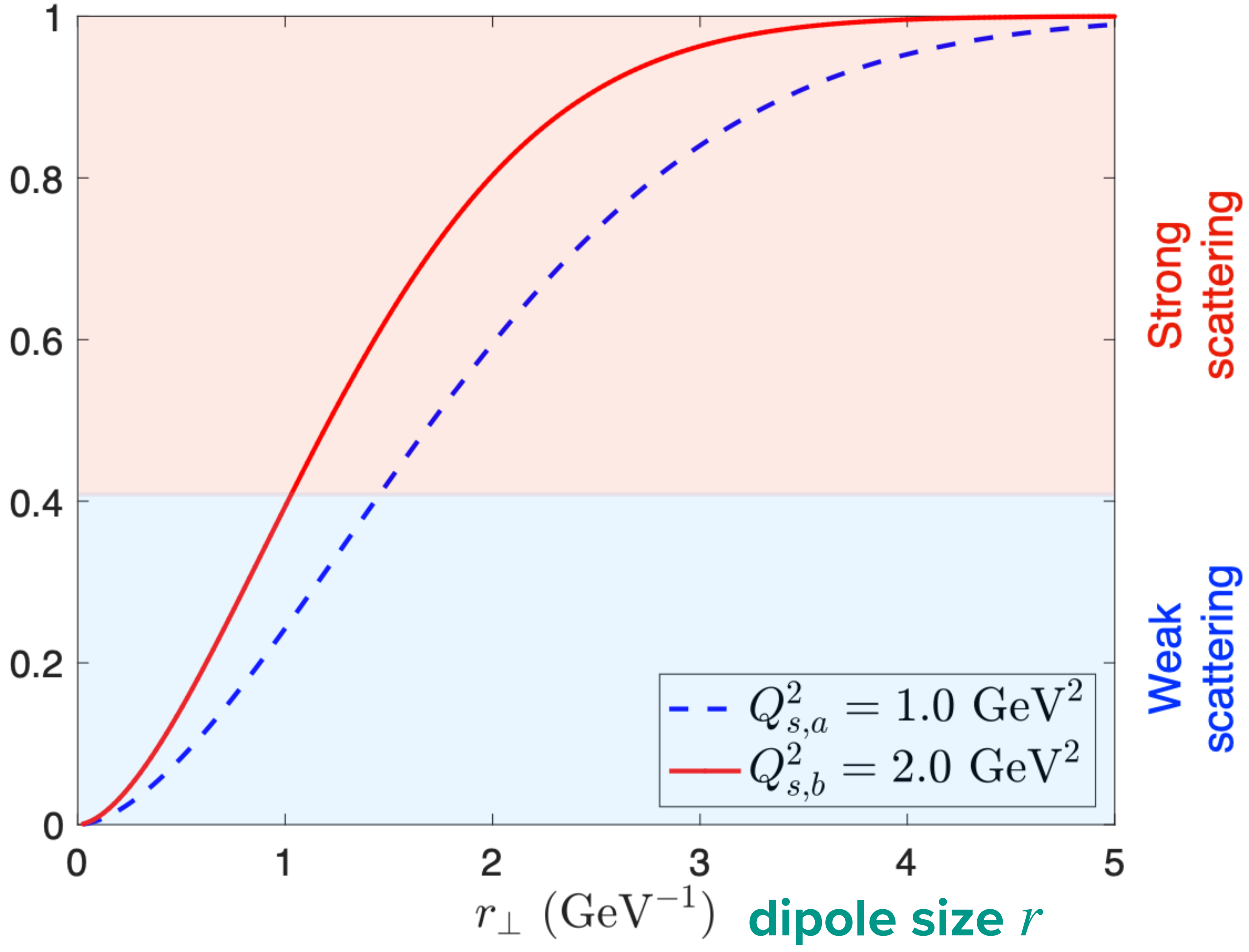

dipole size r

Fourier transform

$\Rightarrow$

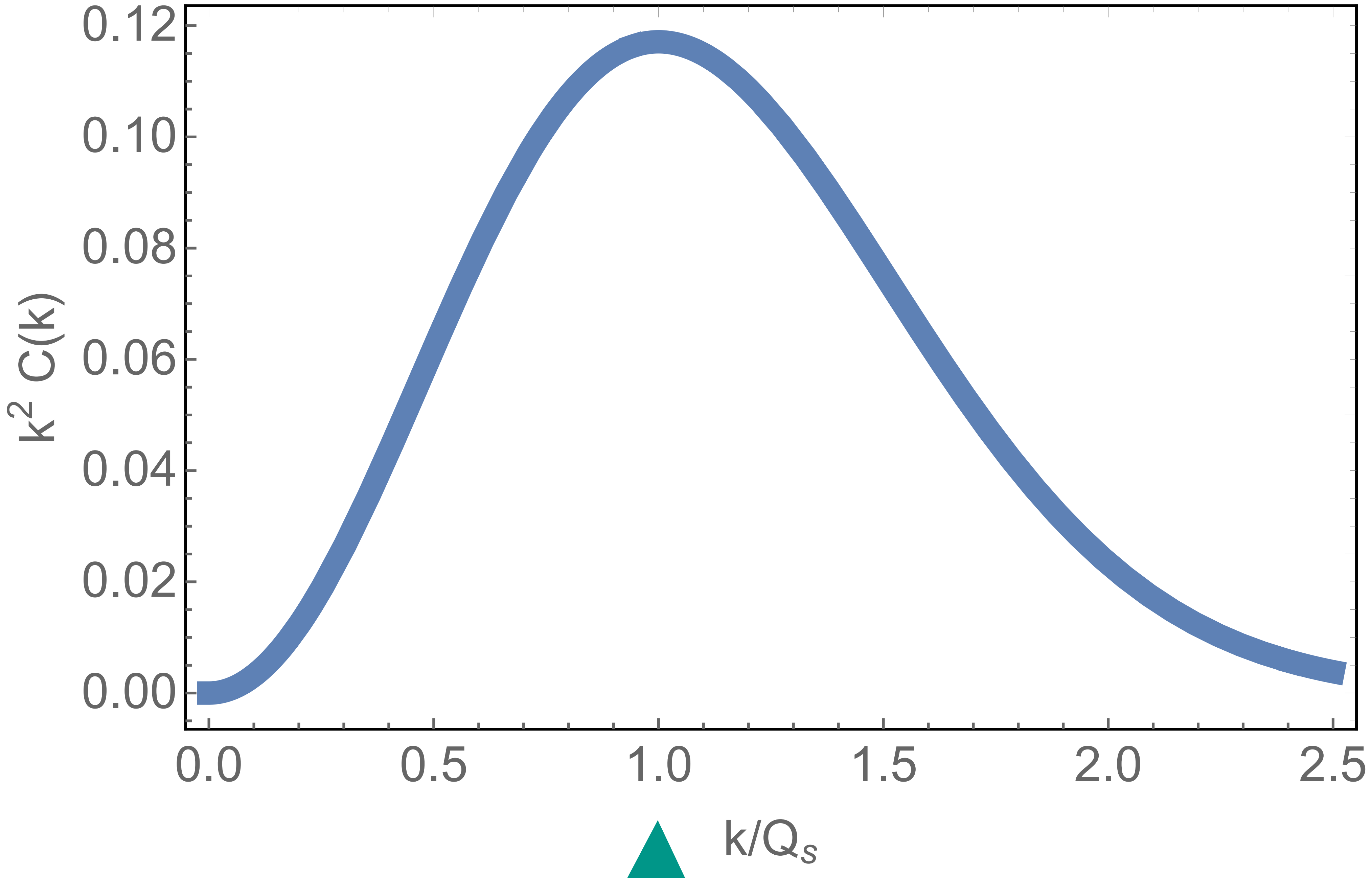

typical momentum $k = Q_s$

EVOLUTION TOWARDS SMALL x - MORE ON THAT LATER

Small-x evolution can be solved numerically. Balitsky-Kovchegov (BK) equation or JIMWLK solved in Langevin form:

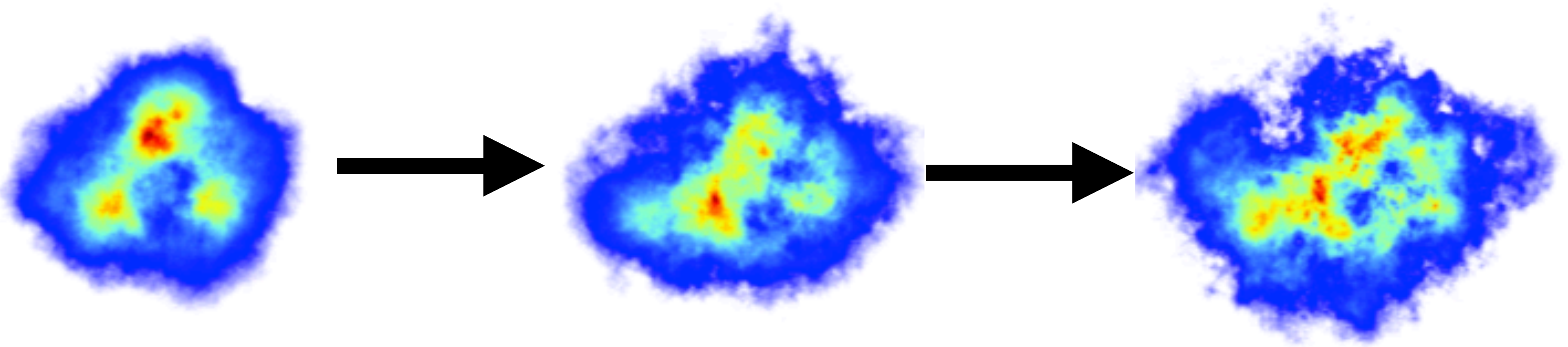

$x \approx 0.01$ $x \approx 0.001$

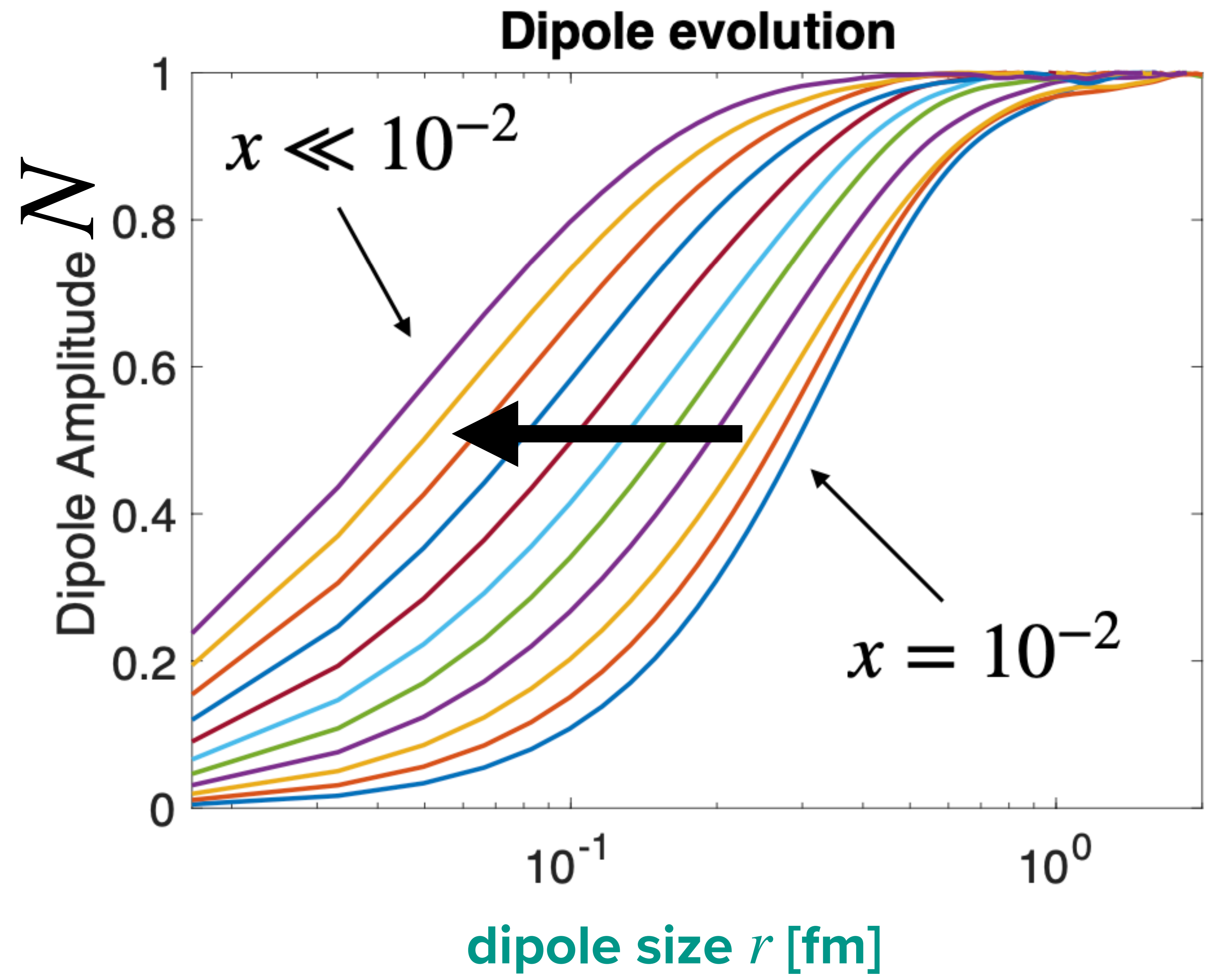

- Evolution leads to growth of typical transverse momentum scale $Q_s(x)$
- The typical correlation length in transverse space decreases $\sim 1/Q_s$
- Proton grows, gluon number increases

SATURATION EFFECTS ON OBSERVABLES

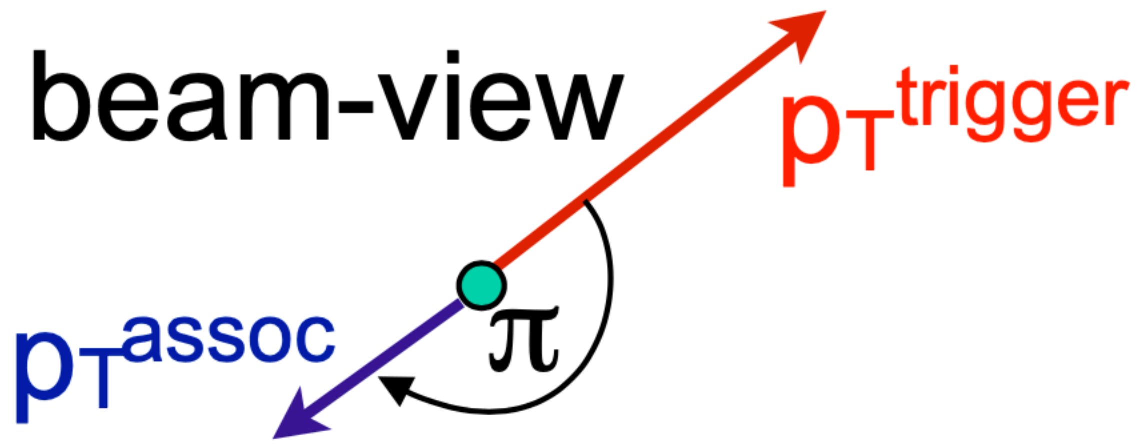

C. Marquet, B. -W. Xiao and F. Yuan, Phys. Lett. B 682 (2009) 207
L. Zheng, E.C. Aschenauer, J.H. Lee, Bo-Wen Xiao, Phys. Rev. D 89, 074037 (2014)

Double inclusive DIS:
Back-to-back peak suppressed more in larger nuclei as momentum imbalance $\sim Q_s$

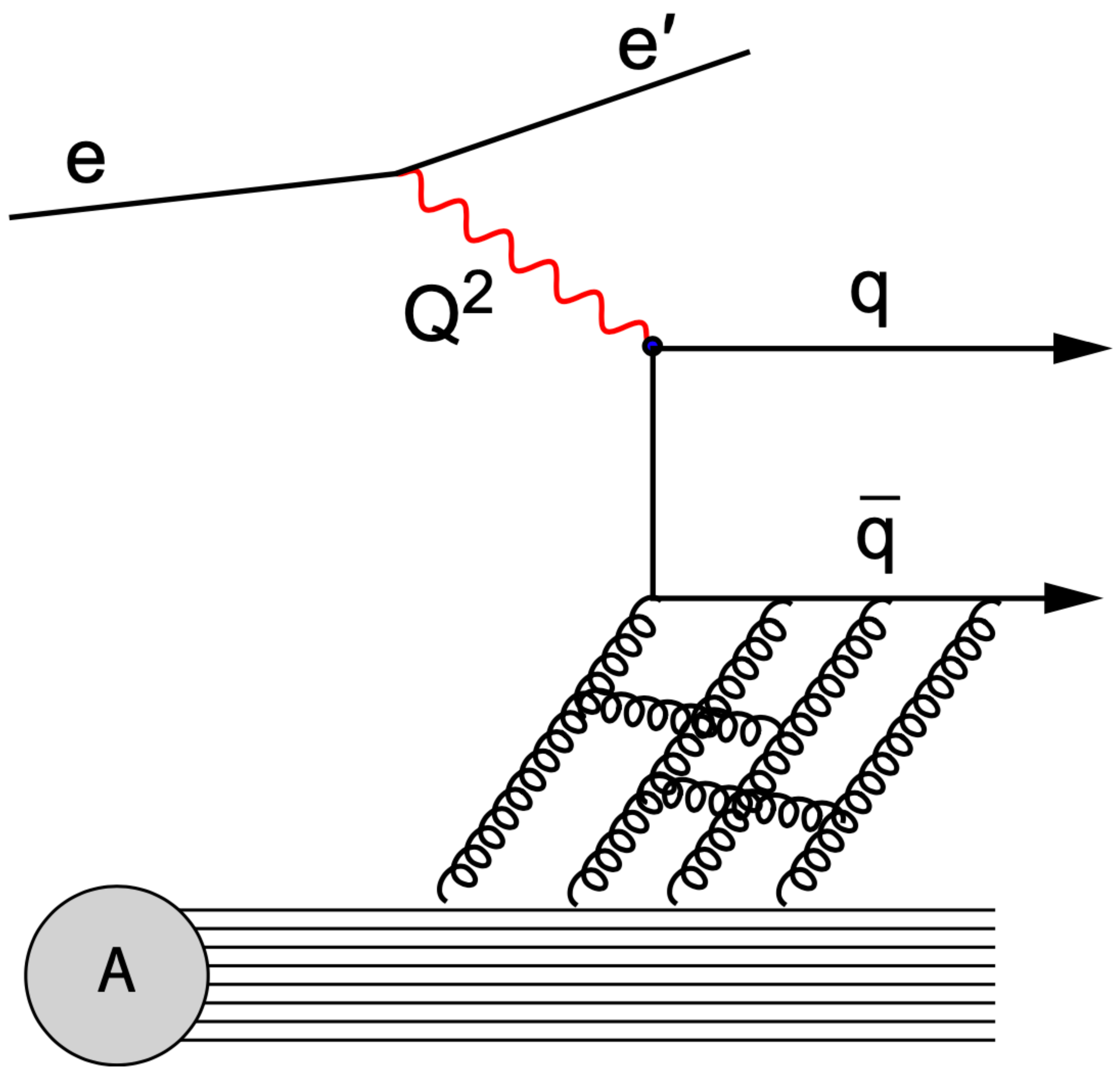

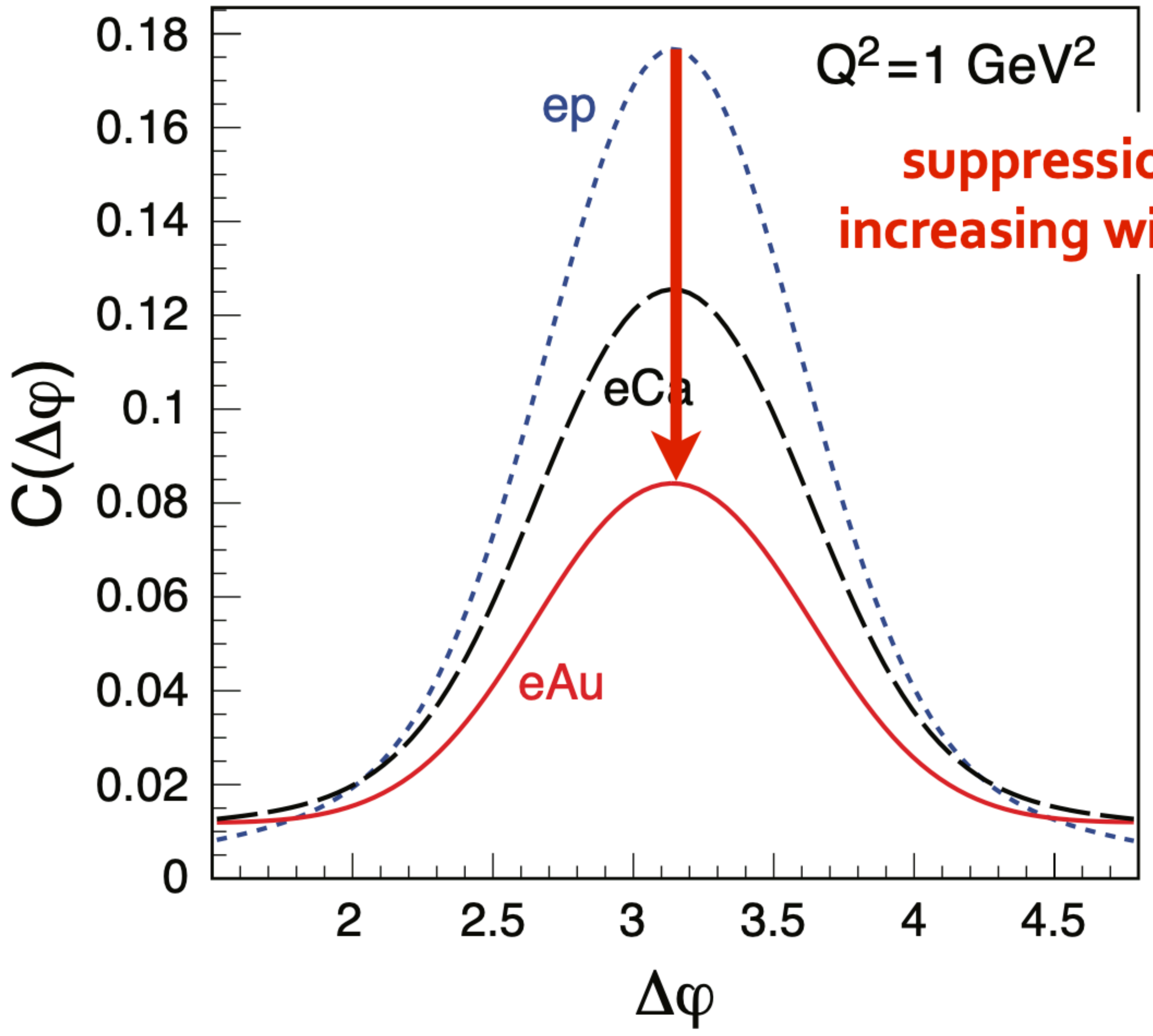

SATURATION EFFECTS ON OBSERVABLES

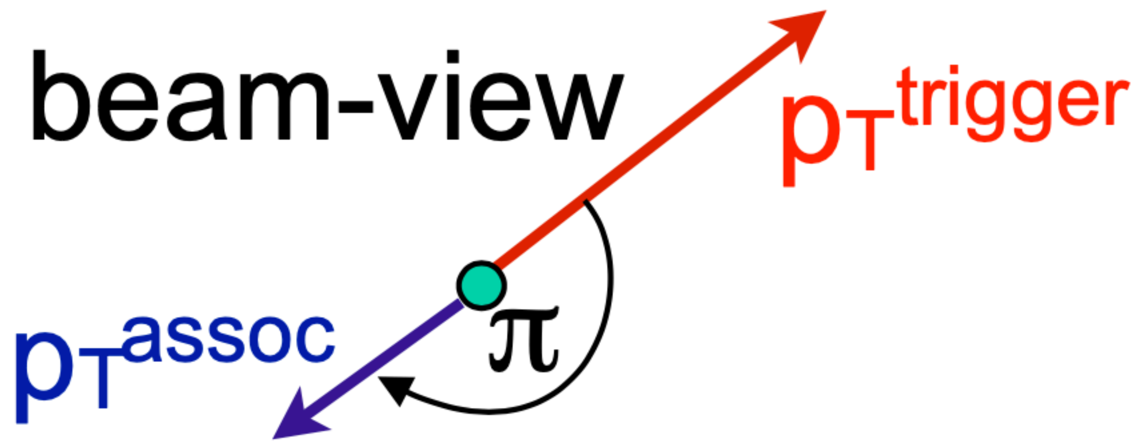

C. Marquet, B. -W. Xiao and F. Yuan, Phys. Lett. B 682 (2009) 207
L. Zheng, E.C. Aschenauer, J.H. Lee, Bo-Wen Xiao, Phys. Rev. D 89, 074037 (2014)

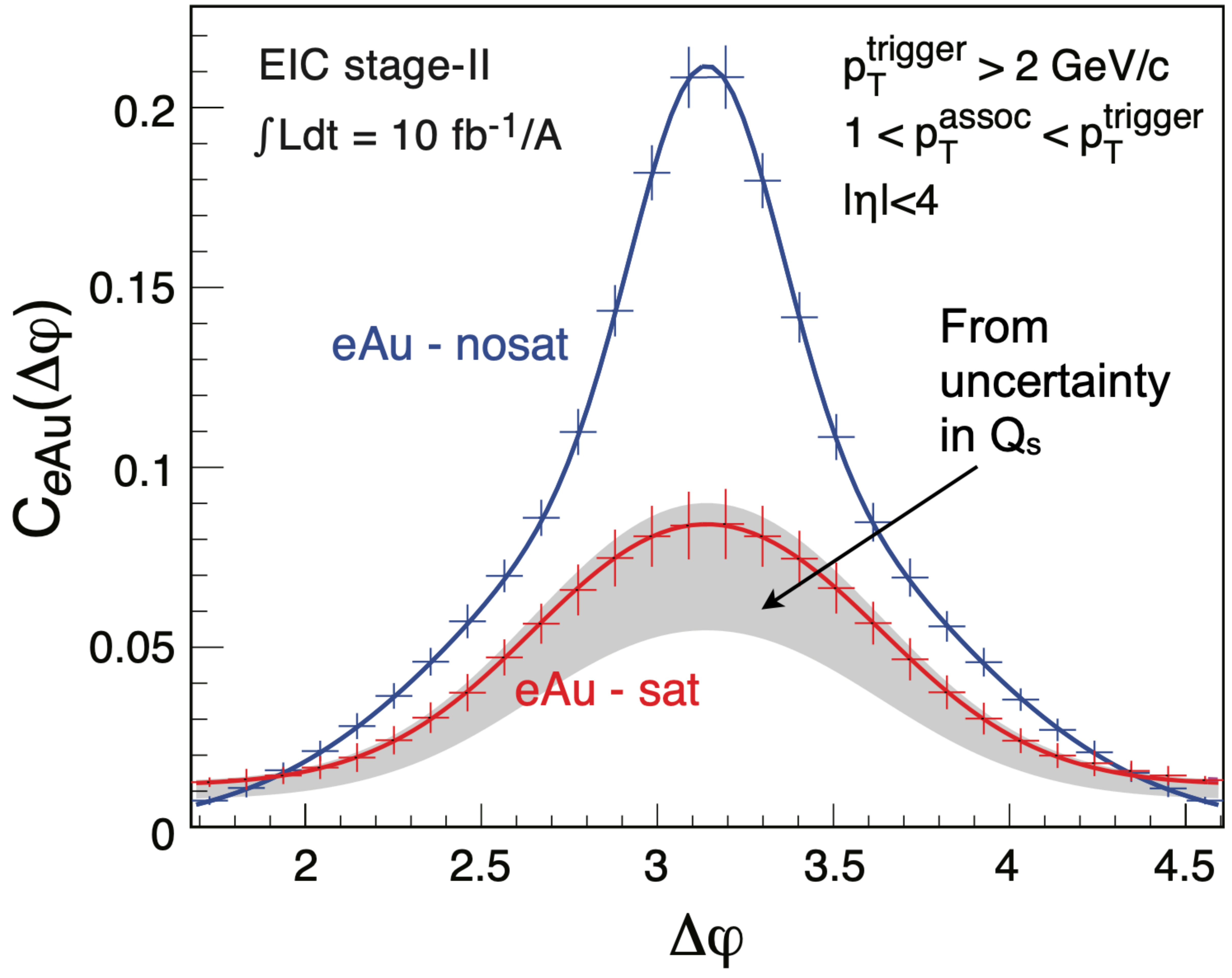

Clear key measurement

- Significant difference between sat and non-sat case
- Has equivalent to pA (e.g. RHIC forward measurements)
- Parton showers (Sudakov logs) can modify predictions

SATURATION EFFECTS ON OBSERVABLES

https://arxiv.org/pdf/1712.02508.pdf

T. Toll, T. Ullrich, Phys.Rev.C 87 (2013) 2, 024913
A. Accardi et al., EIC White Paper, Eur.Phys.J.A 52 (2016) 9, 268

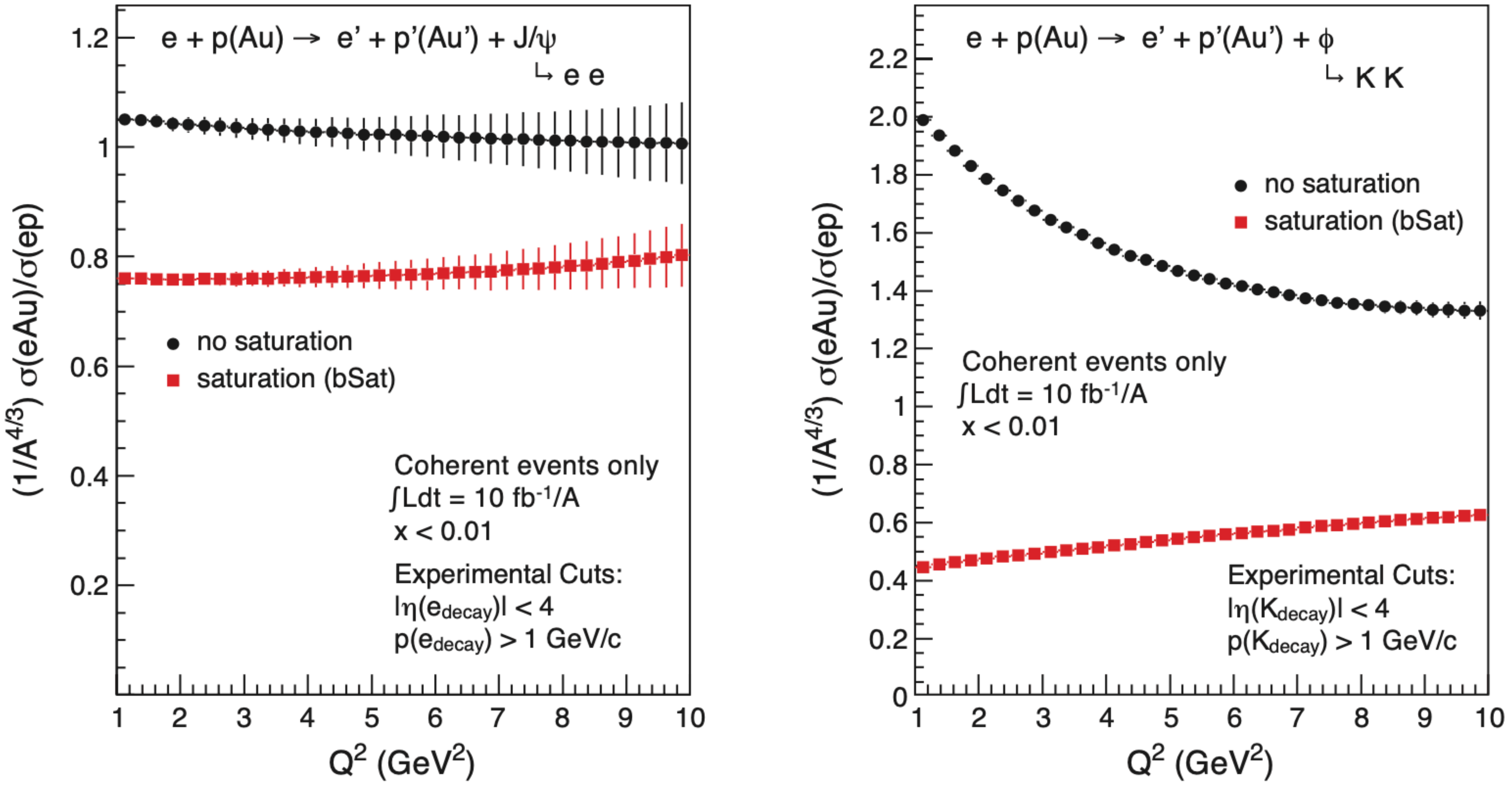

- Diffractive VM production: Sartre event generator (bSat & bNonSat = linearized bSat)
- Big difference for ϕ; less so for J/ψ (larger mass cuts off large dipoles)

Diffractive vector meson production

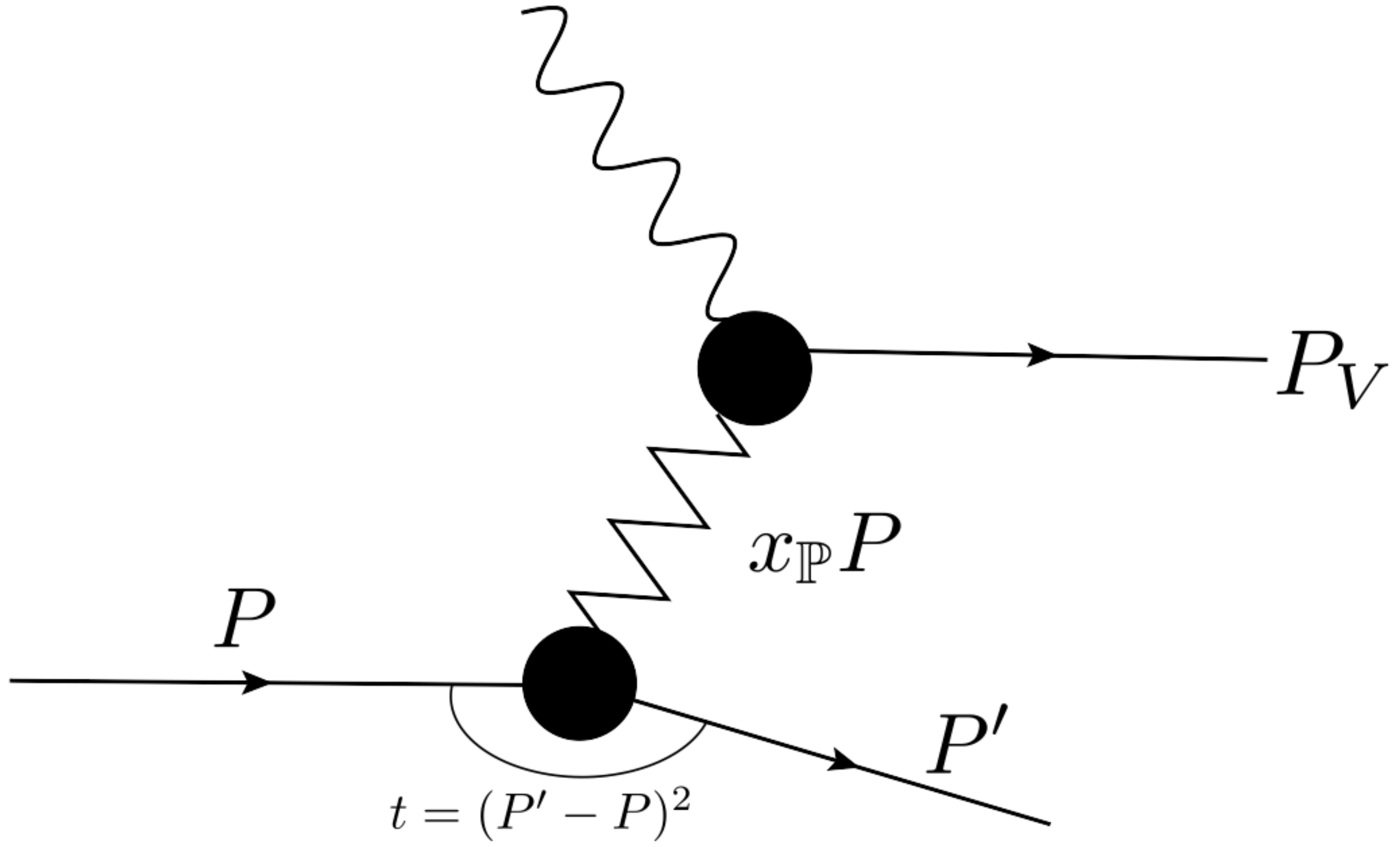

- Coherent diffraction: $$\frac{d\sigma^{\gamma^* p \to Vp}}{dt} = \frac{1}{16\pi} \left| \left\langle A^{\gamma^* p \to Vp}\left(x_P, Q^2, \vec{\Delta}\right) \right\rangle \right|^2$$

sensitive to the average size of the target

- Incoherent diffraction: $$\frac{d\sigma^{\gamma^* p \to Vp^*}}{dt} = \frac{1}{16\pi} \left(\left\langle \left| A^{\gamma^* p \to Vp}\left(x_P, Q^2, \vec{\Delta}\right) \right|^2 \right\rangle - \left| \left\langle A^{\gamma^* p \to Vp}\left(x_P, Q^2, \vec{\Delta}\right) \right\rangle \right|^2 \right)$$

sensitive to fluctuations (including geometric ones)

H. Kowalski, L. Motyka, G. Watt, Phys.Rev. D 74 (2006) 074016
A. Caldwell, H. Kowlaski, EDS 09, 190-192, e-Print: 0909.1254 [hep-ph]
M. L. Good and W. D. Walker, Phys. Rev. 120 (1960) 1857
H. I. Miettinen and J. Pumplin, Phys. Rev. D18 (1978) 1696
Y. V. Kovchegov and L. D. McLerran, Phys. Rev. D60 (1999) 054025
A. Kovner and U. A. Wiedemann, Phys. Rev. D64 (2001) 114002

Dipole picture: Scattering amplitude

H. Mäntysaari, B. Schenke, Phys. Rev. Lett. 117 (2016) 052301; Phys.Rev. D94 (2016) 034042

High energy factorization:

- $\gamma^* \to q\bar{q} : \psi^\gamma(r, Q^2, z)$
- $q\bar{q}$ dipole scatters with amplitude N
- $q\bar{q} \to V : \psi^V(r, Q^2, z)$

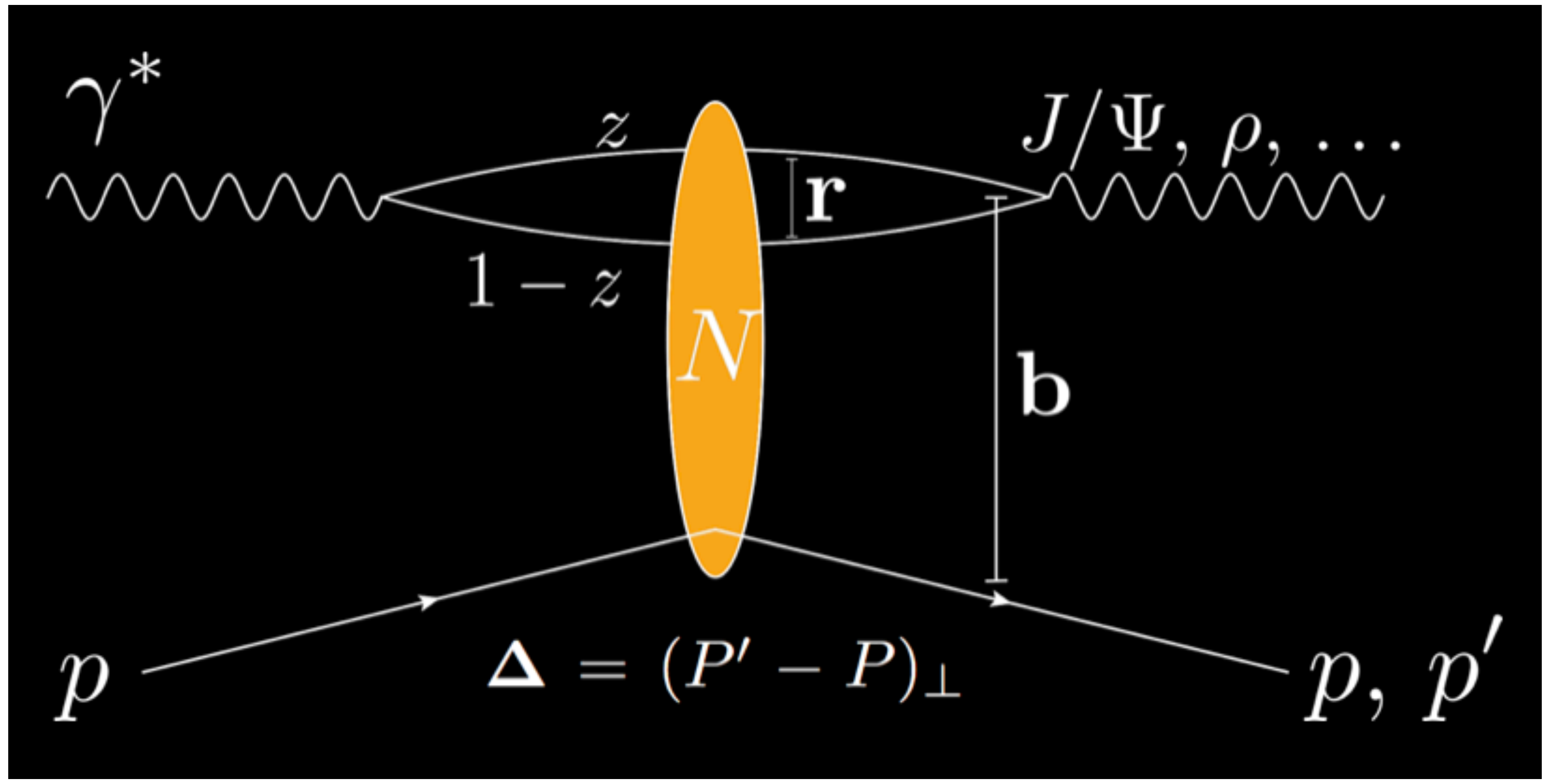

$$A \sim \int d^2b\, dz\, d^2r\, \psi^* \psi^V(\vec{r}, z, Q^2) e^{-i\vec{b}\cdot\vec{\Delta}} N(\vec{r}, x, \vec{b})$$

- Impact parameter ***b*** is the Fourier conjugate of transverse momentum transfer ***Δ*** → Access to spatial structure $(t = -\Delta^2)$

Color glass condensate formalism

H. Mäntysaari, B. Schenke, Phys. Rev. Lett. 117 (2016) 052301; Phys.Rev. D94 (2016) 034042

Compute the Wilson lines using color charges whose correlator depends on $\vec{b}_\perp$

$$\langle \rho^a(\mathbf{b}_\perp)\rho^b(\mathbf{x}_\perp)\rangle = g^2\mu^2(x,\mathbf{b}_\perp)\delta^{ab}\delta^{(2)}(\mathbf{b}_\perp - \mathbf{x}_\perp)$$

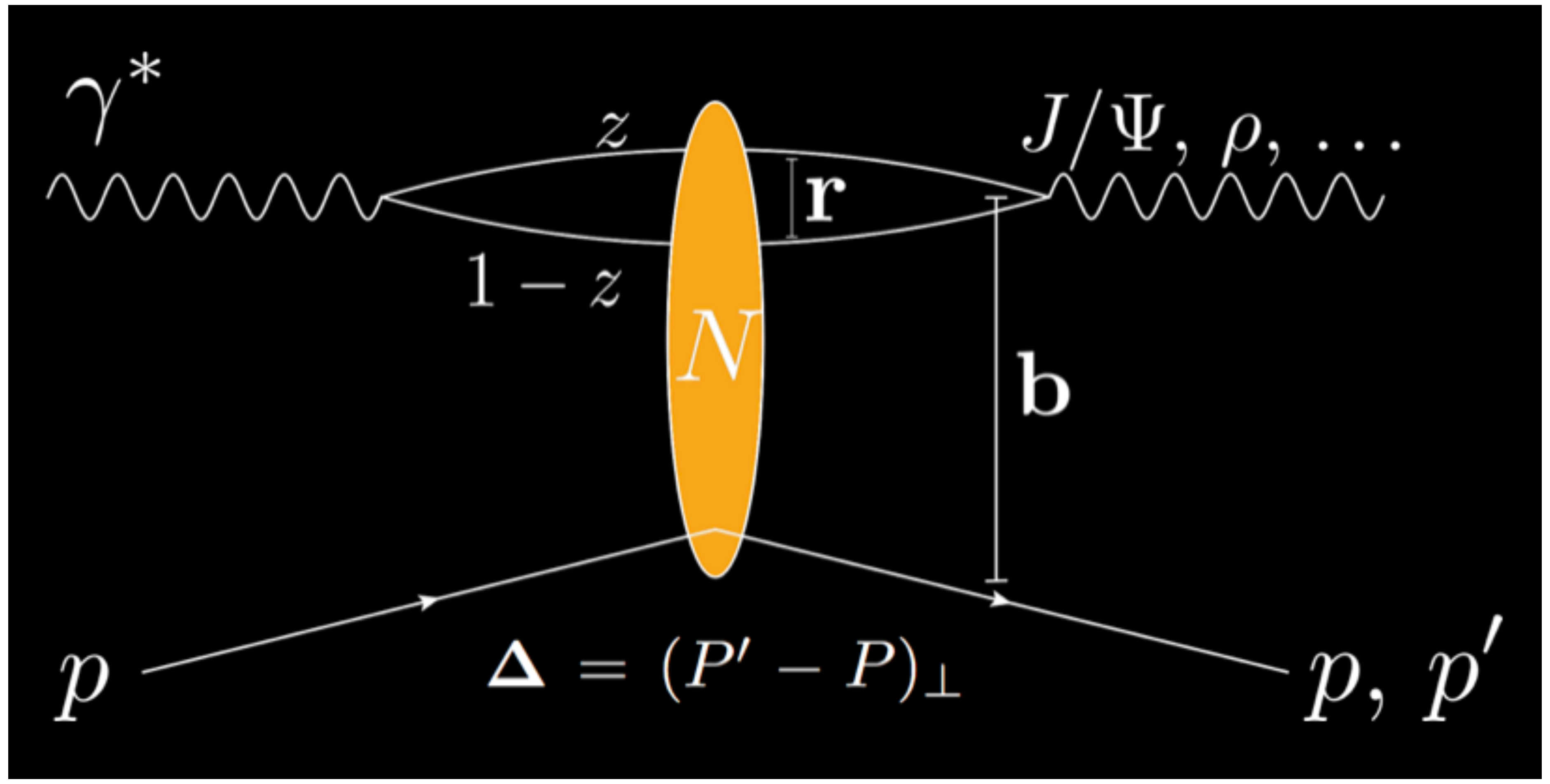

$$N(\vec{r},x,\vec{b}) = N(\vec{x}-\vec{y},x,(\vec{x}+\vec{y})/2) = 1 - \mathrm{Tr}(\mathrm{V}(\vec{\mathrm{x}})\mathrm{V}^\dagger(\vec{\mathrm{y}}))/\mathrm{N_c}$$

The trace appears at the level of the amplitude, because we project on a color singlet

$$A \sim \int d^2b\, dz\, d^2r\, \psi^*\psi^V(\vec{r},z,Q^2)e^{-i\vec{b}\cdot\vec{\Delta}}N(\vec{r},x,\vec{b})$$

Modeling the dipole amplitude

H. Kowalski, D. Teaney, Phys.Rev.D 68 (2003) 114005

Building $N = 1 - \frac{1}{N_c} \langle \mathrm{Tr}\, V(\vec{x}) V^\dagger(\vec{y}) \rangle$ from Wilson lines needs the full CGC average over color charges. In practice one often models N directly --- e.g. the **IPSat** model:

$$N(r, x, \vec{b}) = 1 - \exp\left(-\frac{\pi^2}{2N_c} r^2 \alpha_s(\mu^2)\, xg(x, \mu^2)\, T(\vec{b}) \right), \qquad \mu^2 = \mu_0^2 + \frac{C}{r^2}$$

- Exponential = eikonalized single-gluon exchange ⇒ unitarity, $N \leq 1$ (saturation)
- r^2: small dipoles scatter weakly (color transparency)
- $xg(x, \mu^2)$: gluon density carries the energy (x) and scale (μ^2, DGLAP) dependence
- All transverse geometry enters through the profile $T(\vec{b})$

Model impact parameter dependence (proton, nucleon)

H. Mäntysaari, B. Schenke, Phys. Rev. Lett. 117 (2016) 052301; Phys.Rev. D94 (2016) 034042

1) Assume Gaussian proton shape:

$$T(\vec{b}) = T_\mathrm{p}(\vec{b}) = \frac{1}{2\pi B_\mathrm{p}} e^{-b^2/(2B_\mathrm{p})}$$

2) Assume Gaussian distributed and Gaussian shaped hot spots:

$$P(b_i) = \frac{1}{2\pi B_\mathrm{qc}} e^{-b_i^2/(2B_\mathrm{qc})}$$ (angles uniformly distributed)

$$T_\mathrm{p}(\vec{b}) = \frac{1}{N_\mathrm{q}} \sum_{i=1}^{N_\mathrm{q}} T_\mathrm{G}(\vec{b} - \vec{b}_i)$$ with N_q hot spots; $$T_\mathrm{G}(\vec{b}) = \frac{1}{2\pi B_\mathrm{q}} e^{-b^2/(2B_\mathrm{q})}$$

Diffractive J/ψ production in e+p at HERA

Nucleon parameters B_q, B_{qc}, can be constrained by e+p scattering data from HERA

Exclusive diffractive J/Ψ production in e+p:

Incoherent x-sec sensitive to fluctuations

H. Mäntysaari, B. Schenke, Phys. Rev. Lett. 117 (2016) 052301

Phys.Rev. D94 (2016) 034042

also see:

S. Schlichting, B. Schenke, Phys.Lett. B739 (2014) 313-319

H. Mäntysaari, Rep. Prog. Phys. 83 082201 (2020)

B. Schenke, Rep. Prog. Phys. 84 082301 (2021)

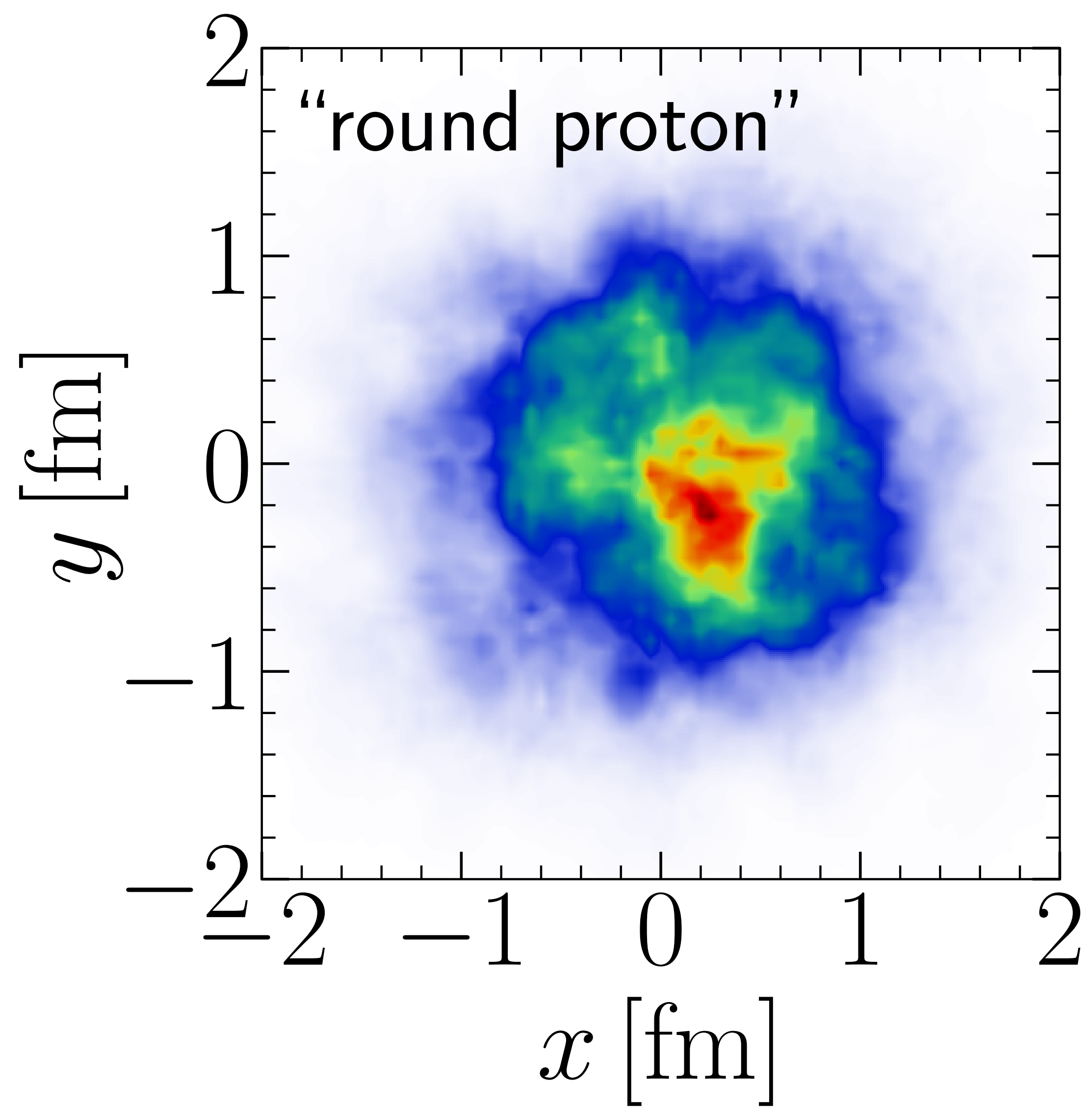

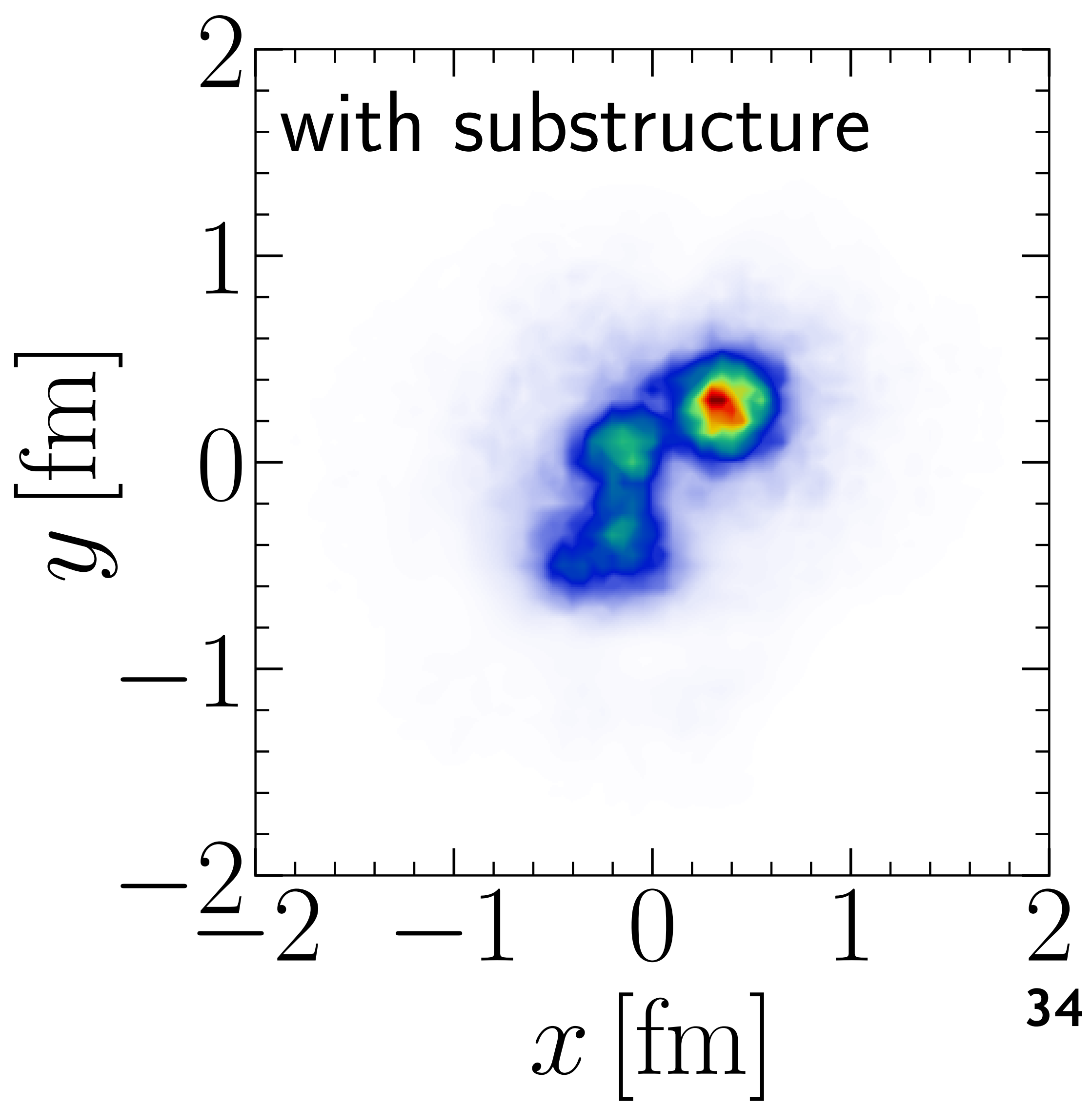

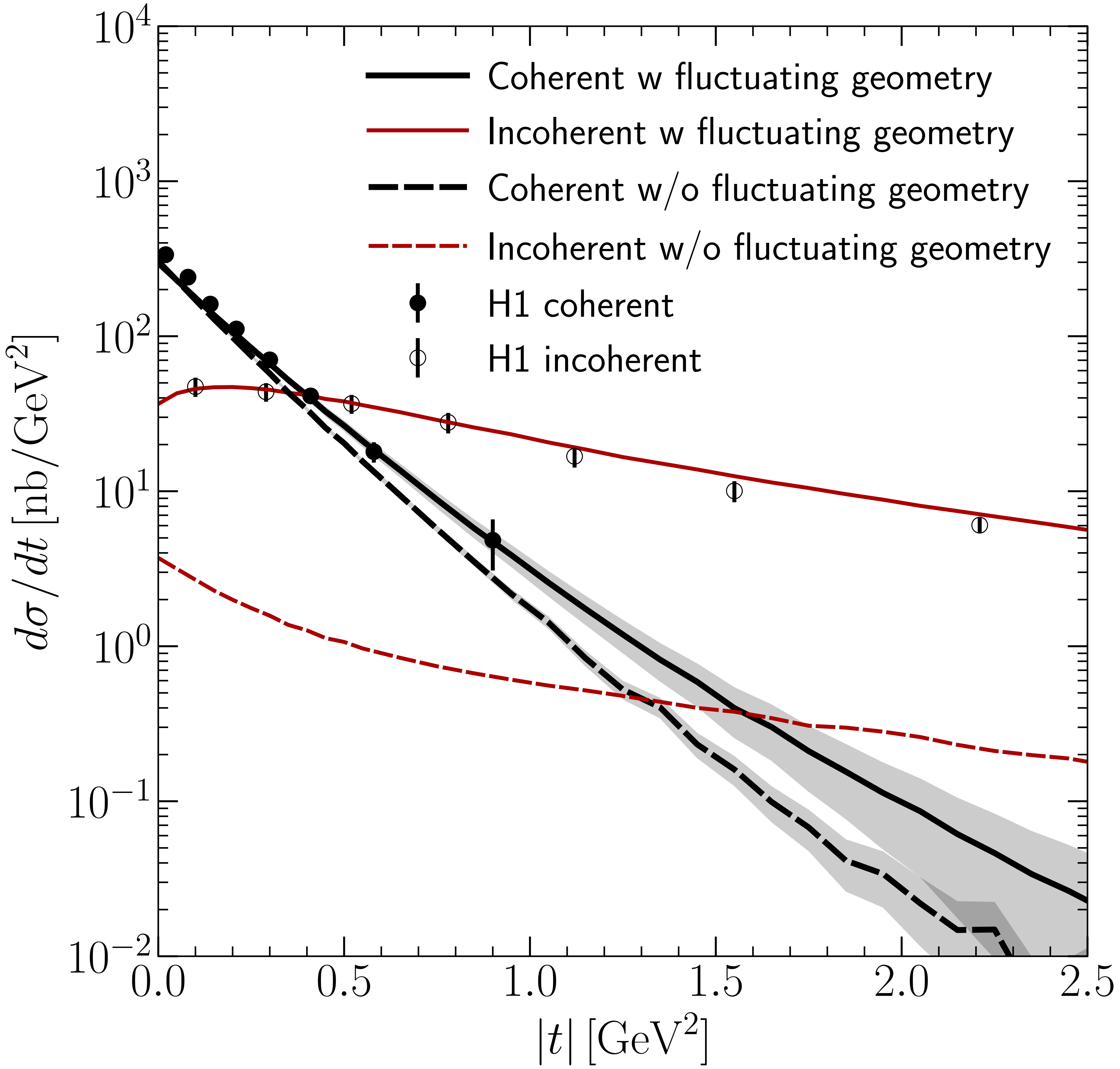

H1 Collaboration, Eur. Phys. J. C73 (2013) no. 6 2466

Information in the diffractive cross sections

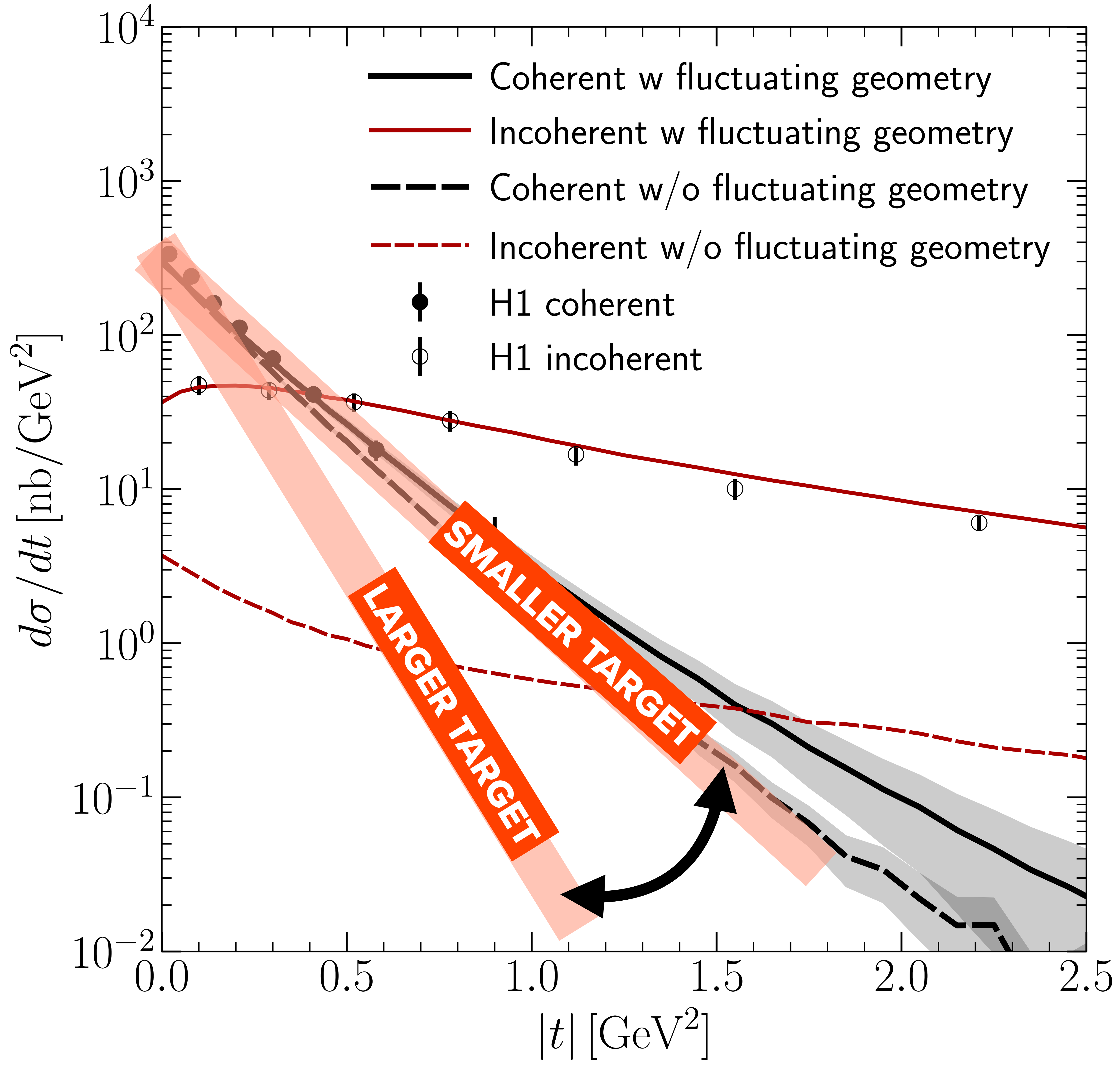

H1 Collaboration, Eur. Phys. J. C73 (2013) no. 6 2466

Information in the diffractive cross sections

larger scale fluctuations (>0.2 fm)

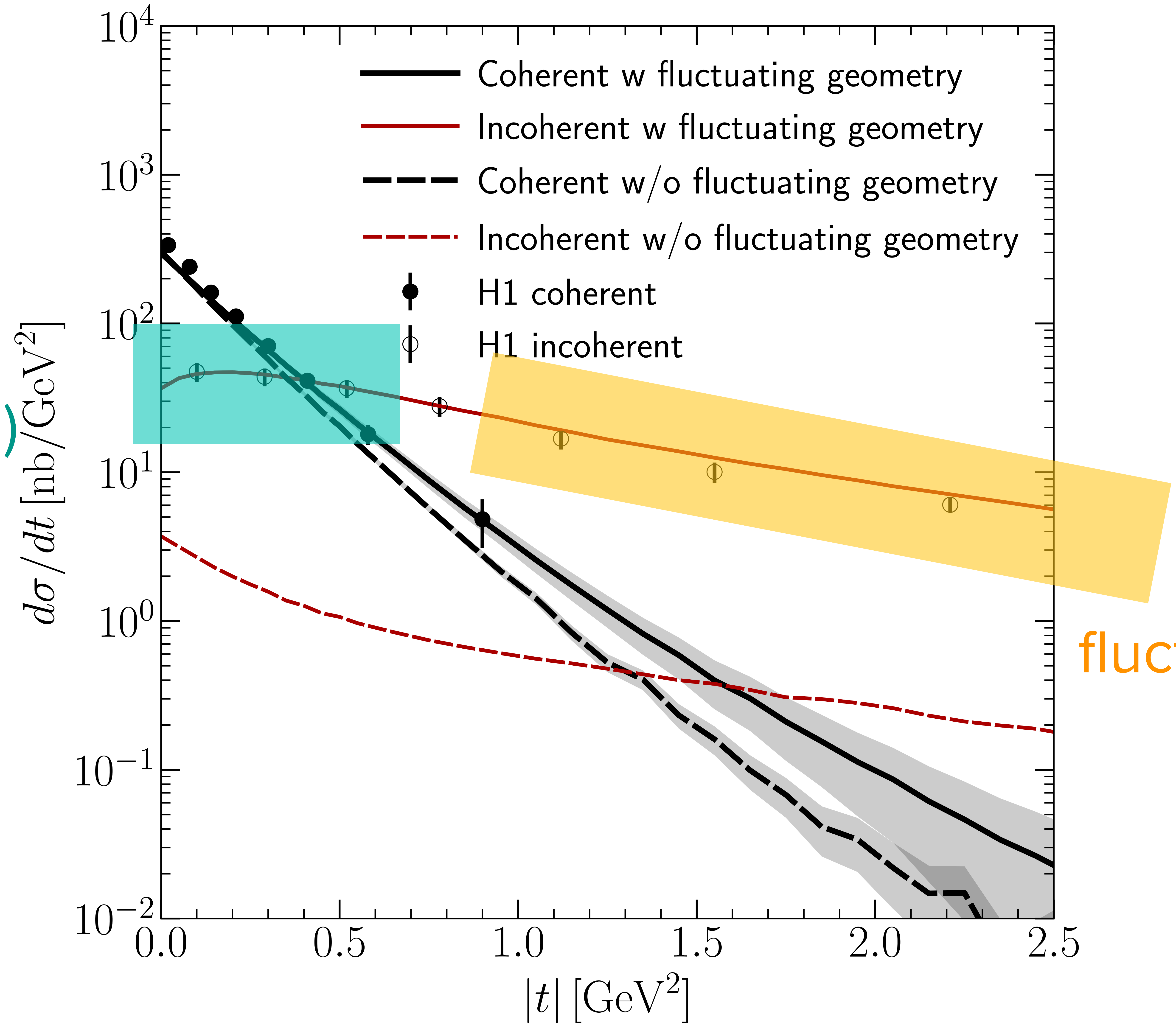

short scale fluctuations (<0.2 fm)

H1 Collaboration, Eur. Phys. J. C73 (2013) no. 6 2466

Center-of-mass energy dependence: $\gamma + p$

H. Mäntysaari, F. Salazar, B. Schenke, Phys.Rev.D 106 (2022) 7, 074019

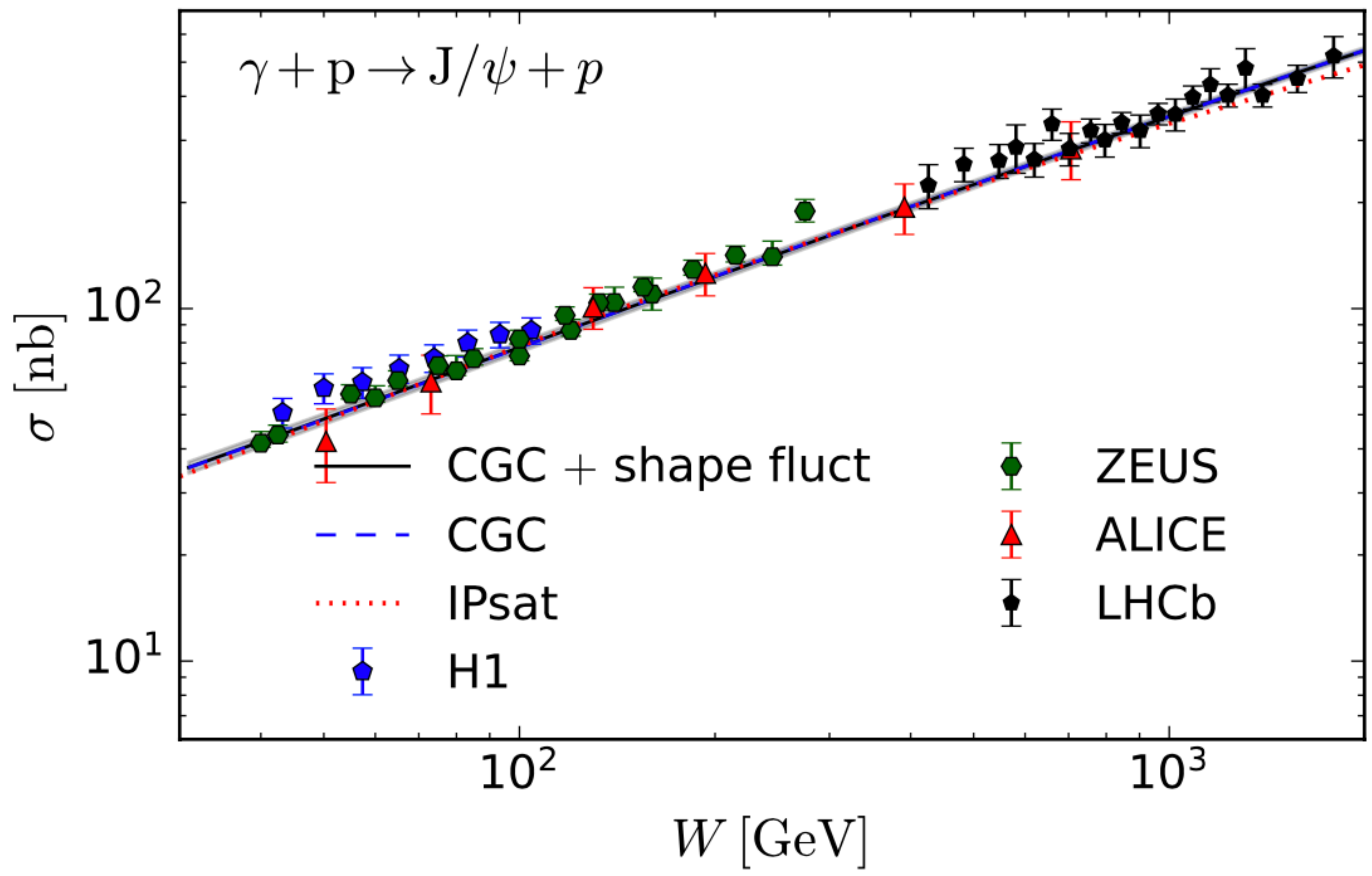

- Coherent cross section measured up to large W
- Compatible with CGC calculations using BK or JIMWLK evolution, but no clear signal of saturation with proton targets

Saturation effects in vector meson production on nuclei

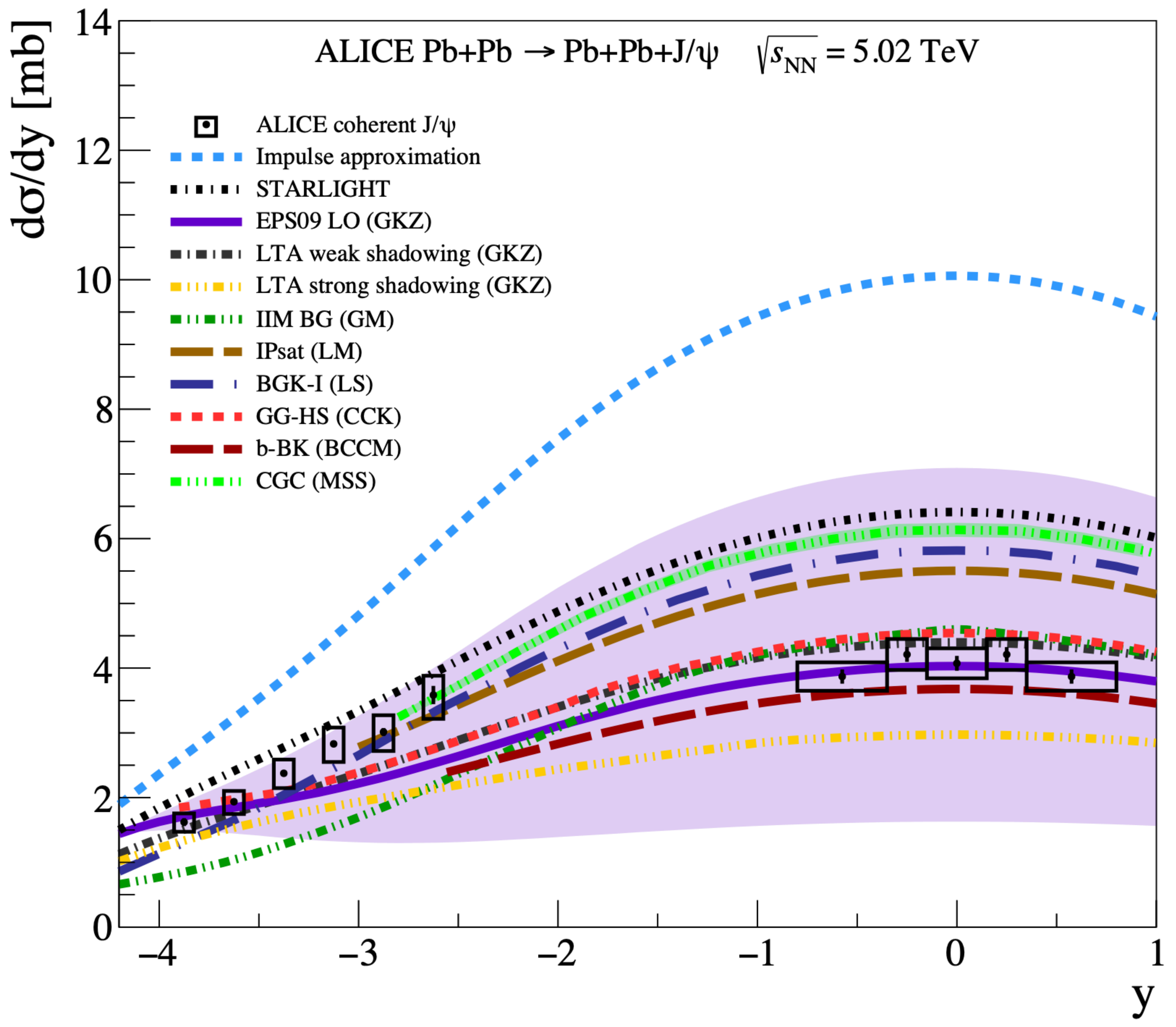

no nuclear suppression

gluon saturation effect

Phys.Proc.UPC 1 (2024) 2

End Lecture 1

Extras

UPCs: γ+Pb measurement - Role of saturation effects

H. Mäntysaari, F. Salazar, B. Schenke, Phys.Rev.D 106 (2022) 7, 074019

Here, ALICE removed interference and photon k_T effects to get the γ+Pb cross section

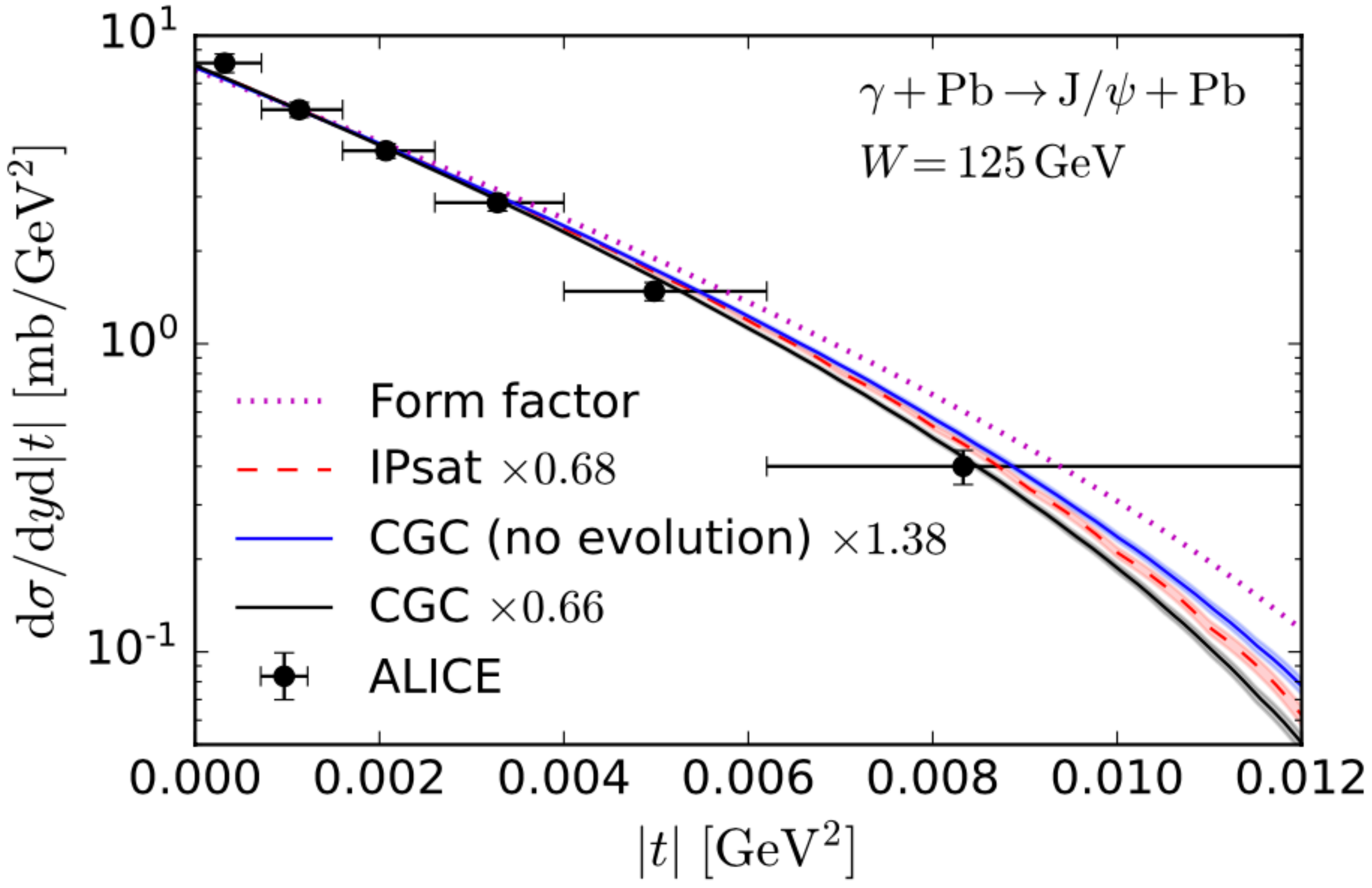

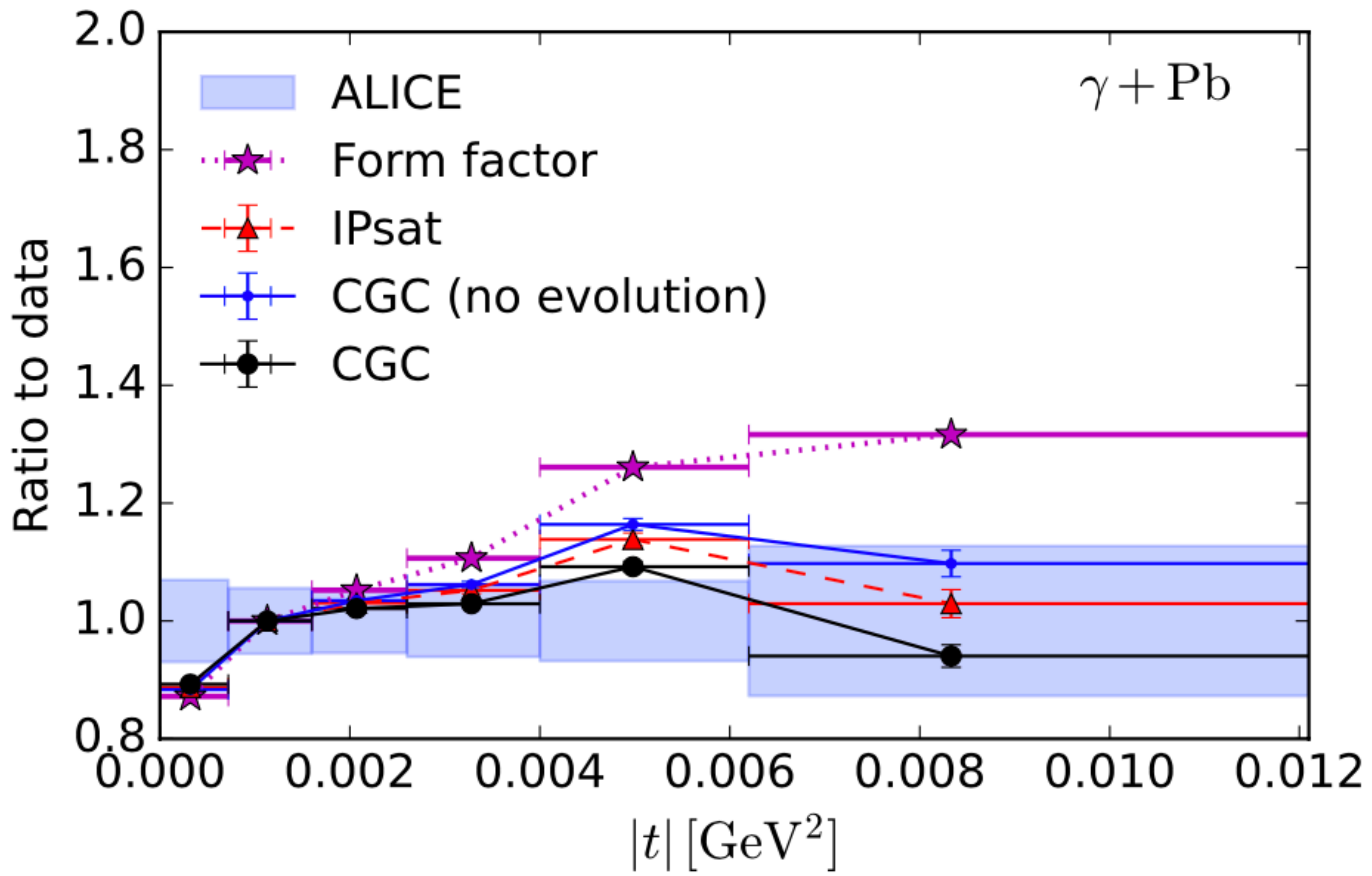

ALICE Collaboration, Phys.Lett.B 817 (2021) 136280

Saturation effects improve agreement with experimental data significantly

Saturation effects on nuclear geometry

H. Mäntysaari, F. Salazar, B. Schenke, Phys.Rev.D 106 (2022) 7, 074019

Fourier transform to coordinate space

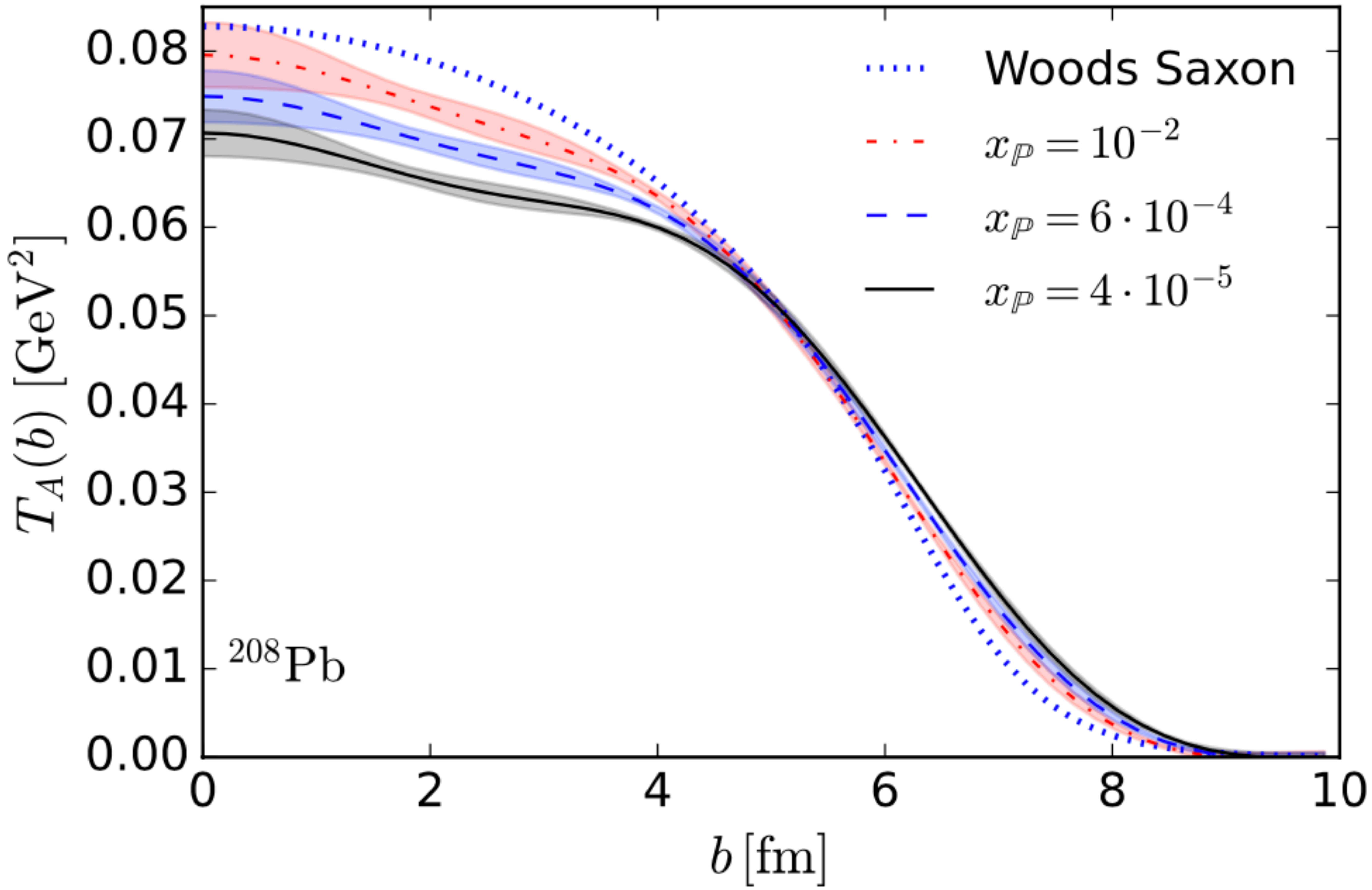

JIMWLK evolution leads to growth of the nucleus towards small x and depletion near the center (normalized so $\int d^2 b T_A(b) = 208$)

Effects of deformation on diffractive cross sections

H. Mäntysaari, B. Schenke, C. Shen, W. Zhao, arXiv:2303.04866

Implement deformation in the Woods-Saxon distribution:

$$\rho(r,\Theta,\Phi) \propto \frac{1}{1+\exp\left(\left[r-R(\Theta,\Phi)\right]/a\right)} \quad , \quad R(\Theta,\Phi) = R_0\left[1+\underline{\beta_2}\left(\cos\underline{\gamma} Y_{20}(\Theta)+\sin\gamma Y_{22}(\Theta,\Phi)\right)+\underline{\beta_3}Y_{30}(\Theta)+\underline{\beta_4}Y_{40}(\Theta)\right]$$

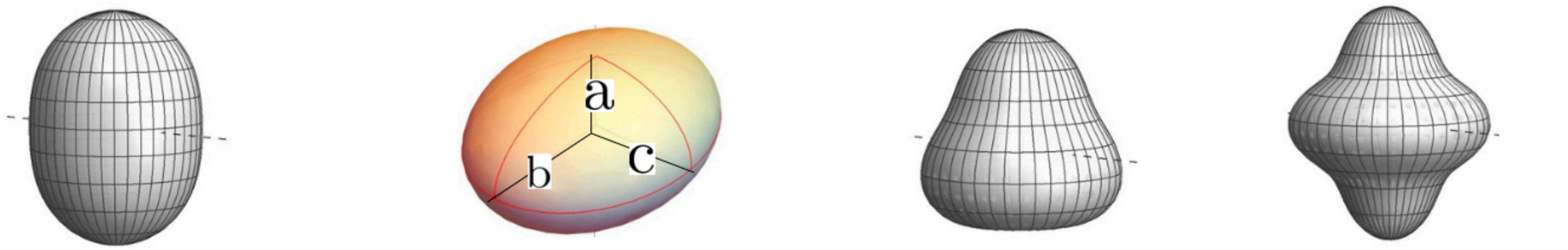

from G. Giacalone

Deformed nuclei exhibit larger fluctuation in the transverse projection:

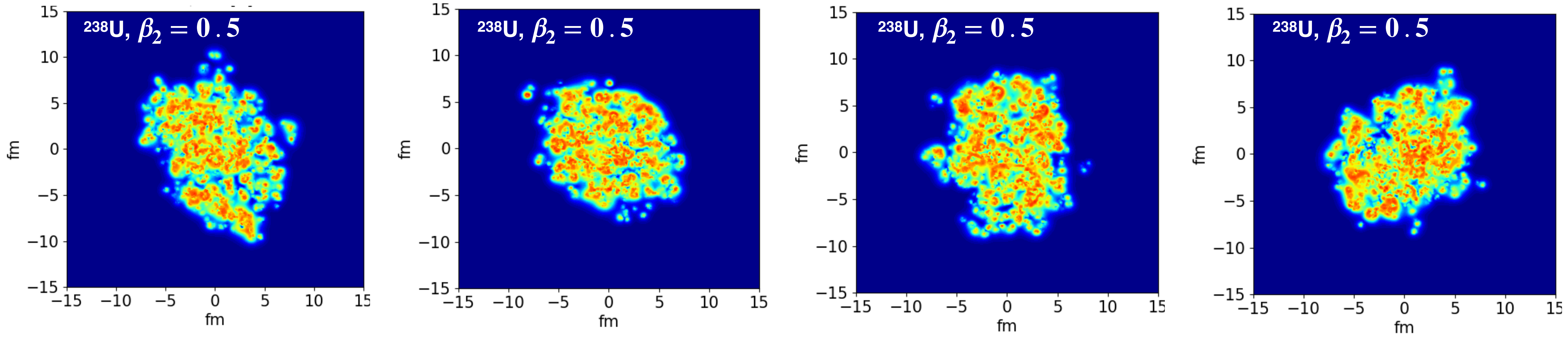

Effects of deformation on diffractive cross sections: Uranium

H. Mäntysaari, B. Schenke, C. Shen, W. Zhao, arXiv:2303.04866

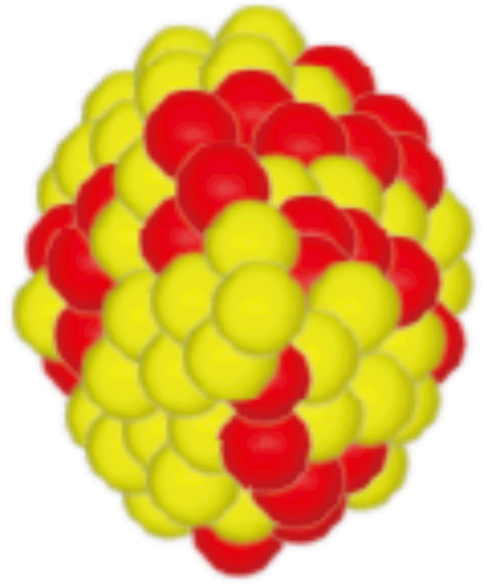

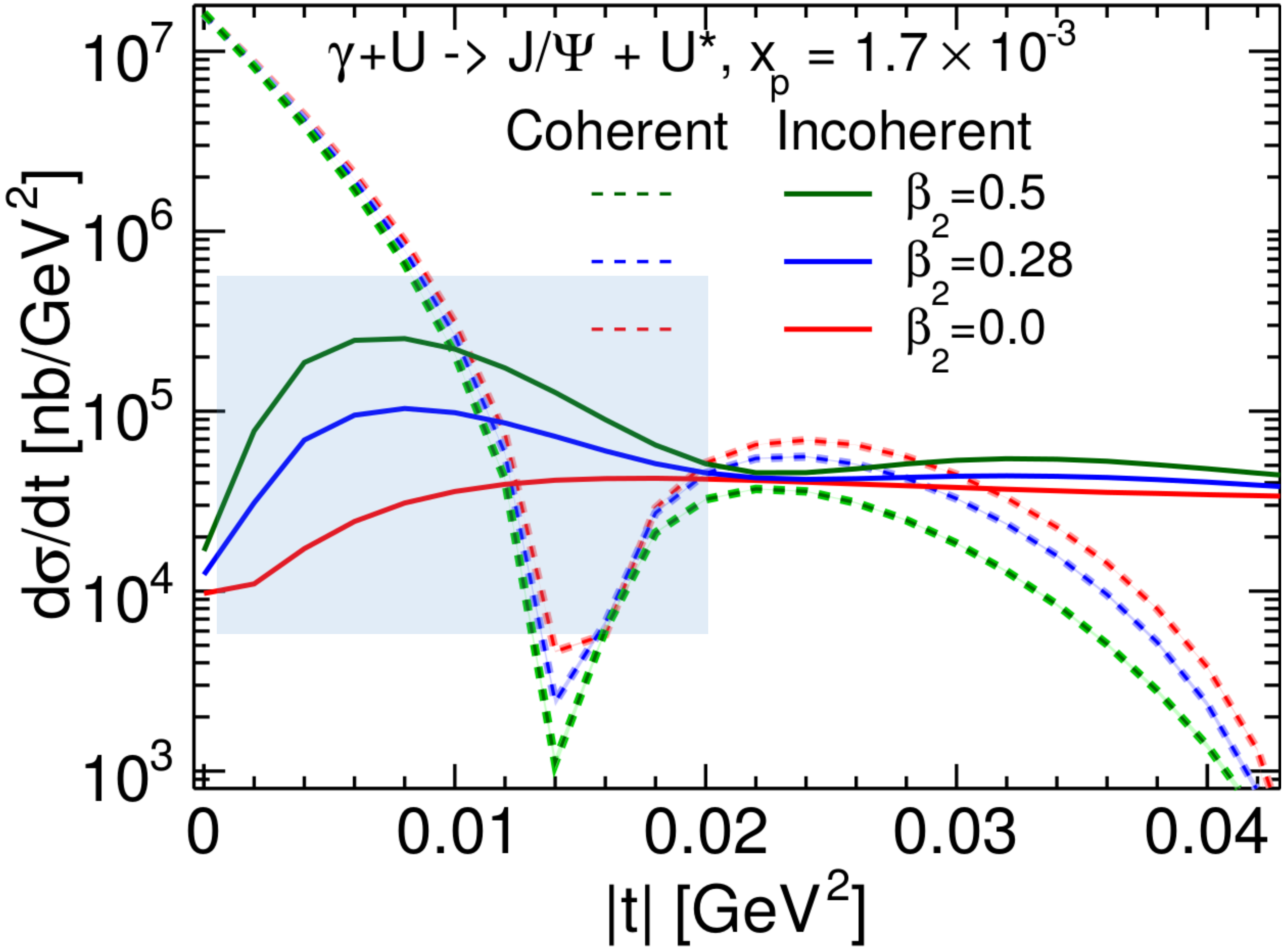

Deformation of the nucleus affects incoherent cross section at small $|t|$ (large length scales)

This observable provides direct information on the small x structure

$Q^2 = 0$

Effects of deformation on diffractive cross sections: Uranium

H. Mäntysaari, B. Schenke, C. Shen, W. Zhao, arXiv:2303.04866

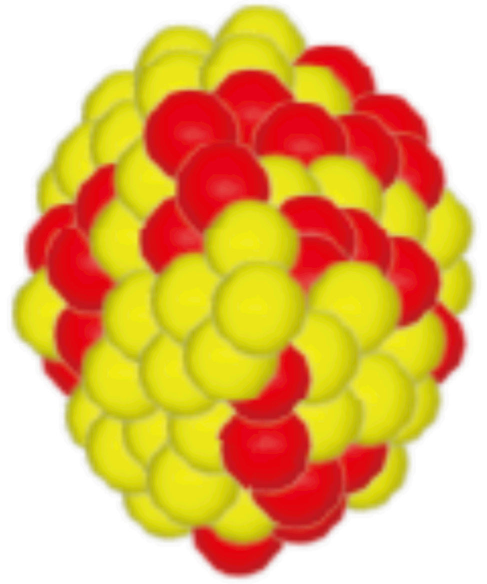

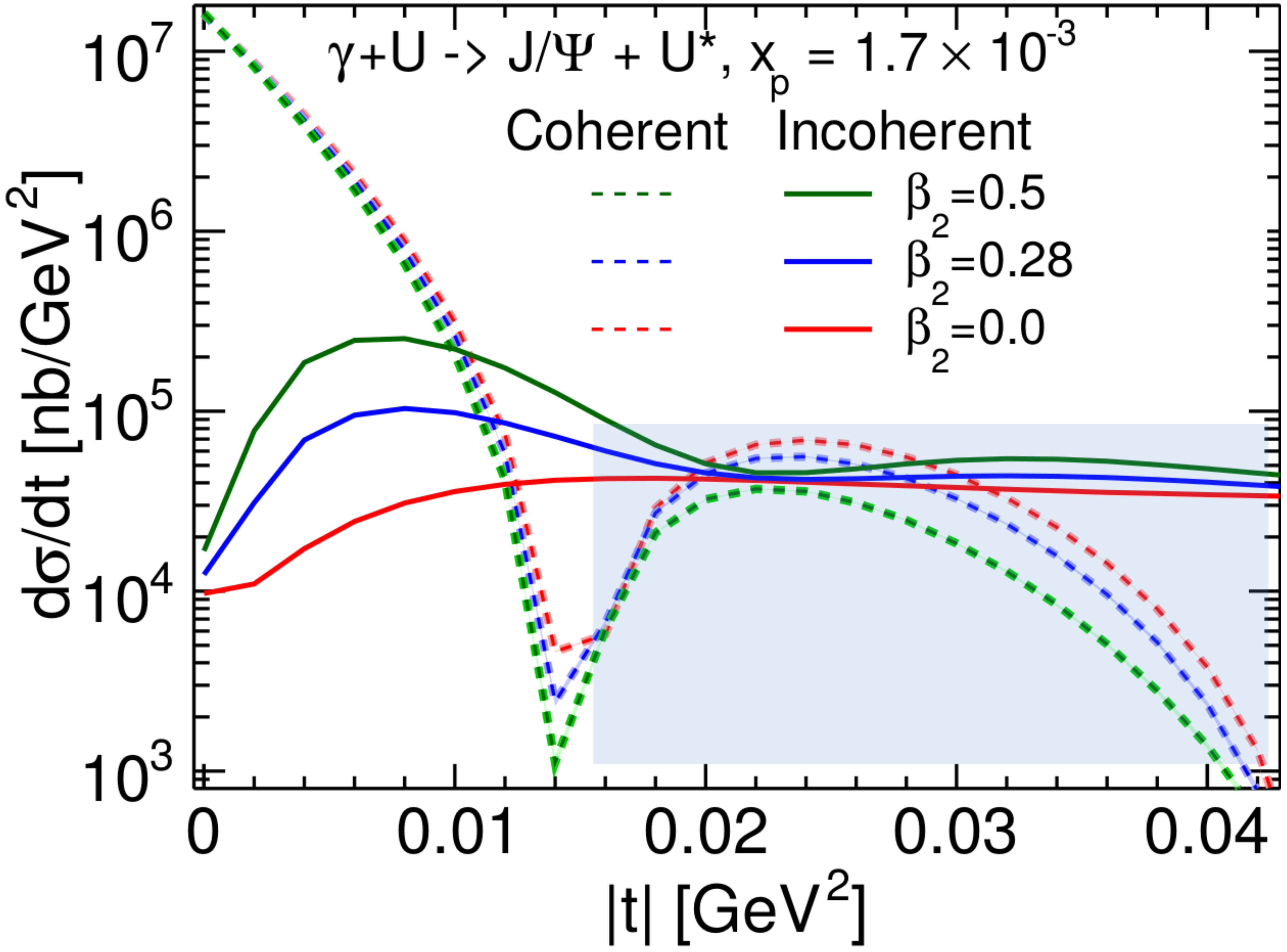

Deformation changes the shape of the average 2D projection of the nucleus

→

Modification of the coherent cross section

Effects of deformation on diffractive cross sections: Uranium

H. Mäntysaari, B. Schenke, C. Shen, W. Zhao, arXiv:2303.04866

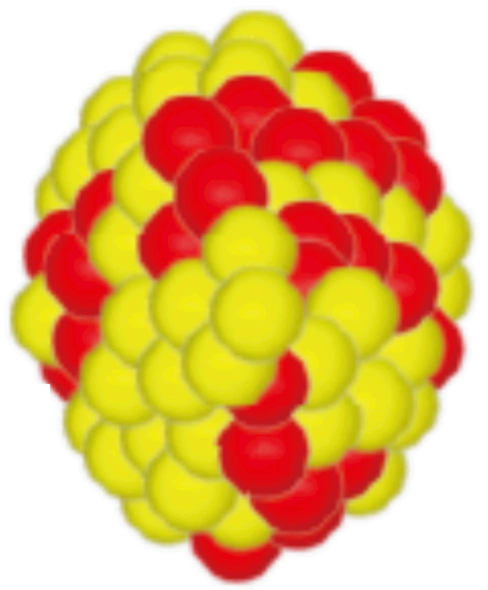

β_2 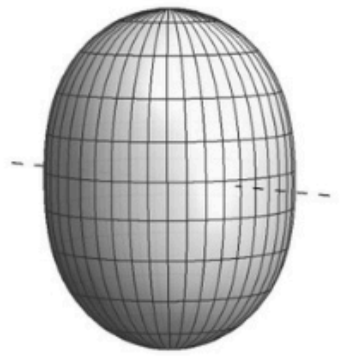 β_3 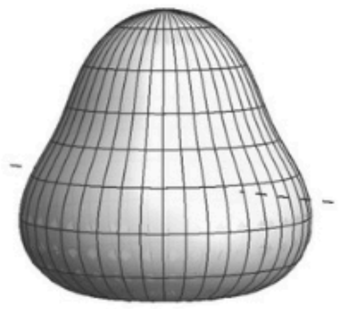 β_4 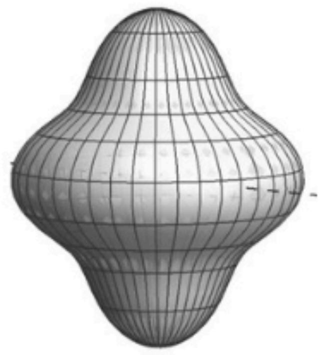

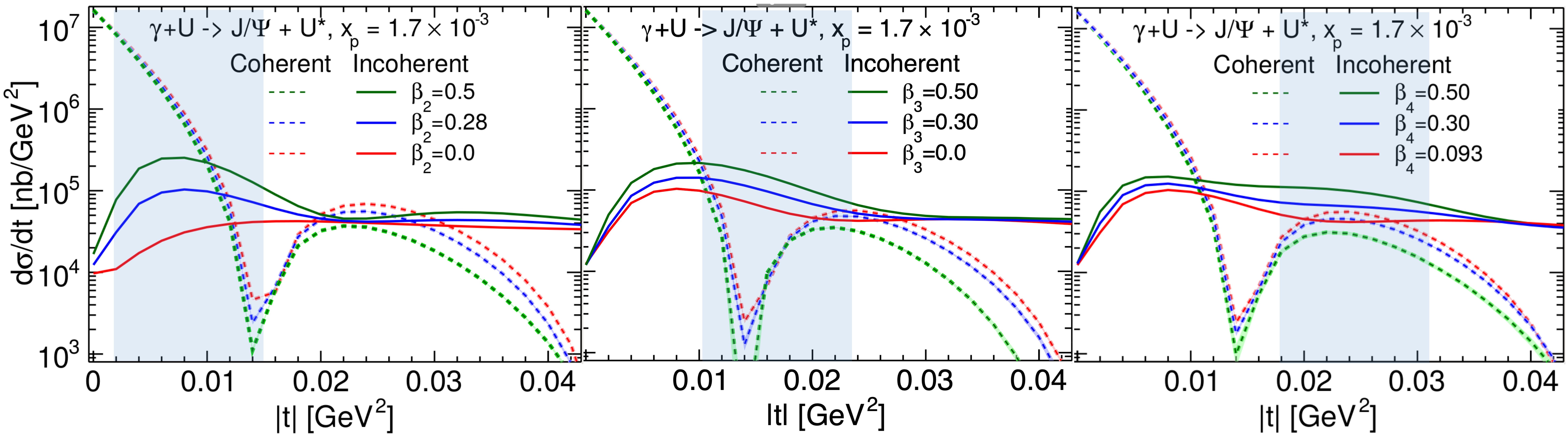

- β_2 , β_3 and β_4 modify fluctuations at different length scales: Change incoherent cross section in different |t| regions

Towards smaller *x*

H. Mäntysaari, B. Schenke, C. Shen, W. Zhao, arXiv:2303.04866

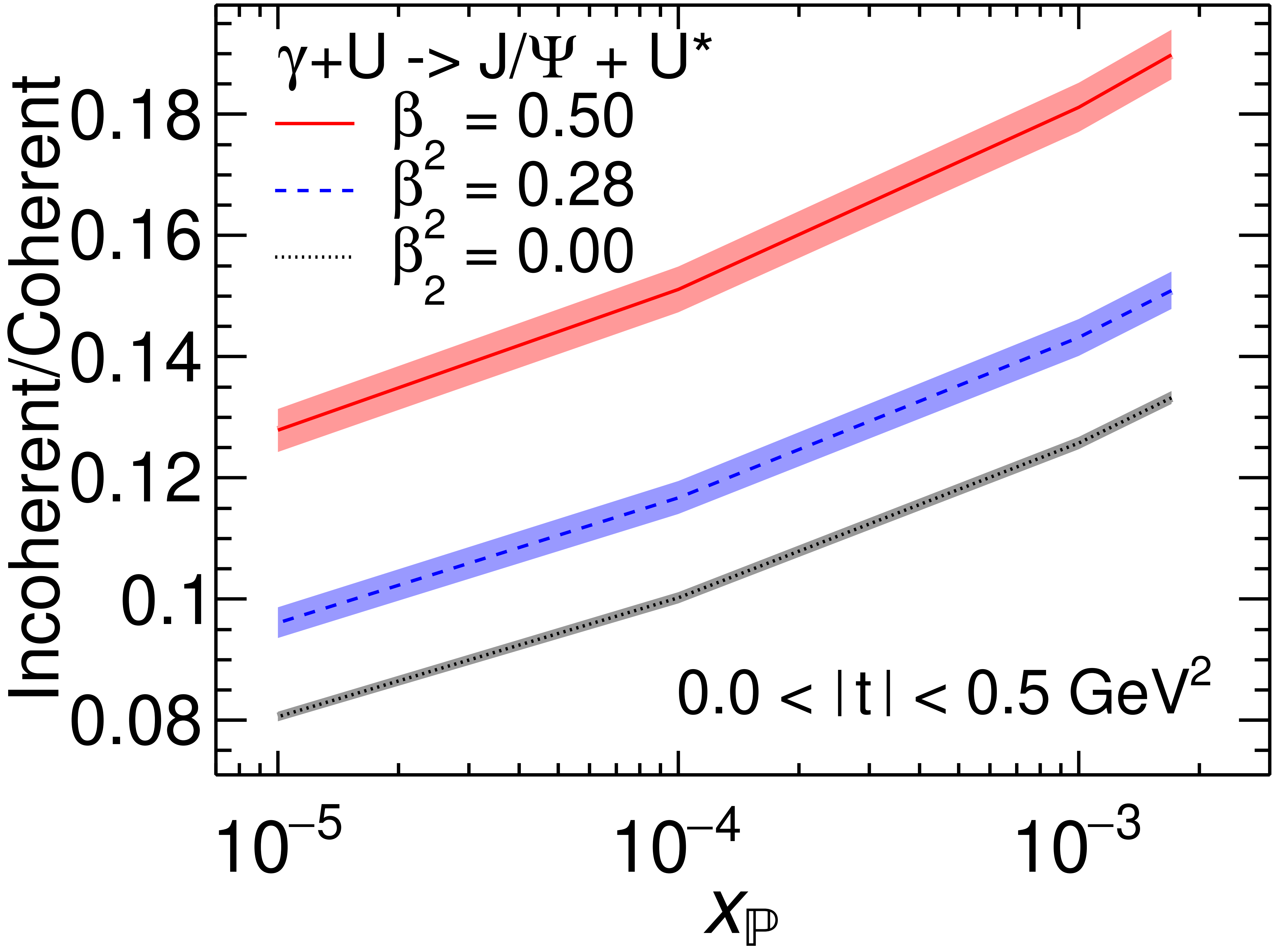

- JIMWLK evolution to smaller *x*
- Both cross sections increase
- Ratio incoherent/coherent decreases because fluctuations are reduced (nucleus becomes smoother)
- Difference between different β_2 does not decrease noticeably in this x range
- Is there a large enough x range we can cover at the EIC (at least 10^{-3} - 10^{-2})?

Neon and Oxygen targets

H. Mäntysaari, B. Schenke, C. Shen, W. Zhao, arXiv:2303.04866

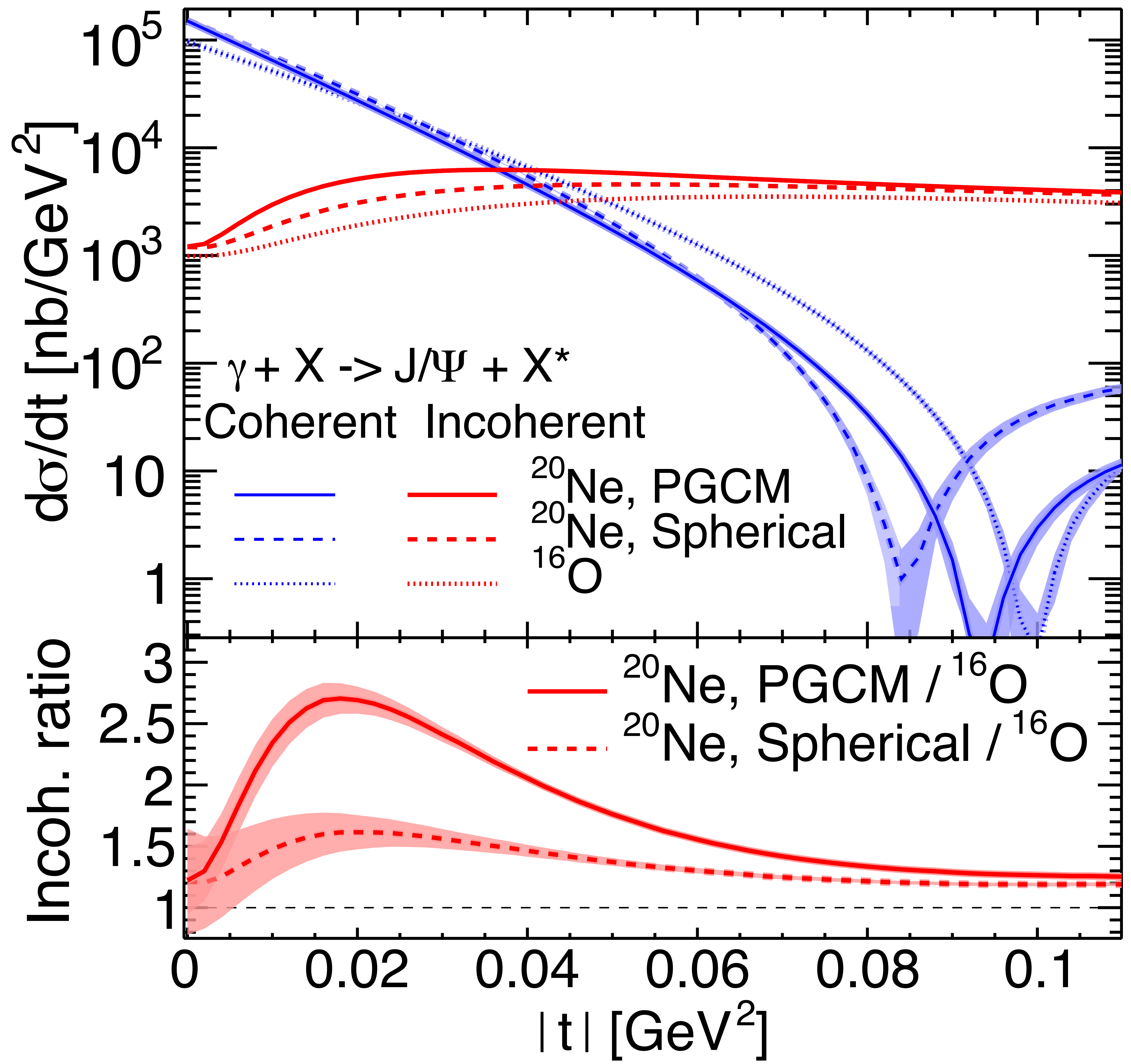

- ^{20}Ne has a bowling pin shape that leads to an increased incoherent cross section relative to an assumed spherical (on average) neon or a spherical oxygen

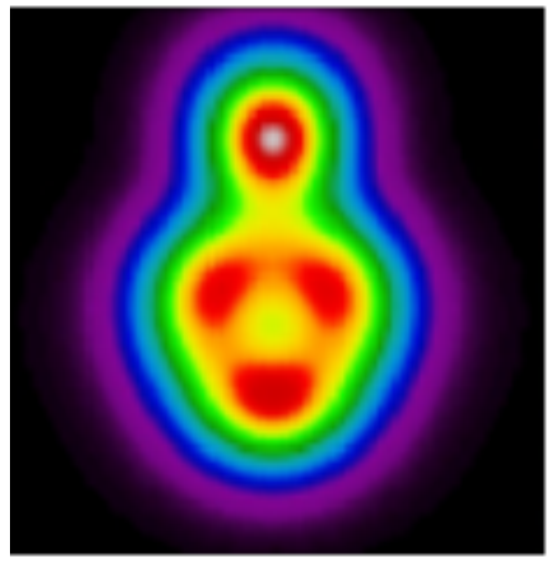

^{20}Ne

PGCM: Projected Generator Coordinate Method: B. Bally et al., "Deciphering small system collectivity with bowling-pin-shaped ^{20}Ne isotopes," in preparation (2023); Mikael Frosini, Thomas Duguet, Jean-Paul Ebran, Benjamin Bally, Tobias Mongelli, Toma´s R. Rodrıguez, Robert Roth, and Vittorio Soma, Eur. Phys. J. A 58, 63 (2022)

Multi-scale sensitivity

H. Mäntysaari, B. Schenke, C. Shen, W. Zhao, arXiv:2303.04866

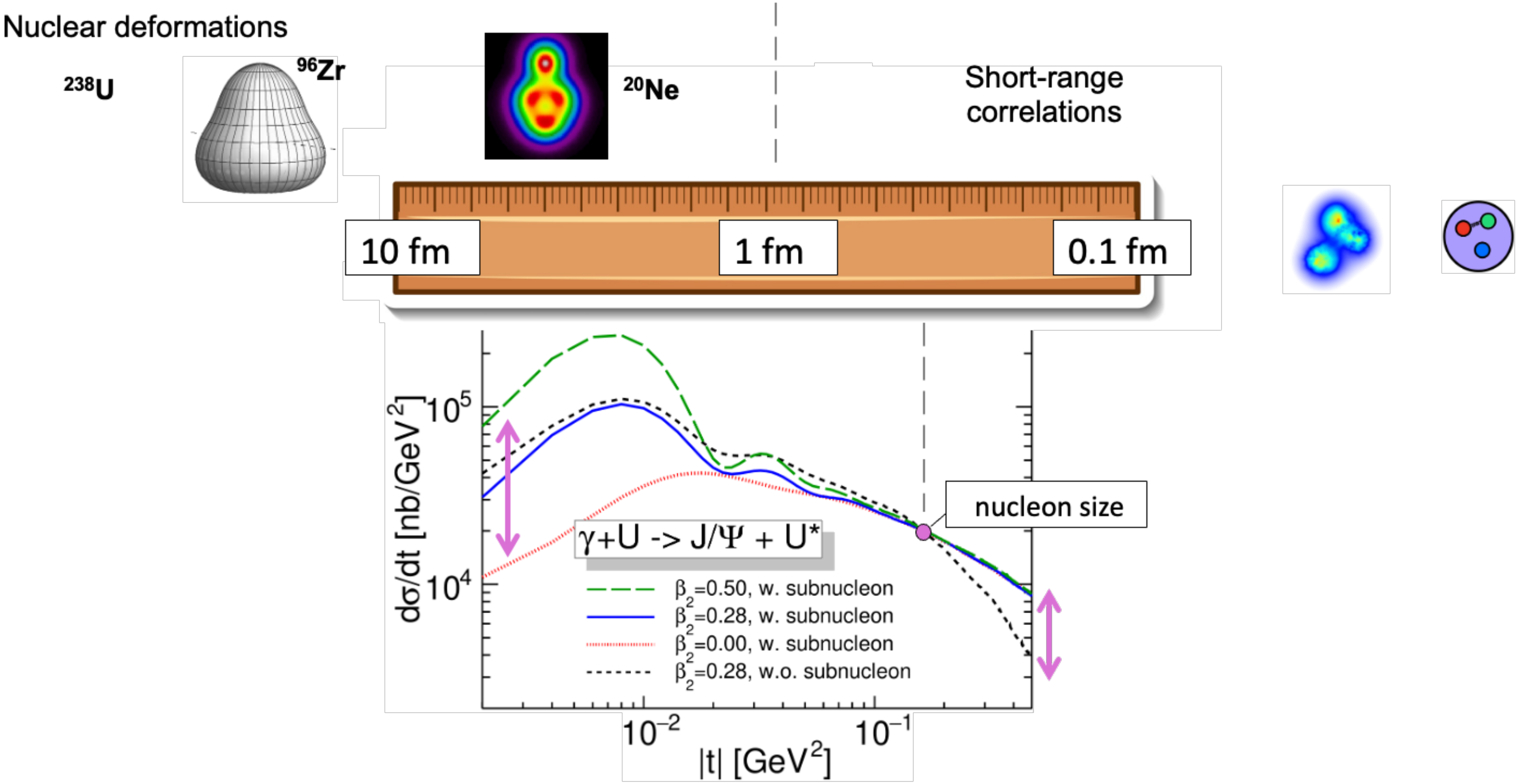

Chiral effective field theory (low-energy QCD) ⟷ **?** ⟷ **CGC effective field theory (high-energy QCD)**

slide from G. Giacalone

Photoproduction of J/ψ in d+Au collisions at STAR

H. Mäntysaari, B. Schenke, Phys. Rev. C101, 015203 (2020)

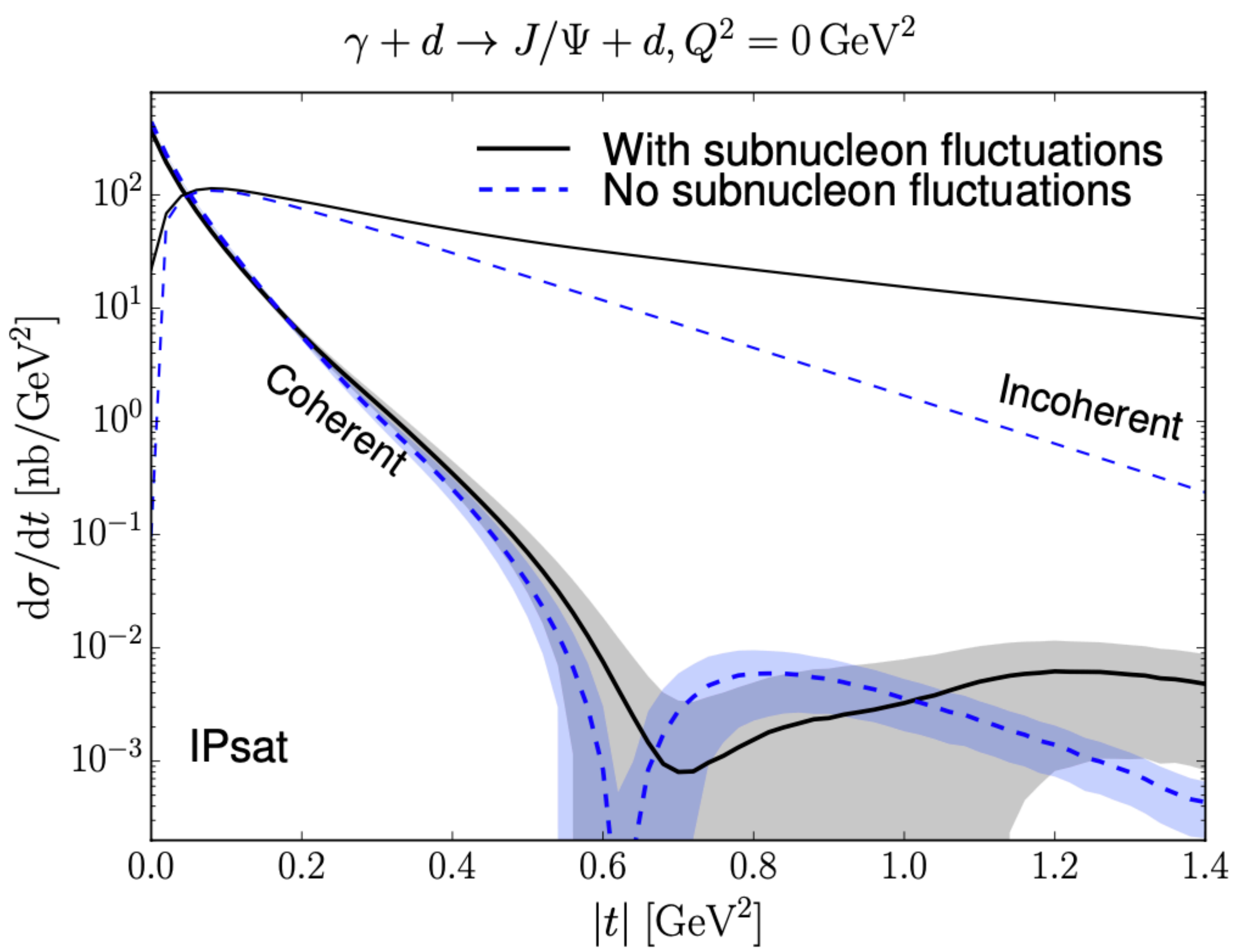

Can also access details of deuteron wave function (BACKUP)

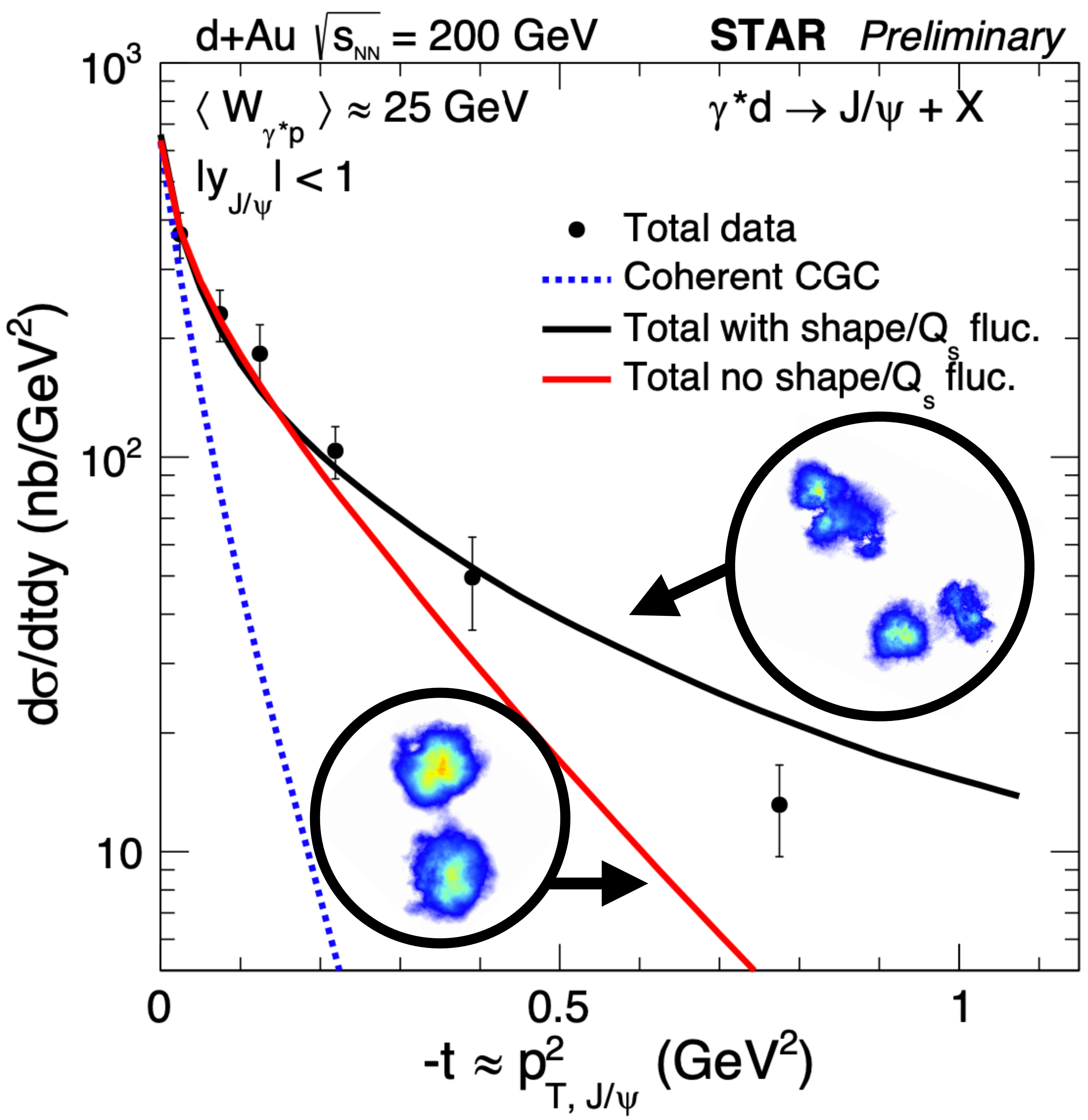

STAR Collaboration at Hard Probes 2020

PoS HardProbes2020 (2021) 100; arXiv:2009.04860

Substructure: large effect on incoherent at $|t| \gtrsim 0.25\mathrm{GeV}^2$ (as in Pb)

STAR data favors substructure

Photoproduction of J/ψ in d+Au collisions at STAR

H. Mäntysaari, B. Schenke, Phys. Rev. C101, 015203 (2020)

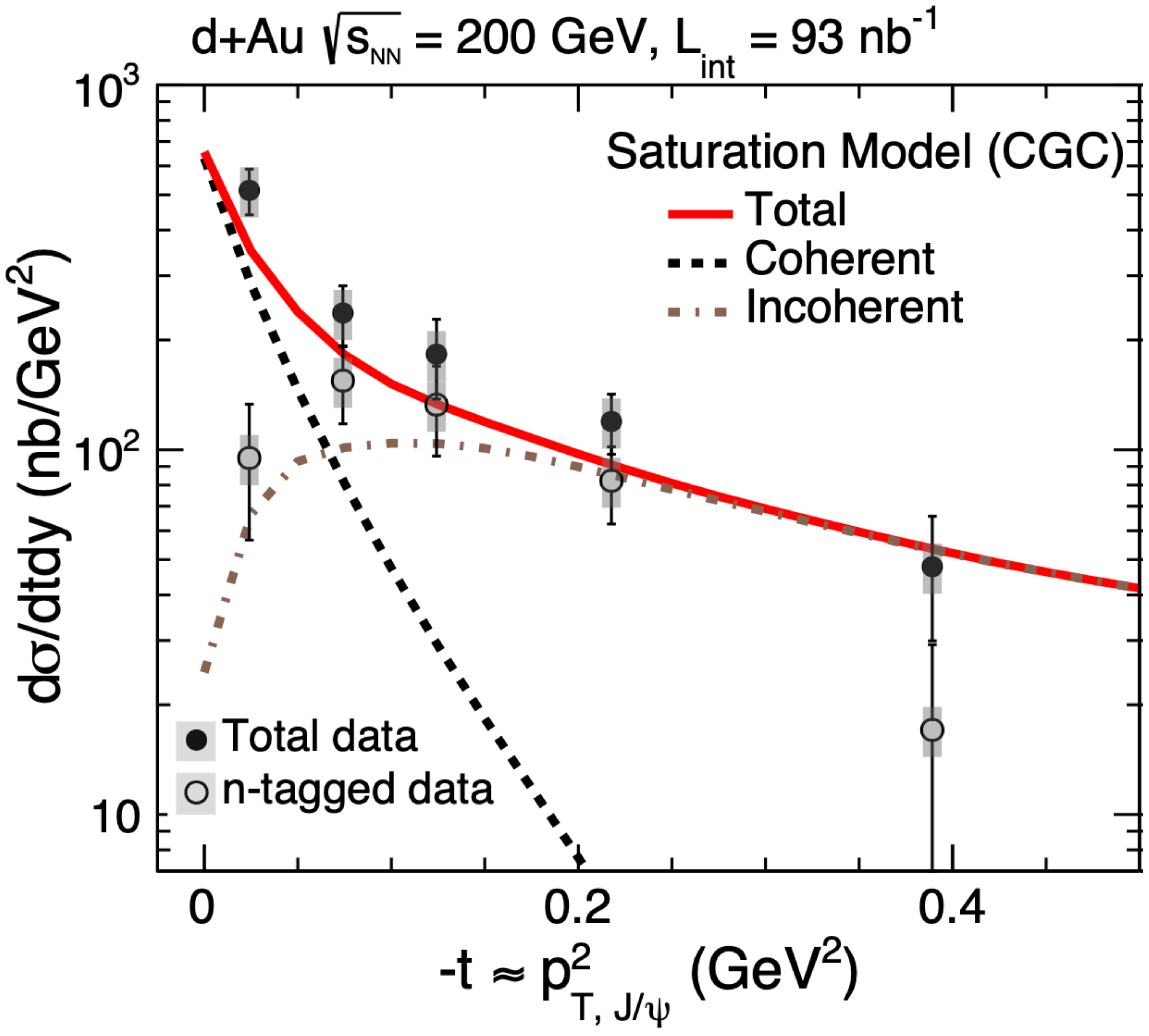

n-tagged results can be compared to incoherent cross section

STAR Collaboration, Phys. Rev. Lett. 128, 122303, (2022) e-Print: 2109.07625